Assessing the Role of *L. brevis* and *S. salivarius* Bacterial-mammalian Cell Interactions in Methotrexate Cytotoxicity in an Imageable *in vitro* Co-Culture Model of the Oral Mucosa Using an Aqueous Two-Phase System

by

Sofía Magaña Lama

Submitted in partial fulfillment of the requirements for the degree of
Master of Applied Science

at

Dalhousie University
Halifax, Nova Scotia
December 2023

Dalhousie University is located in Mi'kma'ki, the ancestral and unceded territory of the Mi'kmaq. We are all Treaty people.

Table of Contents

List of tables

List of Figures

Abstract

Chemotherapy-induced oral mucositis (CIOM) is characterized by the ulceration of the oral mucosal tissues caused by the systemic cytotoxic effects of chemotherapy. It is considered a major side-effect that may lead to the interruption of cancer treatment, which often compromises the treatment prognosis for patients. Recently, there has been interest in exploring the potential of bacteria to treat CIOM, primarily driven by the promising effects of probiotics in reducing the severity of intestinal mucositis. The application of probiotics for treating CIOM has not been properly explored due to the lack of adequate study models and clear mechanisms through which probiotics exert their benefits. We fabricated an imageable *in vitro* model using stained immortalized human oral keratinocytes (OKF6/OKF6-TERT2) and then treated it with Methotrexate aiming to recapitulate the cellular damages that are typically observed in CIOM. The establishment of the microbe-mammalian co-culture was achieved using an aqueous-two phase system (ATPS), a liquid-based scaffold of polyethylene glycol and dextran. An ATPS was optimized for each bacteria to maintain them contained and viable for 48 hours within the DEX-phase without damaging a monolayer of OKF6 cells. This research aimed to provide a tool to fill the knowledge gap in our understanding of the mechanistic effects of specific probiotics in CIOM. The effect of applying *L. brevis* or *S. salivarius* to a monolayer of OKF6 before exposure to MTX was tested. The results suggested that the application of *S. salivarius* to the OKF6 cells before MTX exposure maintained cell viability in comparison to the bacteria-free control. In this study *L. brevis* had a high susceptibility to the tested MTX dosage. The establishment of an *in vitro* model capable of allowing mammalian-microbial interactions in a system with representative damage of CIOM provided the possibility of elucidating the mechanism behind the benefits of probiotics that past studies have demonstrated in clinical trials and using *in vivo m*odels. This is the first study to test *in vitro* the effects of probiotics in an oral mucositis model, furthermore, allowing mammalian-microbial interactions.

List of Abbreviations and Symbols Used

Abbreviation	Definition
µg	Microgram
µL	Microliter
AB	AlamarBlue
ANOVA	Analysis of variance
ATPS	Aqueous two-phase system
BHI	Brain Heart Infusion
BPE	Bovine pituitary extract
CFU	Colony forming unit
CIOM	Chemotherapy-Induced Oral Mucositis
CMRA	CellTracker Orange CMRA
DEX	Dextran
DHFR	dihydrofolate reductase
DMSO	Dimethyl sulfoxide
DNA	Deoxyribonucleic acid
EDTA	Ethylenediaminetetraacetic acid
EGF	Epithelial growth factor
FBS	Fetal bovine serum
GSH	Glutathione
IL-6	Interleukin 6
KSFM	Keratinocyte Serum-Free Media
L	Liters
LB	Luria-Bertani
mg	Milligram
mL	Millilitre
MRS	deMan Rogosa Sharpe
MTX	Methotrexate
NF-κB	Nuclear factor-κB
NRF2	Nuclear factor erythroid 2-related factor 2
OD_{600}	Optical density at 600 nm wavelength
OKF6/OKF6-TERT2	Immortalized human oral keratinocytes

PA CF18	*P. aeruginosa* CF18
PBS	Phosphate-buffered saline
PCR	Polymerase chain reaction
PEG	Polyethylene glycol
RFP	Red fluorescent protein
RNA	Ribonucleic acid
ROS	Reactive Oxygen Species
TNF-α	Tumor-necrosis factor-α
w/v	Weight per volume

Acknowledgements

First and most importantly, I would like to acknowledge and express my profound gratitude to my supervisor Dr. Brendan Leung. For believing in me back when I was in my home country, for giving me the opportunity to come to Canada to work on this project, and for challenging me to think critically. I would like to thank the rest of my committee members, Dr. Zhenyu Cheng and Dr. Daniel Boyd, for their continuous support, guidance, and disposition. I am grateful I got the chance to learn from you.

I would also like to thank my past and present lab members and coworkers for the insightful questions, feedback, constant support, and friendship. To Sarah Spencer, Yuliia Komburleii, Dr. Hanan Moussa, Morgan Pugh-Toole, Max Wolverton, Flora Machovsky, Andrew Smith, Claire Carruthers, Dr. Naeimeh Jafari, and Christian Rempe. To my close friend and lab mate, Magdalena Trocha, thank you for the good company during long nights at the lab, and for your unconditional support and friendship.

Thank you to my parents, Ligia and Arturo, and my family and friends back in Mexico, for encouraging me to always do my best and for supporting me all the way. I would also like to acknowledge my friends in Canada who have been with me every step of the way.

Lastly, I would like to thank all those who helped complete this project. Ashley Kervin, for processing my histology samples. Dr. Lisa Johnson for taking the time to analyze my histology samples and guiding me through the process. And Renee Raudonis for the microbiology training.

CHAPTER 1. Introduction

1.1. Chemotherapy and its Effects on the Oral Microenvironment

The goal of chemotherapy is to inhibit cell proliferation and tumor growth, thus avoiding invasion and metastasis. However, this results in toxic effects due to the lack of specificity of the drug, which affects normal cells as well [1]. Traditional chemotherapy agents primarily affect either macromolecular synthesis and function of neoplastic cells by interfering with DNA, RNA, and protein synthesis or by affecting the functionality of molecules. Ultimately, the treatment leads to cell death due to the chemotherapeutic agents´ direct effect or by triggering apoptosis [2], [3]. Chemotherapeutic agents can be classified according to their mechanism of action, some of them are alkylating agents which yield an unstable alkyl group that reacts with proteins and nucleic acids inhibiting DNA replication and transcription, there are also antimicrotubular agents, that usually inhibit topoisomerase or the assembly of microtubules which stops the cycle in M phase, and among others, there are the antimetabolites, their mechanism of action involves the inhibition of DNA replication, and within this classification, there are the folate antagonists, where one of the most common chemotherapeutic treatments is found, Methotrexate (MTX) [2].

MTX inhibits at least four enzymes in the folate pathway. Its ability to inhibit folate formation comes from its structural similarity to dihydrofolic acid (Figure 1) which allows its competitive inhibition of dihydrofolate reductase (DHFR). The molecular mechanism through which MTX has its effect leads to a significant decrease in purine and pyrimidine synthesis inhibiting cell proliferation, which is why it is considered an antineoplastic drug [4].

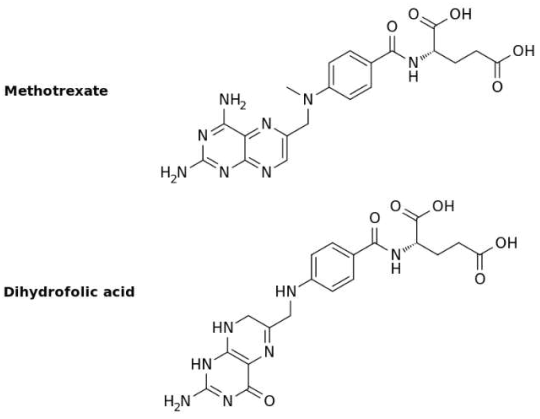

Figure 1. Chemical structure of MTX and dihydrofolic acid

Chemotherapy does not only target malignant cells but also healthy tissue, its effects on the mouth are frequent due to the high division rate of the cells in the oral mucosa. This antineoplastic treatment causes the activation of signaling pathways that lead to the secretion of inflammatory molecules, generation of reactive oxygen species, and other mechanisms that ultimately damage the oral epithelium [5]. These alterations, among others, may contribute to the rupture of the oral mucosal tissue, providing a gateway for opportunistic microorganisms, and leading to infections [6]. In addition, chemotherapeutics can be bacteriostatic, hence, affecting the oral bacterial community in patients. It has also been identified in various studies that oral mucositis is an independent risk factor for the development of bacteremia and systemic infections, involving anaerobic bacteria and other species that are not normally found in the oral cavity [7]. It has been observed in pediatric leukemia patients that during chemotherapy treatment, the oral microbiota plays a role in the metabolism of specific chemotherapeutic agents. It has been identified that the outgrowth of these bacteria leads to the formation of active toxic metabolites of the drug, which directly affects the progression of intestinal mucositis [8]. Although there is still no conclusive evidence correlating the shift in bacterial colonization with oral mucositis severity, multiple studies have suggested potential associations [9]. Nevertheless, further research is required to analyse the different effects of bacteria in oral mucositis.

1.2. Aetiology of Chemotherapy-Induced Oral Mucositis

Mucositis refers to the inflammation and/or ulceration of the mucosal lining of the gastrointestinal tract. When it is present in the mucous membrane that lines the structures within the oral cavity, also called the oropharyngeal mucosa, it is referred to as oral mucositis or stomatitis. These structures include the soft palate, the side and back walls of the throat, the tonsils, and the posterior one-third of the tongue [10] [11].

Chemotherapy interferes with cellular division, thereby inhibiting the spread of rapidly dividing cells. However, it does not differentiate between rapidly dividing cancer cells, and healthy cells that divide at high rates. The oral epithelium, like the skin, is a constantly renewing tissue in which proliferating cells in the basal layer produce daughter cells that migrate to the surface [12]; hence, chemotherapy results in various side effects within the oral cavity [9] (Figure 2). Approximately 40%-70% of patients receiving conventional chemotherapy present oral mucositis [13]. This pathology can seriously

compromise patients' quality of life causing psychological distress but also restricting their ability to eat, speak, and sleep. In severe cases, symptoms often require significant supportive care, including pain management, parenteral nutrition, and anti-microbial agents. In extreme cases, chemotherapy dose reductions or complete cessation of treatment are required, compromising treatment prognosis and patients' survival [14] [12] [15]. The identification of the molecular events and the understanding of the pathobiology leading to this condition provides targets for mechanistically based interventions to adequately manage, but also ideally prevent oral mucositis [5].

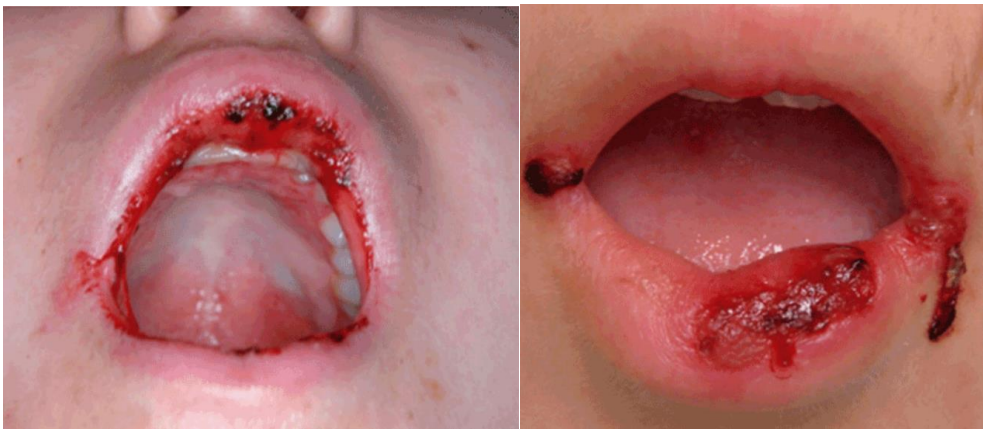

Figure 2. Pediatric chemotherapy patient with oral mucositis grade 3. At this stage, patients consume only liquid foods [16].

Chemotherapy-induced mucositis has mainly been attributed to basal-cell damage. This is the result of the permeation from the submucosal blood supply [12]. As the drug is administered it initiates DNA damage through strand breaks, which result in cell death or injury. Non-DNA injury is initiated through a variety of mechanisms, some of which are mediated by the generation of reactive oxygen species (ROS). Chemotherapy is an effective activator of several injury-producing pathways. The transcription factors involved include nuclear factor-κB (NF-κB) and nuclear factor erythroid 2-related factor 2 (NRF2), which can upregulate genes that modulate the damage response for toxic and oxidative insults. These signaling molecules also participate in a positive feedback loop that amplifies the original effects of the chemotherapy. For instance, TNF-α activates NF-κB and sphingomyelinase activity in the mucosa, which can lead to more cell death. In addition, direct and indirect damage to epithelial stem cells results in a loss of renewal capacity. As a result, the epithelium begins to thin and patients begin to experience the early symptoms of mucositis [12].

1.3. Current Models of Chemotherapy-Induced Oral Mucositis

Current *in vivo* and *in vitro* study models used to understand the cytotoxicity effects of chemotherapy in the mouth and its association with different bacteria are limited and present certain deficiencies. For instance, animal models are ethically challenging, time-consuming, and expensive. Moreover, monitoring dynamic and rapid mucosal biological responses to chemotherapy agents and microorganisms in *in vivo* models is also challenging. The potential of *in vitro* models has not been properly exploited for the study of host-microbial interactions as a potential key treatment to prevent mucosal injury. The ability of physicians to give patients the proper therapy, intervention, or prophylactic treatments, is limited by the molecular background that scientists can provide on the pathology of this condition. Further research is required to define optimal protocols to improve the translatability of findings to humans.

Studies investigating interactions between microbes and mammalian cells both *in vivo* and *in vitro* are challenged by the exponential growth of bacteria. Controlling the growth of microbes in a highly regulated environment, such as a cellular culture, is challenging. Additionally, it constrains the time available for studying cellular interactions because the overgrowth of bacteria results in nutrient depletion for the mammalian cells [17]. However, the interaction between the epithelial cells and bacteria needs to be studied within an ecosystem that allows a realistic environment not only for the mammalian cells but also for the bacteria.

The few models found that have studied *in vitro* the relationship between bacteria and CIOM have focused on the ability of a bacteria species to trigger pathogenicity in the epithelium rather than on the potential of microbes to prevent damage. The use of organotypic models of CIOM allows the reproducing of the main histopathological characteristics of this disease and the assessment of the effect of the MTX on oral opportunistic fungal pathogens and commensal bacteria. These models have also allowed the identification of microbial species that exacerbate the pro-inflammatory signals of the damaged mucosa caused by cytotoxic chemotherapy [18]. Models have not, however, been used to assess the potential protective mechanisms of microbes, nor have they tried modifying the bacterial load to try to improve disease outcomes. Nevertheless, these models have provided a valuable tool to study the mechanism of commensals in the mouth and the relevance of biofilm formation.

Another *in vitro* model capable of recapitulating histological organization and functional characteristics of the oral mucosal epithelium is patient-derived organoids.

These structures consist of a functional stratified epithelium that can be maintained in culture for over six months. Upon passaging, organoids grown from primary oral mucosa tissue can be broken into smaller fragments, which will proliferate and result in the formation of new organoids [19]. As such, organoids allow the multiplication of human wild-type epithelial cells for a wide variety of applications. These include testing for optimal MTX regimens to reduce mucosal toxicity in patient-derived oral mucosal organoids [20]. Given that this model is capable of accurately mimicking the mouth's physiological environment, its application to study the relationship between the cells of the lining of the mouth and the oral microbiota offers great potential. However, given the origin of the structures and the potential risk of cancer cell contamination, the wild-type status of the organoids needs to be constantly confirmed by whole exome sequencing, which is an important factor to take into consideration. Primary cells must be used in early passages given their limited potential for self-renewal and differentiation, and the risk of cells undergoing senescence [21].

Animal models of mucositis have provided extensive information concerning the mechanisms of cancer therapy-induced mucosal injury [22]. The most common *in vivo* model organisms for oral mucositis in the published literature are Hamsters [22] [23]. An article published in 2023 by Huang *et al.* reported that a limiting factor preventing 75% of *in vivo* models from accurately reproducing a common clinical scenario is the use of alternate routes of administration of the antineoplastic agent when compared to patients [23]. Additionally, these studies stray from clinical relevance through the use of non-physiological stimuli to induce representative damage such as mechanical irritation or chemical injury. There is still significant variability among studies and further research is required to define optimal experimental conditions for a reproducible animal model suitable for preclinical studies [23].

The previously mentioned models have allowed the reproduction of the histological organization of the oral mucosa, recapitulate histopathological damage caused by chemotherapy, and understand complex molecular processes of CIOM, nevertheless, these studies have not exploited their potential or have important constraints that prevent them from studying the protective mechanisms that bacteria could exert on the epithelium.

1.4. Probiotics as a Potential Treatment to Target CIOM

The health effects that have been attributed to the use of probiotics in the past years

are numerous, which has increased scientific interest in the healing potential of bacteria. Probiotics are defined as live, non-pathogenic bacteria that confer health benefits beyond their nutritional value when administered at an adequate concentration [24]. Some of the most documented outcomes associated with the use of probiotics are the stimulation of humoral and cellular immunity, the decrease in unfavorable metabolites (such as ammonium and cancerogenic enzymes), the reduction of diarrhea associated with chemotherapy, the reduction of allergic symptoms, and cancer prevention [24]. The increasing interest in the applicability of probiotics to treat oral mucositis has been largely driven by the effectiveness of probiotics in treating intestinal mucositis [25]. However, it is important to mention that different strains of bacteria may exert different effects based on specific capabilities and enzymatic activities, even within a single species [24].

The efficacy and safety of *L. brevis* lozenges have been tested to prevent oral mucositis in patients undergoing chemotherapy. It has been observed that patients with hematological malignancies receiving high-dose chemotherapy that used *L. brevis* CD2 lozenges as a supportive care treatment, did not develop severe CIOM as often as patients taking a placebo [26]. Additionally, it has been reported that chemotherapy treatment completion rates in patients receiving *L. brevis* CD2 treatment are higher (92%) than those receiving placebo (70%). Furthermore, it has been identified that a larger proportion of patients remain mucositis-free when treated with *L. brevis* CD2 (28%) compared to the placebo (7%) [27]. However, there are also studies in the literature with inconclusive results about the beneficial effects of *L. brevis* CD2 [28].

The safety of probiotics has been assessed by evaluating translocation potential to the blood, spleen, and liver in mouse models. Species of *lactobacillus* have demonstrated protection of the oral mucosa against damage induced by 5-FU via the activation of cell antioxidant defense systems and reduction of inflammatory responses [25]. In these studies, no bacteria isolates were found in blood samples or tissues [25]. These findings have been observed for different strains of lactobacilli within the same genus [29].

Other protective mechanisms that have been identified in oral probiotics include the modification of the oral microbiota. *S. salivarius* K12 decreases the abundance of oral anaerobes. The application of this bacteria to treat radiation-induced oral mucositis has resulted in a significant reduction of ulceration, increased thickness of tongue mucosa and the density of basal cells, enhanced basal cell proliferation, and attenuated apoptosis. These effects have been in part attributed to its ability to alter the oral microbiota [30].

As previously mentioned, probiotic bacteria can differ in their mode of action in the disease processes depending on the microenvironment, the presence of other bacteria, or exogenous factors, such as anti-neoplastic treatments. These are all fundamental factors to take into consideration when conducting mechanistic analysis of probiotics in CIOM pathogenesis, which is a key step to its successful clinical adoption for CIOM management.

The use of probiotics can prevent or mitigate oral mucositis by reducing inflammatory or oxidative responses, improving the dysregulation of the oral microbiota, and promoting epithelial cell protection. However, the underlying mechanisms of various bacterial species or strains in the prevention and mitigation of oral mucositis vary [25].

Despite the benefits of probiotics, their misuse can cause adverse events. Some of these include gastrointestinal symptoms such as abdominal cramping or diarrhea, skin manifestations, excessive immune stimulation, and systemic infections such as bacteremia and endocarditis [31].

Systemic infections are considered the most severe side effects, and patients who are immunosuppressed, critically ill, or have cancer are at high risk [32]. In cases of bacteremia, *Lactobacillus* spp. strains had the highest reported involvement. Nevertheless, no deaths have been attributed to their use in the published literature [18]. The use of *Lactobacillus brevis* CD2 has been implemented in patients with hematological disorders undergoing high-dose chemotherapy and HSCT to reduce oral mucositis severity. Analysis showed no blood cultures were positive for *L. brevis* [26].

Different strains of probiotics have demonstrated great potential to treat oral mucositis, and when used correctly, they are generally safe with a low incidence of adverse events. However, for patients with certain clinical conditions, such as immunosuppression, the evidence suggests careful evaluation of the risk-benefit ratio before prescription or recommendation to use [32].

1.5. *L. brevis* and *S. salivarius*

Lactobacilli are Gram-positive, facultative anaerobic or microaerophilic, rod-shaped, and non-spore-forming bacteria. They are capable of fermenting hexose sugars to produce lactic acid, which results in the generation of an acidic environment that often inhibits the growth of other bacterial species [31]. In patients with cancer, *lactobacilli* have been demonstrated to be capable of helping to reduce the side effects of cancer antineoplastic treatments, including diarrhea and oral mucositis [33]. This bacteria is one

of the main probiotic genera that has been used to treat oral infections [34]. It has been reported in the literature that *lactobacilli* are capable of modulating immune responses causing cytotoxic effects in cancer cells, which shows great promise for the development of future cancer therapies [31]. The probiotic *Lactobacillus brevis CD2* was previously shown to inhibit gingival inflammation in humans, and potential to inhibit periodontal bone loss. The CD2 strain of *L. brevis* secretes high levels of arginine deiminase, an enzyme that inhibits the production of nitric oxide by competing with the enzyme nitric oxide synthase for the same substrate, arginine [35]. *Lactobacilli* can be used in various medical fields; species and strain identification is fundamental because different species or strains may lead to different therapeutic effects [31].

Levilactobacillus brevis demonstrated to be capable of inhibiting the growth of opportunistic pathogens, it has been reported in the literature that this strain can secrete antimicrobial compounds such as hydrogen peroxide and lactic acid. It has been demonstrated that this strain can adhere to oral epithelial cells. Additionally, it has been found to alleviate inflammation and might confer benefits to host health by modulating the immune system [34].

Streptococcus salivarius is a gram-positive, non-motile, facultative anaerobic lactic acid bacteria, that acts as a commensal in the oral cavity [36]. This species has been recognized as an oral probiotic for the treatment of multiple oropharyngeal pathogen-related diseases including oral candidiasis, pharyngitis, and halitosis [30]. It has been demonstrated that it has a regulatory effect on oral microflora [37], likely due to its production of bacteriocin-like inhibitory substances which strongly antagonize the growth of *Streptococcus pyogenes*, the most common bacterial cause of pharyngeal infections in humans [38] [30]. The use of *S. salivarius* has also been used as a prophylactic treatment for children with a history of recurrent oral *streptococcal* disease, and it has resulted in a reduction of *streptococcal* and viral infections and reduced the number of days under antibiotic and antipyretic therapy [39]. It has also been recorded that diverse strains of *S. salivarius* have significant antioxidant and protective properties against cell oxidative stress [40].

1.6. Research Aims, Objectives, and Thesis Hypothesis

Research question:

1. Can the application of bacteria with probiotic potential reduce the effects of Methotrexate cytotoxicity in an *in vitro* microbial co-culture model of the oral

mucosa?

The overall goal of this project was to develop a study model that would allow the analysis of the effects of bacteria with probiotic potential in the oral microenvironment of CIOM patients. It was hypothesized that the application of probiotics in the oral microenvironment would reduce the effects of CIOM in an *in vitro* co-culture model of the oral mucosa. In the following subsections the research aims along with their objectives are described.

Aim 1

The first aim of this project was the establishment of an imageable *in vitro* model that allowed the study of the probiotic potentials of bacteria on a system recapitulating CIOM-like damage. For this purpose, a 2D oral epithelium model was established using human basal keratinocytes on a system capable of recapitulating CIOM effects by causing representative cell damage with MTX. To verify that the engineered *in vitro* model could reflect the effect of MTX and of the application of bacteria, a MTX dose-response curve was established through the observation of a signal emitted by live cells on the assembled system over time using fluorescent microscopy. At the same time, the assay of preference had to be capable of reflecting different types of cell damage (microbial and chemical) to ensure the effect of MTX was being observed. To test the effectiveness of the model in replicating CIOM responses in the epithelium, MTX was administered at a dosage that was carefully selected, and the damage was characterized using cell viability assays that evaluated the effect in the system following drug exposure (Obj. 1. B). MTX is one of the most commonly used antineoplastic agents associated with mucositis, is one of the most studied chemotherapeutic drugs, and its effects in the epithelium and its connection with the oral microbiota are highly documented in the literature. However, correlating the MTX treatment of cell cultures to a general clinical situation is not realistic because chemotherapy regimens, whether it is a continuous dosage versus repeated infusions and its duration, differ upon the type of tumor, organ affected, presence of metastases, and other clinical factors. Therefore, this project will aim to define the proper test dosage (concentration and time) as one that causes 50-70% of the cells in the model to undergo apoptosis, rather than trying to match the *in vivo* local drug dose to which the oral tissue is exposed. In a clinical setup, this level of cell death mimics the full onset of CIOM and also allows the study of changes in cellular response caused by the presence of microbes. However, given the antimicrobial effect that MTX may exert on the bacteria, the selected

dosage will also be adjusted upon the susceptibility that the selected strains may show toward the drug.

Aim 2

The effectiveness of probiotics in OM has been proven by multiple clinical trials, but the results are still controversial and sometimes inconclusive because the interactions between the bacteria and the epithelium have not been fully understood. In the second aim, the bacteria that were going to be studied in this research project were chosen following specific parameters. In Objective 2.A., After an extensive literature review, two bacteria with probiotic potential towards CIOM that could safely be administered to a patient were selected per at least two of the following criteria: they modulated host inflammatory response; increased resistance to oxidative stress; or they had proven to displace pathogenic bacteria or prevent dysbiosis by maintaining host-microbiome balance in the oral milieu. Once selected, the characterization process included performing the growth curve of each one of them and making their OD_{600}-CFU/mL correlation graphs.

To be able to incorporate the bacteria into the *in vitro* co-culture model, the bacteria needed to be compatible with an aqueous-two phase system (ATPS), which implied that it could be contained and maintain viability within it. This was assessed in objective 2.B. This system limited bacterial spread but allowed their metabolites to be sensed by mammalian cells underneath the system. The ATPS formulation that was used consisted of polyethylene glycol (PEG) and dextran (DEX), given that they have been extensively studied, are non-cytotoxic, and are the most commonly used. This objective also involved the optimization of the formulation and bacterial concentration that was used for each strain in the system.

Once the bacteria were selected and proven to be compatible with ATPS, it had to be assessed if they could maintain viability with clinically relevant chemotherapy dosage (Obj. 2.C.). It has been demonstrated that some commensal bacteria in the mouth remain prevalent regardless of the application of chemotherapy [41], [42]. Nevertheless, MTX, in the same way as its antimicrobial counterpart trimethoprim, acts by inhibiting the bacterial DHFR, which leads to reduced purine, pyrimidine, and amino acid biosynthesis and thus inhibits cell replication [43]. Additionally, it has been reported in the literature that MTX has relevant activity against *Streptococcus spp*. The highest activity was observed against certain species of *V. streptococci* which were inhibited at concentrations $\geq 5x10^4$ mg/mL. The relevance of verifying bacterial tolerance to the

chosen chemotherapy dosage was evident.

Aim 3

The third and last aim of the project was to test the protective effects of probiotics and to identify the mechanism through which probiotics protect the oral epithelium from MTX-mediated damage. Although it has been proven in the literature that the chosen bacteria can be safely administered to patients [26], [44], the first objective was to verify that they did not damage the mammalian cells at selected concentrations (Obj. 3.A.). In the second objective for this aim, the protective effect of the bacteria was studied through the addition of the bacteria on top of the cells 24 hours before the application of the MTX dosage (Obj. 3. B). The next feature that aimed to be evaluated on the system was if the probiotics were capable of modulating molecular markers of cell damage (Obj. 3.C.), *In vivo* models have suggested positive outcomes concerning this matter. However, the mechanisms through which the probiotics achieve this remain unclear.

CHAPTER 2. Materials and Methods

2.1. Mammalian and Bacterial Cell Culture Conditions

An immortalized human oral keratinocyte cell line, OKF6/TERT2 kindly provided by Dr. Cathie Garnis (BC Cancer Centre) was used for this study. These cells were isolated from human oral mucosa. They were incubated at 37ºC and 5% CO_2 in Keratinocyte Serum-Free media (KSFM, Thermo Fisher Scientific, Gibco, Cat. No. 17005042). The media was supplemented with $5x10^{-5}$ mg/mL bovine pituitary extract (BPE), $5x10^{-6}$ mg/mL of human recombinant epithelial growth factor (EGF) (Thermo Fisher, GIBCO, 37000-015), and for experiments that did not require an ATPS, 1% antibiotic-antimycotic was added (AA, 100x, Thermo Fisher Scientific, Gibco, Cat. No. 15240062).

Streptococcus salivarius strain M18 (*S. salivarius*) and *Levilactobacillus brevis* strain Bb14 (*L. brevis*), were studied during this research. *S. salivarius* (ATCC 14869) was originally isolated from a human oral cavity. Frozen stocks of this bacteria were stored in Brain Heart Infusion (BHI) broth (Millipore 110493) containing 25% (v/v) glycerol stored at -80ºC. *L. brevis* (ATCC 14869) frozen stocks were stored in Difco Lactobacilli deMan Rogosa Sharpe (MRS) (Fisher Scientific 288130) containing 25% (v/v) glycerol stored at -80ºC. For use of the *S. salivarius* in experiments, frozen stocks were streaked on 1.5% (w/v) BHI agar (Sigma-Aldrich) plates and incubated overnight at 37ºC, for 16 to 18 hours. *L. brevis* frozen stocks were streaked on MRS on 1.5% (w/v) MRS agar plates and incubated overnight at 37ºC for approximately 36 to 48 hours. Overnight cultures were prepared by using a loop to pick single colonies from the streaked plates and inoculating 5 mL of bacteria culture broth.

BHI broth was used for *S. salivarius* overnight cultures, while MRS broth was used for *L. brevis*. The inoculated broth was placed in a shaking incubator (VWR) shaking at 200 rpm and 37ºC for 16 to 18 hours.

2.2. Assessment of CFU/mL of *L. brevis* and *S. salivarius* per OD_{600}

Given that the bacterial concentration of starting stock solutions was obtained by reading their optical density, it was necessary to determine the concentration of colony-forming units per milliliter (CFU/mL) in a solution given its optical density (OD_{600}), which was read at 600 nm. For this purpose, an overnight culture was established for *L. brevis* and *S. salivarius* in MRS and BHI broth respectively; an isolated colony from each

strain was obtained from a freshly streaked agar plate, no more than a week old, using a sterile loop to inoculate 5 mL of the broth of preference of each bacteria. A negative control was kept at all times for each broth; in the same incubation process an extra 5 mL tube with the broth was kept and it was inoculated with a loop without bacteria to guarantee a lack of external bacterial contamination neither in the broth nor in loops. The 5 mL broth tubes were placed in a shaking incubator at 200 rpm and 37ºC for 16 to 18 hours.

After the incubation time, *S. salivarius* culture was diluted to a 2:5 ratio in BHI, while *L. brevis* was diluted 3:5 ratio in MRS. Both strains were left to further incubate for 3 hours in the same conditions. After this period, *L. brevis* was diluted into 0.1, 0.2, 0.3, 0.4, 0.5 and 0.6 OD_{600}. While *S. salivarius* was diluted into 0.1, 0.2, 0.3, 0.4, and 0.5 OD_{600}. These dilutions were calculated (Equation 1) given the initial OD_{600} read from the overnight cultures.

$$C_1 \cdot V_1 = C_2 \cdot V_2 \qquad [1]$$

Each one of the mentioned dilutions for each bacteria was further diluted from 10^{-1} to 10^{-6} and these dilutions were spot-plated to quantify bacterial concentration. Negative control was spread-plated to verify the lack of bacterial contamination in broth or loop. Using Equation 2, the concentration of CFU/mL was calculated. Where N is the concentration of viable bacteria in CFU/mL, which is determined by the number of individual colonies counted (C), the volume of the plated sample (V) in mL, and the dilution factor (D) out of which this colonies were counted.

$$N = \frac{C}{(V)(10^{-D})} \qquad [2]$$

2.3. Assessment of Growth Curves for *L. brevis* and *S. salivarius*

In order to establish the growth curves of each strain, the two bacteria were inoculated in 5 mL of their broth of preference, and two tubes of each broth were kept just with broth as a negative control as established in Section 2.3. For *S. salivarius*, the optical density was read every 2 hours until the 12-hour mark after that the OD_{600} was read again after 4 hours. This process involved vortexing the culture and then adding 200

µl of bacterial solution to three wells of a 96-well plate out of which the absorbance was read at 600 nm for the three technical replicates. For *L. brevis* the optical density was read approximately every 2 hours for the first 15 hours, and then again from hour 23 to hour 34 every 2 hours, and then once again at hour 52. The sampling and analysis process of the culture was the same for both strains.

2.2. Collagen Coating

To enhance and promote a more even distribution of cells in the inserts, a collagen coating was added to the membrane of the inserts used for all experiments that involved OKF6s. A 3.0 mg/mL collagen (Advanced BioMatrix PureCol® bovine collagen solution, Type I, Cat. No. 5005) was diluted to .05 mg/mL (1:60) in cell culture grade water in a sterile 15 mL tube. 100 µl of solution was added to each insert and they were allowed to incubate inside the biosafety cabinet at room temperature for 2 hours. After incubation, the collagen solution was carefully aspirated, and they were washed with 100 µl of PBS. The plate was air-dried in the biosafety cabinet for 45 minutes and used immediately or sealed with a parafilm laboratory film cover till the next day.

2.3. Alginate Hydrogel Preparation

A thin layer of alginate hydrogel was added to the inserts between the ATPS and the OKF6 monolayer in all experiments to enhance cell viability and adhesion. This alginate cushion was made with 1.5% (w/v) alginate, and 0.5 mg/mL CaCl2. Two stock solutions were prepared for this purpose, the first one was a 10 mg/mL CaCl2 solution prepared in DI water, it was sterilized through filtration (0.22 µm diameter filter) before storage at -4°C. The second one was a 30 mg/mL sodium alginate stock solution, to prepare it, sodium alginate was weighed in a 50 mL Falcon tube and UV sterilized for 60 minutes by turning it over every 20 minutes. Then it was dissolved in PBS to a concentration of 30 mg/mL. HEPES buffer was added to a concentration of 75 mm. Lastly, the sodium alginate was left on a rocking platform shaker (VWR) overnight to allow it to fully dissolve.

The sodium alginate stock solution was diluted with PBS to a final concentration of 22.5 mg/mL while the $CaCl_2$ stock solution was diluted in 0.9% NaCl until a 2 mg/mL concentration was reached. These two solutions were mixed in a 3:1 ratio, three parts of the 22.5 mg/mL sodium alginate solution and one of the 2 mg/mL $CaCl_2$ [NaCl] solution, and then vortexed for 10 seconds. However, the addition of the $CaCl_2$ solution to the

alginate solution starts the crosslinking of the hydrogel, for this reason, the mixing of these two solutions was done right before adding the gel to the cells and if more than 12 inserts needed the hydrogel the crosslinking was started in two batches one after the other to delay the gelation. Once the alginate hydrogel was applied to the inserts, the plate was left in incubation at 37°C and 5% CO_2 for ten minutes to allow the completion of the gelation process. A volume of 15 µl of alginate hydrogel was sufficient to cover evenly the entire bottom surface of a collagen-coated insert in a 24-well plate with 12 inserts.

2.4. Preparation of Aqueous Two-Phase System (ATPS)

The ATPS formulations used for this research were prepared with polyethylene glycol (PEG) (Mw: 35 kDa, Sigma Aldrich) and dextran (DEX) (Mw: 500 kDa, Pharmacosmos). To prepare the ATPS suitable for *L. brevis,* two separate ATPS had to be prepared, to obtain the PEG-phase*,* 10% (w/v) PEG and 5% (w/v) DEX were dissolved together in keratinocyte Serum-Free Media (KSFM) as well as in MRS broth in equal proportions (50/50-KSFM/MRS). The second ATPS would provide the DEX-phase, and it was prepared with the same DEX-PEG ratio but dissolved fully on MRS media. The preparation of the ATPS formulation suitable for *S. salivarius* involved preparing two separate ATPS as well, the PEG-phase was obtained from an ATPS prepared with 10% (w/v) PEG and 5% (w/v) DEX dissolved together in KSFM. The second ATPS used the same PEG-DEX proportions, but it was dissolved in BHI. The cell culture medium used to prepare all ATPS was free of any antibiotics or antimycotics. The solutions were mixed on a rocking platform shaker (VWR) until both polymers were fully dissolved. Once dissolved, the four ATPS prepared were sterilized using suction filtration with a 0.2 µm pore size filter (Thermo Scientific), then the tubes were centrifuged at 3000 x g for 90 minutes which allowed the polymers to separate into distinct phases. The PEG-rich top phase and the DEX-rich bottom phase were collected into separate sterile tubes and stored at 4°C.

All experiments that involved the application of *L. brevis*, involved the use of an ATPS prepared with 50/50-KSFM-MRS PEG-phase, which allowed OKF6 growth, and the DEX-phase made up with MRS media which supported *L. brevis* growth. On the other hand, all experiments that involved the application of *S. salivarius*, used an ATPS with the PEG-phase made up of KSFM, and the DEX-phase made up of BHI media which supported *S. salivarius* growth (Figure 3).

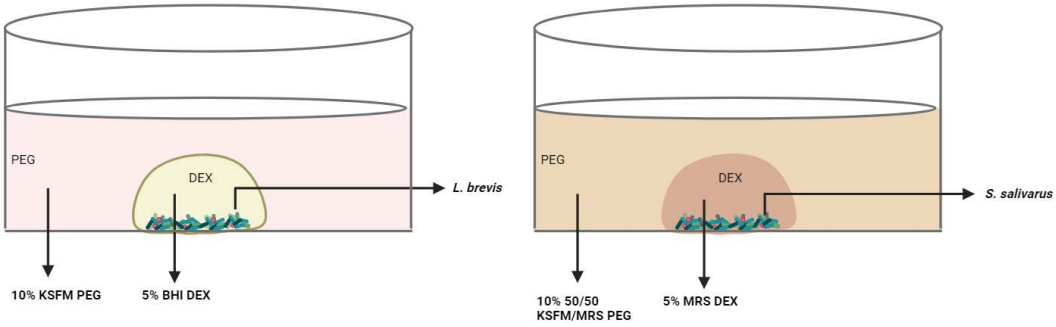

Figure 3. ATPS formulation for *L. brevis* and *S. salivarius.*

It is important to point out that given that the DEX and the PEG used in this study come from different mixtures and are prepared with different solutions, the polymeric solutions are not in perfect equilibrium with one another at the time of assembling the ATPS. Therefore, there will likely be a small amount of flux of DEX into the PEG-rich phase and vice versa. Over time the structure of the DEX droplet was likely altered due to this. However, the working concentrations of the solutions in the ATPS used were greater than the critical point to avoid loss of the phase system as concentrations drop below the critical point, this helped ensure that the ATPS remained after the polymers equilibrate with respect to each other [45].

2.4. Assessment of the *in vitro* Model's Ability to Reflect Cell Damage

For all experiments involving the use of stained OKF6 cells, a 24-well plate with 12 inserts was used (VWR, Avantor. Cat. No. 76313-906). The inserts had a 0.4 µm pore size, a polyethylene-terephthalate (PET) membrane, and a 6.5mm diameter. Approximately 9,000 cells were seeded per well, and they were grown for 24 hours prior to use for experiments.

2.4.1. MTX Dose Response Curve with CellTracker Orange CMRA

The OKF6s were stained with a fluorescent probe (CellTracker Orange CMRA, ThermoFisher, Cat. No. C34551, 550.4 g/mol). To prepare the stock solution, the lyophilized dye was allowed to warm to room temperature in its vial, then, the product was dissolved in Dimethyl Sulfoxide (DMSO) to a final concentration of 10 mM and stored at -20 °C. The working solution was prepared the same day on which the cells were going to be stained. For this purpose, the stock solution was diluted down to 20 µM by diluting 2 µl of stock solution in 998 µl of keratinocytes serum-free medium. The cells were resuspended in 1 mL of the working solution and incubated at 37ºC, 5% CO_2 for 40 minutes. After the incubation period, the cells were centrifuged, the supernatant was

discarded, and the pellet was resuspended in KSFM to the desired concentration. 9000 cells were seeded in 100µl on top of the collagen-treated inserts, and 600 µl of pre-warmed KSFM filled the basolateral compartment of the inserts. The cells were allowed to adhere overnight.

After verifying the confluency ranged between 50-60%, 5 different concentrations of MTX (Millipore, Sigma-Aldrich, Cat. No. A6770) were added to the basolateral compartment of the inserts: 10^{-10}, 10^{-8}, 10^{-6}, 10^{-4}, and 10^{-3} mg/mL MTX. Each concentration had two technical replicates. Five pictures were taken in the center of the insert in the red fluorescent protein (RFP) channel using a fluorescent microscope (EVOS ™ FL Auto 2 Imaging System. ThermoFisher Scientific) (Figure 4). Ten pictures were taken in total out of each treatment every 24 hours. Cell viability was calculated from a healthy control of cells that did not contain MTX diluted in the cell medium. Cell count was calculated using the Smart Segmentation tool of Celleste Image Analysis Software (ThermoFisher) (Figure 5).

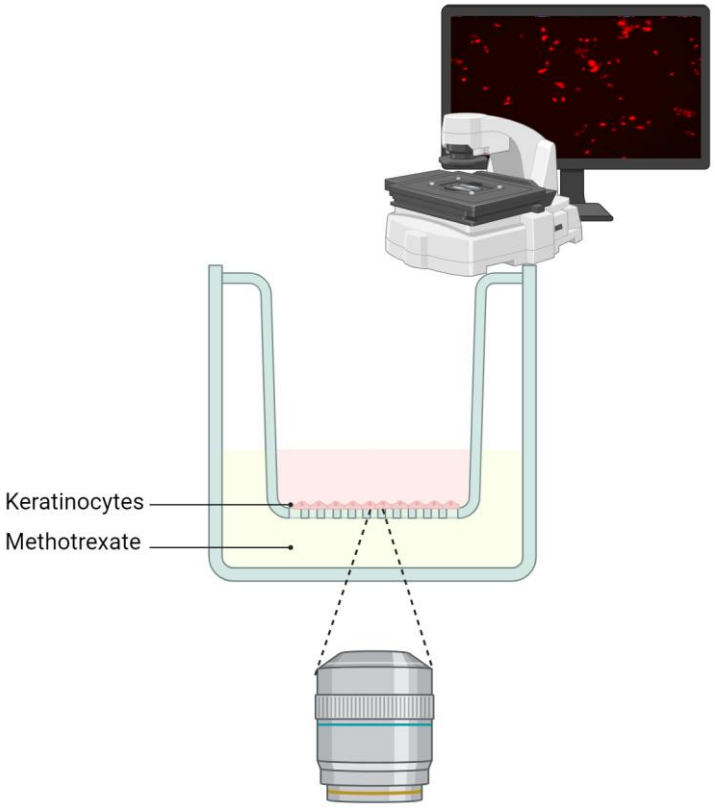

Figure 4. Fluorescent imaging arrangement of a 6.5mm insert with CellTracker-stained keratinocytes exposed to different concentrations of MTX from the basolateral compartment.

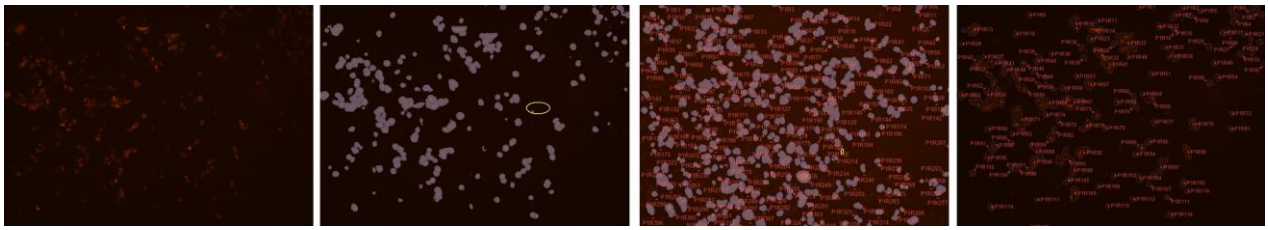

Figure 5. Celleste Image Analysis Software. the Smart Segmentation tool within Celleste allows the segmenting and counting of objects with a determined pixel intensity and a specified size (ThermoFisher)

2.4.2. Dimethyl Sulfoxide (DMSO) Induced Damage on CellTracker-stained OKF6 Cells

To test that the cell tracker was capable of reflecting cell death induced by different mechanisms a monolayer of CellTracker-stained OKF6 was exposed to DMSO. The CellTracker-stained OKF6s were seeded at a 50-60% confluency on the membrane of the inserts. The plate was left in incubation at 37°C and 5% CO_2 for approximately 24 hours to allow cell adherence and test the accuracy of the confluency. Then, an alginate hydrogel was added as established in Section 2.5. After gelation, KSFM with 5% dimethyl sulfoxide (DMSO) was added to the basal compartment of the inserts. Three technical replicates were used for the 5% DMSO treatment and three others for the control that used fresh and pre-warmed KSFM.

2.4.3. *Pseudomonas aeruginosa* (PACF18) Induced Damage on CellTracker-stained OKF6 Cells

To test that the cell tracker was capable of reflecting cell death induced by a microbe contained in an ATPS a monolayer of CellTracker-stained OKF6 was exposed to *P. aeruginosa* in an ATPS. A monolayer of CellTracker-stained OKF6 was seeded at a 50-60% confluency on the membrane of the inserts. The plate was left in incubation at 37°C and 5% CO_2 for approximately 24h to allow cell adherence and test the accuracy of the confluency. An alginate hydrogel was added as established in Section 2.5. An ATPS containing *P. aeruginosa* was added on top of the hydrogel, this system had 5% DEX prepared in Luria-Bertani (LB, Sigma-Aldrich) broth, and a 10% PEG-phase made with KSFM without antibiotics. The containment of *P. aeruginosa* CF18 within the ATPS was already assessed by previous lab members. A phase contrast image (scale bar 650um) was taken at times 0h, 24h, and 48h to track the growth of the bacteria, at the same time points, five fluorescent images (scale bar 275um) of the stained cells underneath each DEX

droplet were taken to track cell viability. A control was kept with the same ATPS formulation and assembled on top of a stained monolayer of OKF6 but without PACF18.

2.5. Assessment of *S. salivarius* and *L. brevis* Compatibility with Aqueous Two-Phase System

The compatibility of *S. salivarius* and *L. brevis* with the ATPS was first assessed by testing the adequate bacterial concentration that would allow the containment of the bacteria for 48h in an ATPS prepared with both DEX and PEG-phase made with the broth of preference of each strain. An initial 5% DEX 5% PEG ATPS was prepared with both phases made with the broth of preference of the bacteria, for *S. salivarius* BHI, and *L. brevis,* MRS. Following the same steps as established in Section 2.7.

An overnight culture was established for *L. brevis* and *S. salivarius* in MRS and BHI broth respectively by taking an isolated colony from an agar plate of each bacteria and inoculating 5 mL of the broth of preference of each bacteria. A negative control was kept at all times for each broth, as established in Section 2.3. The overnight cultures were left in a shaking incubator at 200 rpm and 37ºC for 16 to 18 hours. After the incubation time, *S. salivarius* culture was diluted to a 2:5 ratio in BHI, while *L. brevis* was diluted 3:5 ratio in MRS. Both strains were left for 3 more hours for further incubation.

After the second incubation, the OD_{600} of both bacteria and their controls was read. The absorbance of the broth without bacteria was subtracted from the OD_{600} of the broth with the strains. Using equation 1, *L. brevis* was diluted into 0.1, 0.3, and 0.5 OD_{600}. While *S. salivarius* was diluted into 0.1, 0.2, 0.3, and 0.5 OD_{600} into their broths of preference to a final volume of 400 µl in Eppendorf tubes. Then, the tubes were centrifuged at 10000 x g for 10 minutes, which allowed the bacteria to sediment. The supernatant was discarded, and the bacteria pellet of each tube with different bacterial concentrations was resuspended in 400 µl of DEX prepared whether in MRS or BHI for each strain. 250 µl of PEG at 10% and 5% concentrations prepared with MRS or BHI, was added to the wells of a 48-well plate, and a 1 µl droplet of DEX with bacteria at the mentioned concentrations was added with three technical replicates.

The assessment of the compatibility of the bacteria with an ATPS capable of satisfying the nutritional requirements of the mammalian cells involved preparing a second ATPS using KSFM media both with 5% and 10% PEG. Out of this ATPS, the PEG-phase was extracted and 250 µl of it was applied to a 48-well plate where a 1 µl DEX droplet containing *L. brevis* or *S. salivarius* at a 0.5 OD_{600} concentration was added.

Given the selective nutritional requirements of *L. brevis*, a second assessment was required in which the PEG-phase was prepared with 50% MRS and 50% KSFM.

After finding an ATPS formulation suitable for each bacteria that allowed containment for 48h and was capable of satisfying the nutritional requirements of the microbes and the mammalian cells, it was necessary to validate that the bacteria within the DEX was still viable. After 72h of starting the ATPS, the bacteria was spot plated (Adapted from Wang *et al.* [46]) into MRS and BHI agar plates, respectively.

2.5. Assessment of MTX Dosage on OKF6

The CellTiter-Glo® Luminescent Cell Viability Assay (Promega, Cat. No. G7570) was performed into OKF6 cells seeded at a 60% confluency in a white-walled 96-well plate. 24h after seeding, the different dilutions of MTX in (Millipore, Sigma-Aldrich, Cat. No. A6770, and Accord Pharma DIN 02474733) were prepared and applied with two technical replicates to each corresponding well of the 96-well plate. The MTX was aliquoted into 1N NaOH and stored at -20°C for a maximum period of a month. It has been observed that after 48 h of MTX exposure, an effect is visible on the apoptotic index and the proliferation of HaCaT keratinocytes in contrast to cells exposed for 24 hours [3]. Thus, the assay was performed 48 hours after MTX application by adding a volume of CellTiter-Glo® Reagent equal to the volume of cell culture medium present in each well. The content was mixed for 2 minutes in an orbital shaker and then it was allowed to stabilize the luminescent signal for 10 minutes covered from direct light. The luminescence was recorded using the Varioskan LUX plate reader (ThermoFisher Scientific).

The AlamarBlue assay was performed on a 96-well plate, where healthy OKF6 cells at 50-60% cell viability had been seeded. MTX in five different concentrations 10^{-11}, 10^{-8}, 10^{-6}, 10^{-5}, and 10^{-3} mg/mL MTX, was added to the well plate 48 hours prior to the assay diluted in KSFM. Each treatment was applied with three technical replicates. After 48h of exposure to the concentrations of MTX, the media was discarded and the cells were washed twice with PBS, then, 100 µl of KSFM with 10% AlamarBlue reagent was added to each well. After 3 hours of incubation at 37°C the fluorescence was read in the Varioskan LUX plate reader (ThermoFisher Scientific).

A live/dead assay was performed on a 48-well plate after exposing a monolayer of OKF6 cells to five different concentrations of MTX. This assay consists of calcein AM and ethidium homodimer-1 (ThermoFisher Scientific). In parallel to these stains, an

additional Hoechst stain (Hoechst 33342, ThermoFisher Scientific) was added to the wells to assess the total cell count. Calcein AM and ethidium homodimer-1 were diluted together in PBS to final concentrations of 2 µM and 4 µM, respectively, while the Hoechst was diluted in PBS to a concentration of 8.1 µM. Before adding the stains, the monolayer was washed with PBS once, then the calcein AM/ethidium homodimer-1 solution was added and the plate was incubated at 37ºC for 30 minutes. After incubation, the cells were washed and incubated with the Hoechst stain solution for 10 minutes at room temperature. The last stain was washed once more with PBS and then more PBS was added for imaging. The EVOS™ FL Auto 2 Imaging System (ThermoFisher Scientific) was used for phase contrast and fluorescence microscopy, which allowed the visualization of live cells (green fluorescent protein channel, GFP), non-viable cells (red fluorescent protein channel, RFP), and the stained cellular DNA (DAPI channel). ImageJ was used for image processing and cell viability quantification. Cell viability for each condition was calculated based on cell counts using Equation 3.

$$Cell\ Viability\ (\%) = \left(\frac{Total\ Cells - Dead\ Cells}{Total\ Cells}\right)(100\%) \qquad [3]$$

2.6. Assessment of Bacteria Susceptibility to MTX dosages

The susceptibility of *L. brevis* and *S. salivarius* to MTX was tested with two different concentrations. An overnight culture was established for *L. brevis* and *S. salivarius* in MRS and BHI broth with the respective MTX dilutions. An isolated colony from each strain was picked from a previously streaked agar plate using a sterile loop, and 5 mL of the broth of preference of each bacteria was used to dilute MTX to 10^{-1} and 10^{-6} mg/mL. These solutions were then inoculated. A negative control was kept at all times for each broth; in the same incubation process an extra 5mL tube with broth with the same MTX dilutions was kept and it was inoculated with a loop without bacteria to guarantee a lack of external bacterial contamination in the broth nor in loops. The 5mL broth tubes were placed in a shaking incubator at 200 rpm and 37ºC for 16 to 18 hours. After incubation, three technical replicates of each tube were taken into the plate reader where the optical density was measured. This experiment was performed with two biological replicates.

To further validate the ability of bacteria to stay metabolically active after exposure to the MTX dosage during ATPS containment, an ATPS containing each

bacteria was established on a 24-well plate with inserts (Section 2.9). The MTX was diluted to 10^{-1} and 10^{-6} mg/mL MTX in KSFM without antibiotics. Using the EVOS ™ FL Auto 2 Imaging System, phase contrast images were taken of the DEX droplets every 24h starting at time zero until the 48h mark. This allowed us to visualize an increase in density within the DEX that would suggest bacteria proliferation. To validate cell viability, the inside of the inserts containing the ATPS with the bacteria and the controls were transferred to a 96-well plate where the samples were diluted in PBS down to a 10^{-5} concentration where the isolated CFUs were observed.

2.6. Assessment of Effect of *S. salivarius* and *L. brevis* on Healthy Cell Culture

To assess the effect of *S. salivarius* and *L. brevis* on a healthy culture of OKF6s, the cells were seeded at a 60% confluency on a 48-well plate and left for incubation for 24h at 37°C. After incubation, the media was discarded, the wells were washed with PBS twice and an alginate hydrogel (Section 2.6) was applied evenly on top of the monolayer. In parallel to the incubation step of the hydrogel, an ATPS was assembled (Section 2.7) with each bacteria in their corresponding formulations of ATPS, both at 0.5 OD_{600} concentration. After resuspending the bacteria pellet on DEX, 250 µl of KSFM PEG was applied to half of the wells, and 50/50 MRS/KSFM PEG was applied to the others. 1 µl of DEX containing *L. brevis* was manually deposited on wells containing 50/50 MRS/KSFM PEG, while 1 µl of *S. salivarius* was deposited on wells containing KSFM PEG (Figure 6). As a control, 1 µl of BHI and MRS DEX without each strain was deposited in their corresponding ATPS formulation on top of healthy cells. Each treatment was applied with three technical and was performed with two biological replicates.

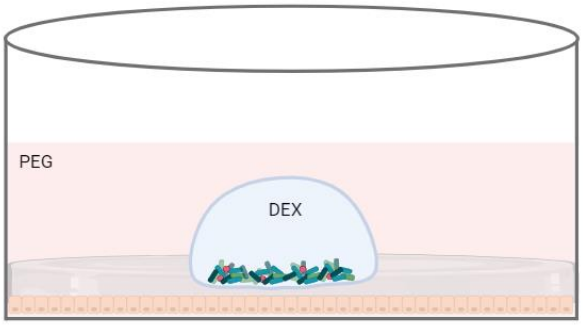

Figure 6. 48-well plate ATPS containing PEG and L. brevis or S. salivarius in DEX droplet on top of an alginate hydrogel covering a monolayer of CellTracker-stained keratinocytes.

2.7. Assessment of Effect of *S. salivarius* and *L. brevis* on Cell Culture with CIOM-like Damage

To assess the effect of *S. salivarius* and *L. brevis* on a cell culture with CIOM-like damage, OKF6 cells were seeded on collagen-treated inserts (Section 2.5) at a 50-60% confluency and left for incubation for 24h at 37°C at 5% CO_2. After incubation, the media was discarded, the inserts and the wells were washed with PBS twice and an alginate hydrogel (Section 2.6) was applied evenly on top of the monolayer. During the incubation process of the hydrogel, an ATPS was assembled (Section 2.7) with each bacteria in their corresponding formulations of ATPS, both at 0.5 OD_{600} concentration. The basolateral compartment of the inserts was filled with 600 µl of KSFM without antibiotics. 24 hours after the application of the bacteria on top of the monolayer, the KSFM media in the outer well was replaced with MTX solution at 10^{-6} mg/mL diluted in KSFM (Figure 7). Phase contrast images of each DEX droplet were taken every 24 hours for a total of 72 hours to verify bacterial growth. At the same time, 5 fluorescent images of the cells were taken from underneath the DEX droplet at the same 5 time points. The cells in the fluorescent images were counted using Celleste Software.

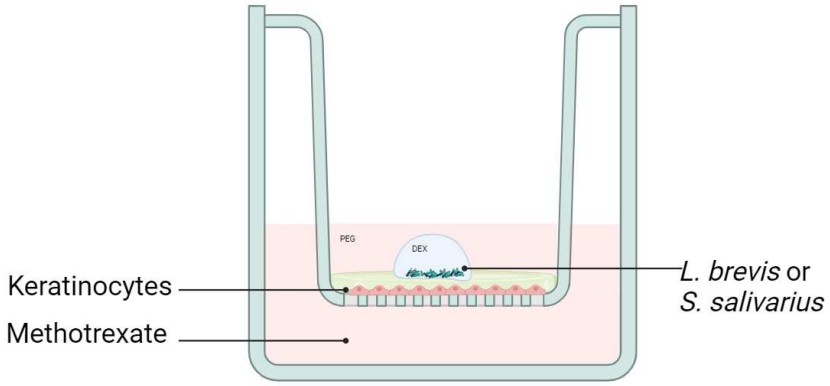

Figure 7. 6.5mm diameter insert with an ATPS containing PEG and L. brevis or S. salivarius in DEX droplet on top of an alginate hydrogel covering a monolayer of CellTracker-stained keratinocytes exposed to MTX from the basolateral compartment.

2.7. Statistical Analysis

Minitab Statistical software (Version 21.4.1.0) was used to analyze the cell count of OKF6 cells exposed to bacteria plus MTX and the cell count of cells just exposed to MTX. Statistical significance of cell count differences was determined using a two-way analysis of variance (ANOVA) test with p values represented as *$p < 0.05$, **$p < 0.01$,

***p < 0.001 and ****p<0.0001. The two factors analyzed were: time, with four levels: 0, 24, 48, and 72h; and treatment, with two levels, whether the cells had had bacteria applied or not.

GraphPad Prism (Version 10.1.0) was used to generate the visual representations of the two-way ANOVA paired with Tukey´s multiple comparison posthoc test with 95% confidence which allowed us to identify which means were different from the others after the ANOVA test indicated a statistical difference in the means of the multiple groups of the analyzed data.

2.8. Assessment of Molecular Markers on a Cell Culture Exposed to Bacteria and MTX

Aiming to assess the effect of *S. salivarius* and *L. brevis* on a cell culture with CIOM-like damage, OKF6 cells were seeded on 6-well inserts (Merck Millipore. Millicell Cell REF PIHA03050) with a polycarbonate membrane, at a 50-60% confluency and left for incubation for 24h at 37°C at 5% CO_2. After incubation, the media was discarded, the inserts and the wells were washed with PBS twice and 400 µL of an alginate hydrogel (Section 2.6) was applied evenly on top of the monolayer. During the incubation process of the hydrogel, an ATPS started being assembled with each bacteria in their corresponding formulations of ATPS as shown in Figure 8, both at 0.5 OD_{600} concentration. 740 µL of PEG were added on top of the hydrogel after the hydrogel had solidified. 4 droplets of DEX containing the bacteria were added, 1 µL each one, into the PEG. The basolateral compartment of the inserts was filled with 1500 µL of KSFM without antibiotics. 24 hours after the application of the bacteria on top of the monolayer, the KSFM media in the outer well was replaced with MTX solution at 10^{-6} mg/mL diluted in KSFM (Figure 8).

Forty-eight hours after the application of the MTX, the inserts were taken out of the incubator. The media in the basal compartment as well as the ATPS were discarded. One wash of PBS was gently done to the insert without removing the alginate hydrogel. 200 µL of 4.5% (w/v) Ethylenediaminetetraacetic acid (EDTA) in PBS was added to the inserts to solubilize the hydrogel and avoid detaching the cells from the membrane. 200 µL of pre-warmed trypsin were added to the membranes and allowed to incubate for 5 minutes at 37°C. 400 µL of DMEM with 10% fetal bovine serum (FBS) were added to neutralize the trypsin. Each treatment had a total of 3 technical replicates, 3 inserts, the cells were pulled from the three inserts from the same treatment into one microcentrifuge

tube and the cells from the other treatments were in other tubes. The cells were centrifuged at 3000 x g for 5 min, the supernatant was discarded. The pellet was washed twice with PBS using the centrifuge with the same setup. 10 µL of cell suspension was taken into the hemacytometer to verify that there were cells in the solution. 350 µL of lysis solution was added to the pellet. A matching volume (350 µL) of 70% EtOH prepared in ribonuclease (RNase) free water was added to each tube to reduce the viscosity. The 700 µL of solution was transferred to the columns and centrifuged for 30 sec, the flow through was discarded. 700 µL of Low stringency wash solution was added, centrifuged for 30 sec, and the flow through was discarded again. 80 µL of diluted DNase I was added to the membrane in the column and allowed to digest at room temperature for 15 minutes. 700 µL of High stringency wash solution was added, centrifuged for 30 sec, and the flow through was discarded again. 700 µL of Low stringency wash solution was added to the columns, they were centrifuged for 1 min, and the flow through was discarded. After drying the columns for 2 minutes, the columns were placed into a 1.5 mL Eppendorf tube for the collection of mRNA. 40 µL of elution solution was added directly to the spin column membrane and centrifuged at full speed for 1 min. The columns were discarded and the tubes with the mRNA were placed on ice. 2 µL of each sample were taken to quantify mRNA using the Varioskan LUX plate reader (ThermoFisher Scientific).

This protocol was adapted from an initial attempt to isolate RNA from a 24-well plate that used inserts with 6.5 mm in diameter inserts. As shown in Section 2.13. Initially, the cells were ruptured directly in the insert using the lysis buffer, and the solution was collected into RNase-free microcentrifuge tubes. No RNA was detected in the plate reader, given the surface area of the inserts it was believed that one of the factors contributing to the lack of RNA was that there were not enough cells to yield sufficient genetic material for the experiment, which is why a second attempt was tried using 6-well plates.

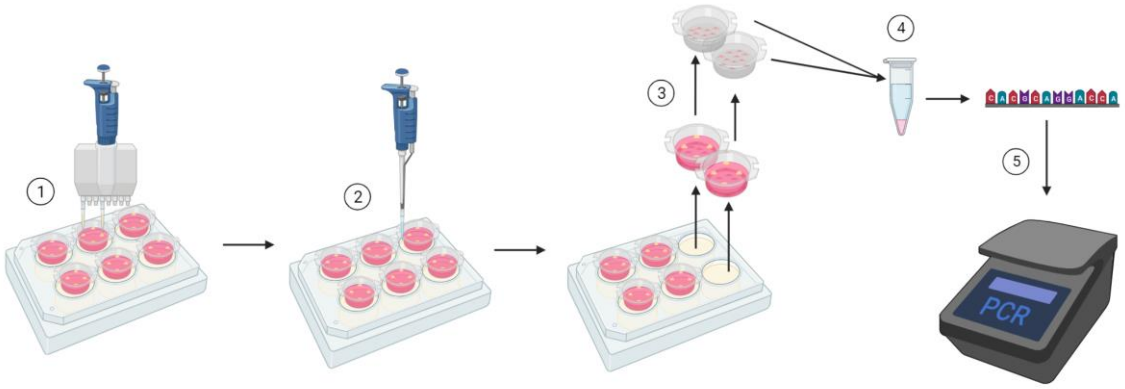

Figure 8. Insert setup for RNA isolation and nucleic acid analysis. 1) ATPS is assembled on top of alginate hydrogel and OKF6 monolayer. 2) MTX is added to the basal compartment in a 10^{-6} mg/mL concentration. 3) ATPS and alginate hydrogel is removed. 4) Genetic material is extracted from the cells and RNA is isolated and purified. 5) RNA is quantified, after this step cDNA would be synthesized, and specific genes would be amplified using a PCR.

Eleven genes were selected to test for potential effects that the bacteria could have been exerting in the cells (Appendix H). The primers were obtained from different studies that had tested them in human cell lines ideally keratinocytes or oral keratinocytes. A primer BLAST was run for each pair to assess their specificity, all the primers chosen had high specificity.

CHAPTER 3. Results

3.1. Assessment of *in vitro* Model´s Ability to Reflect Cell Death

The following graph (Figure 9) shows that at every given concentration of MTX, the cell viability percentage is affected by the drug at a greater magnitude 48 hours after the drug was administered. After 24 hours, concentrations smaller than 10^{-6} mg/mL MTX do not seem to have completely inhibited proliferation, as a small increase in cell viability can be observed. However, at this same point, a decrease in cell viability is observed for concentrations greater than 10^{-6} mg/mL MTX and this increases in magnitude as the concentration rises. At 72 hours, the cell viability reaches its lowest point for each MTX concentration and also for the MTX-free control. This could potentially mean that the decrease in cell viability after 48 hours in all treatments involving MTX is not exclusively caused by the cytotoxic effects of MTX but also by other factors present in the MTX-free control, possibly nutrient depletion. The MTX-free control was shown to have proliferated for 48 hours and it decreased considerably at 72 hours.

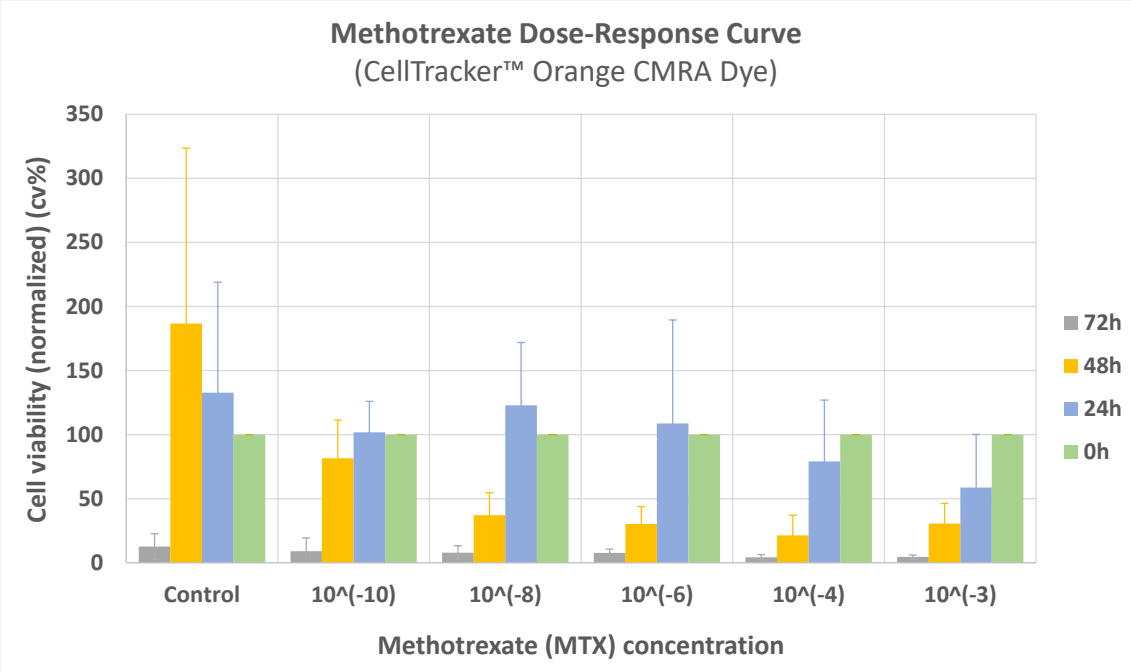

Figure 9. Dose-response curve of human immortalized oral keratinocytes (OKF6) exposed to five MTX concentrations: 10^{-10}, 10^{-8}, 10^{-6}, 10^{-4}, and 10^{-3} mg/mL of MTX. The graph is normalized assuming 100% is cell viability at time zero hours in each treatment. Error bars indicate the standard deviation of technical replicates. n=2

To test that the CellTracker™ Orange CMRA Dye was accurately reflecting cell death, the following two experiments were used to validate the reliability of data obtained

from live fluorescent imaging. The inserts were assembled in the same way as the previous experiment with the same cell density (9000 cells/insert = 50-60% confluency), the cells were stained before seeding them in the imageable insert, an alginate hydrogel was added, and on top of an ATPS containing *Pseudomonas aeruginosa* (PA CF18), a well-studied pathogen that according to the literature, has virulence factors with high probability of affecting OKF6 cell viability (Figure 10). It can be observed that the CellTracker drastically decreases fluorescence as PA CF18 proliferates, by the 48th hour, no fluorescent signal from viable cells is observed (Figure 11).

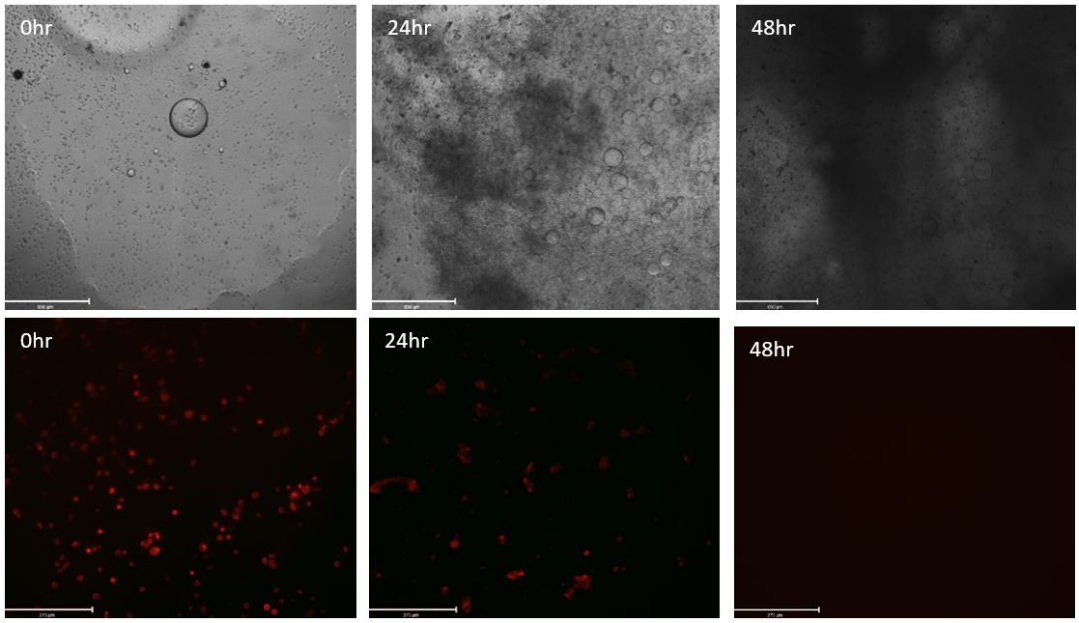

Figure 10. Effect of P. aeruginosa (PA CF18) in an aqueous two-phase system (ATPS) on oral keratinocytes (OKF6). Phase contrast images of a DEX droplet with P. aeruginosa on top of cells are shown on the first row, the second row shows fluorescent live cell images of CellTracker-stained OKF6 of the same wells exposed to P. aeruginosa. The cells were seeded below an alginate hydrogel in a 48-well plate, 150 µl of 10% PEG prepared with KSFM was added followed by 1 µl droplet of DEX prepared with LB. Shown from left to right are the three time points in which the cells were monitored, 0h, 24h, and 48h respectively.

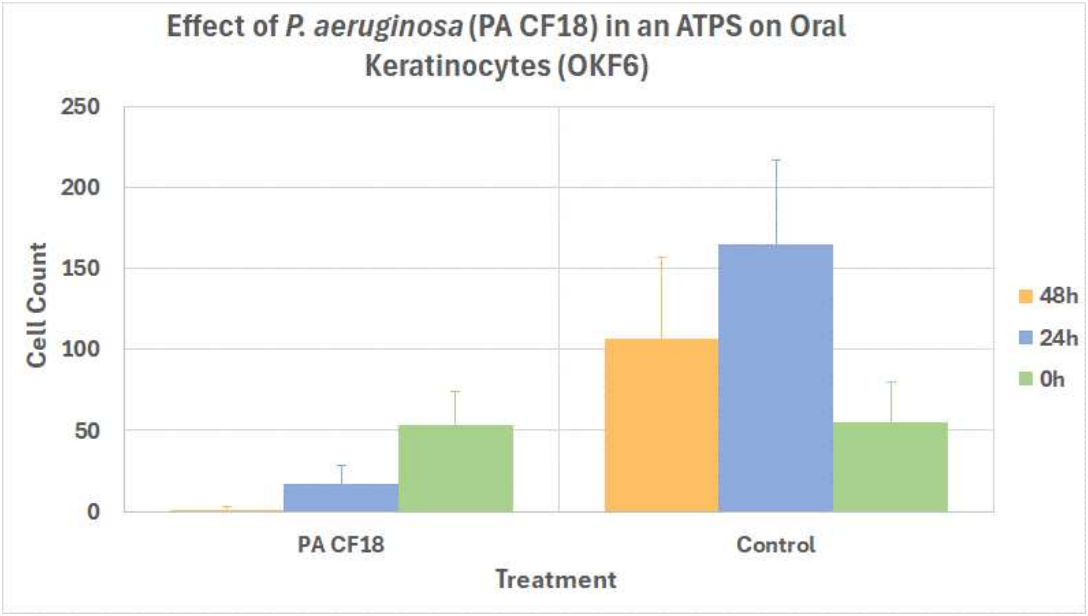

Figure 11. Effect of P. aeruginosa (PA CF18) in an aqueous two-phase system (ATPS) on oral keratinocytes (OKF6). Error bars indicate the standard deviation of technical replicates (n=2)

A second experiment was performed to validate that the cell tracker was capable of reflecting cell death through different mechanisms and over time. The OKF6 monolayer was stained and seeded. An alginate hydrogel was added on top of the cells on the apical compartment instead of an ATPS and KSFM with 5% DMSO was added. Figure 12 shows that after 90 minutes the fluorescent signal from the cells is considerable lower that the signal from the control. Correspondingly, Figure 13 shows the decrease in cell count observed after applying the DMSO, reported by the CellTracker.

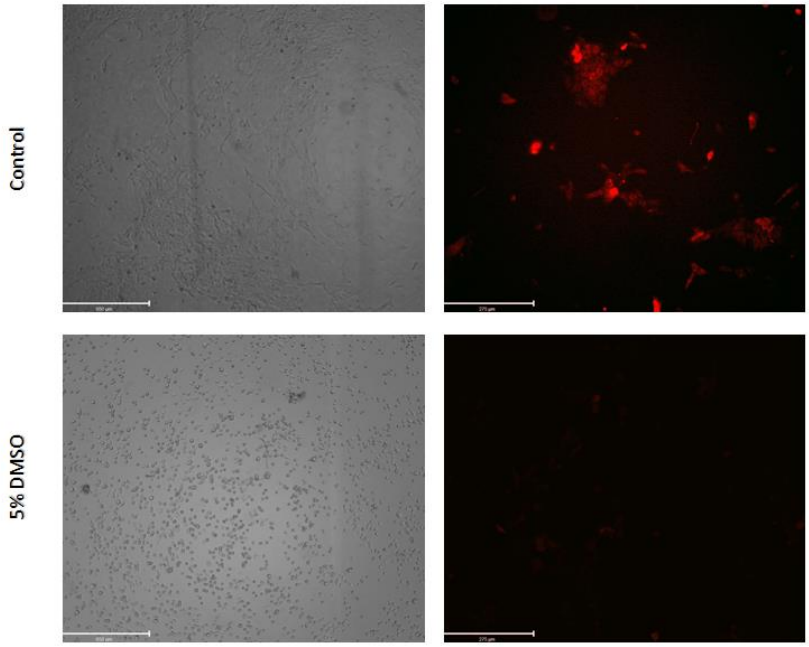

Figure 12. Effect of 5% DMSO on oral keratinocytes (OKF6) stained with stained CellTracker™ Orange CMRA below alginate hydrogel. Fluorescent live imaging (scale bar 275 µm) and phase contrast imaging (scale bar 650 µm). Cells were exposed to 5% DMSO diluted in KFSM for 90 minutes.

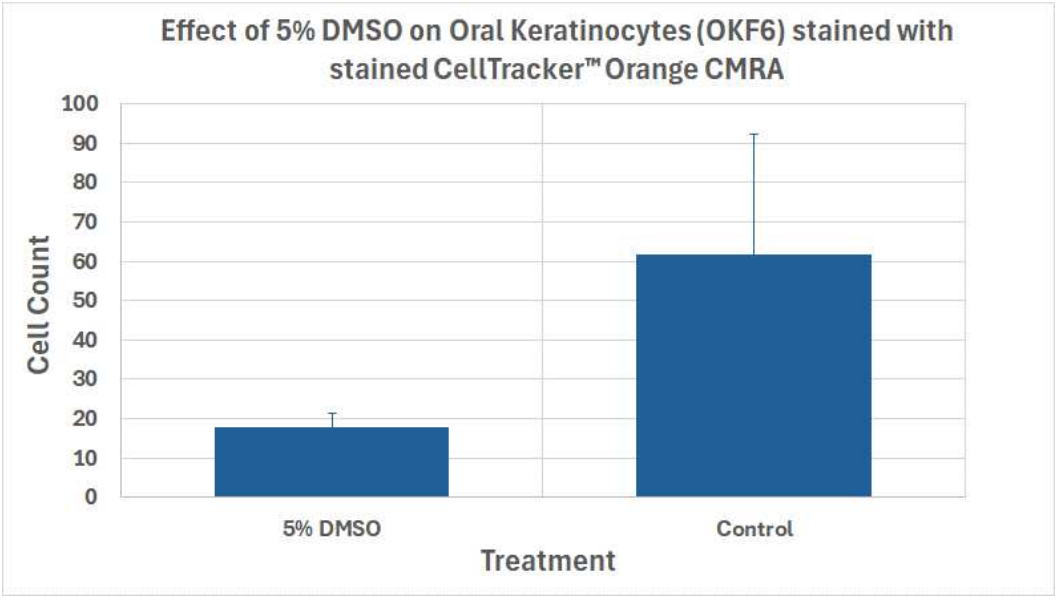

Figure 13. Effect of 5% DMSO on oral keratinocytes (OKF6) stained with stained CellTracker™ Orange CMRA below alginate hydrogel. Error bars indicate the standard deviation of technical replicates (n=2)

3.2. Selection of MTX Dosage and Characterization of CIOM-Like Damage

In order to find a chemotherapy dosage that would lead to a decrease in cell viability representative of CIOM epithelial damage, three different assays were performed after exposing a monolayer of OKF6 seeded in a 60% confluency to different

concentrations of MTX for 48h. The observed decrease in cell viability is shown in the following sections.

3.2.1. Live/Dead Assay

The first technique that was performed was a Live/Dead assay on a monolayer of OKF6 cells seeded 24h before the application of chemotherapy in a 96-well plate (Figure 14). The dilutions were prepared in KSFM media with MTX in its solution presentation. Cell viability was calculated standardizing from a healthy control with three technical replicates that reached full confluency before the treated cells. Cell adherence was found to be poor even with the most diluted concentrations. The red fluorescent signal from the ethidium homodimer-1 could not be detected. Thus, the number of dead cells was calculated through the subtraction of live cells by the total amount of cells, which were stained with Hoechst stain.

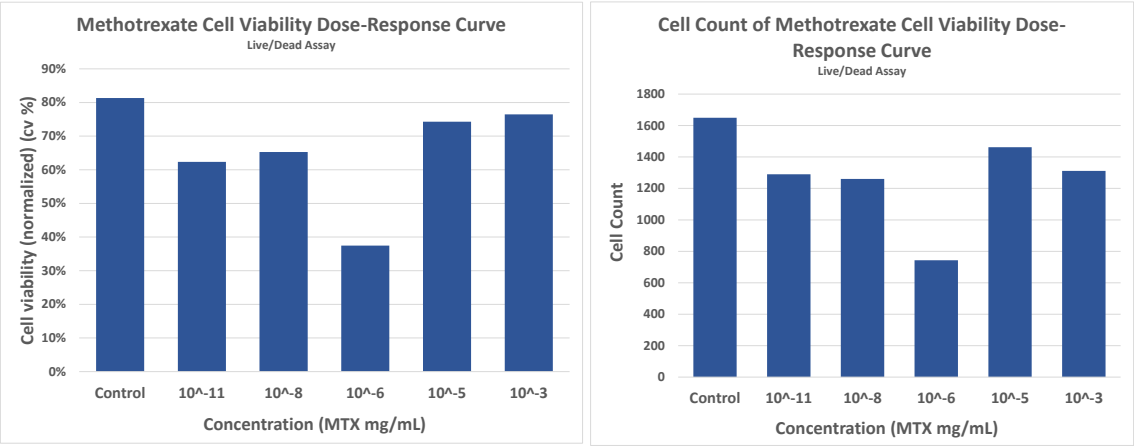

Figure 14. Dose-response curve of OKF6 cells with five different concentrations of MTX. Cell viability normalized to time zero hours (left) and cell count of same samples (right). Hoechst staining and Live/dead assay with calcein AM and ethidium homodimer-1 were performed after 48 hours of treatment application. Images captured with EVOS™ FL Auto 2 Imaging System using GFP and DAPI channels. Cells were counted from five images taken of each of the three technical replicates for each treatment. n=1

3.2.3. AlamarBlue Assay

Due to the lack of reproducibility that the Live/Dead assay demonstrated towards the goal of the experiment an Alamar Blue assay was run to validate the reliability of the experiments after 48h of exposure to MTX (Figure 15). The mean cell viability for all treatments decreased by ~15% with respect to the control.

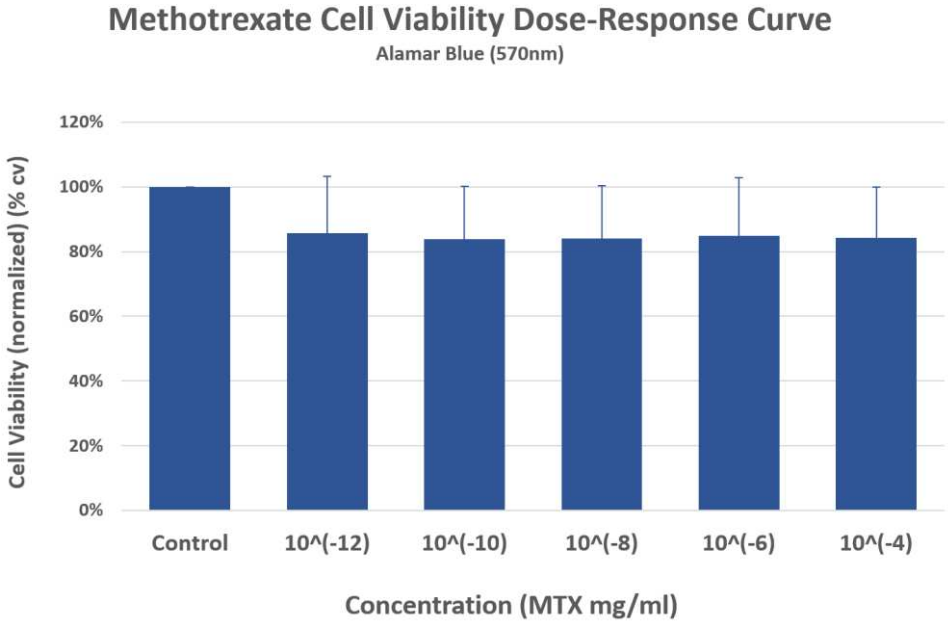

Figure 15. *Normalized dose-response curve of OKF6 cells with five different concentrations of MTX. AlamarBlue (AB) assay at 550nm was performed after 48 hours of exposure to treatments. Error bars indicate the standard deviation of technical replicates (n=2)*

3.2.2. CellTiter-Glo Assay

The following CellTiter-Glo assay shows an MTX dose-response curve made with the drug in its solution presentation from an initial concentration of 25 mg/mL. there appeared to be no difference between concentrations 10^{-8}, 10^{-6}, and 10^{-3} mg/mL nor between 10^{-10} and 10^{-4} after 48 hours of treatment exposure (Figure 16). Adding treatment in a 10^{-12} mg/mL concentration decreased the cell viability a 21.7%, while 10^{-8} and 10^{-6} mg mg/mL decreased it by 49.59% and 44.7% respectively. The lowest cell viability observed was in treatment 10^{-10} and 10^{-4} mg/mL. These two values also had the lowest variability among their replicates. Regardless of the lack of difference between treatments, which was validated by more than one assay, the chosen concentration would most likely generate approximately 50% of the cells to die, which was 10^{-8} mg/mL. Based on these results and data generated with Live/Dead and the Alamar Blue assays, the bacteria susceptibility was tested to this concentration (Figure 45, Figure 46, Figure 47, and Figure 48).

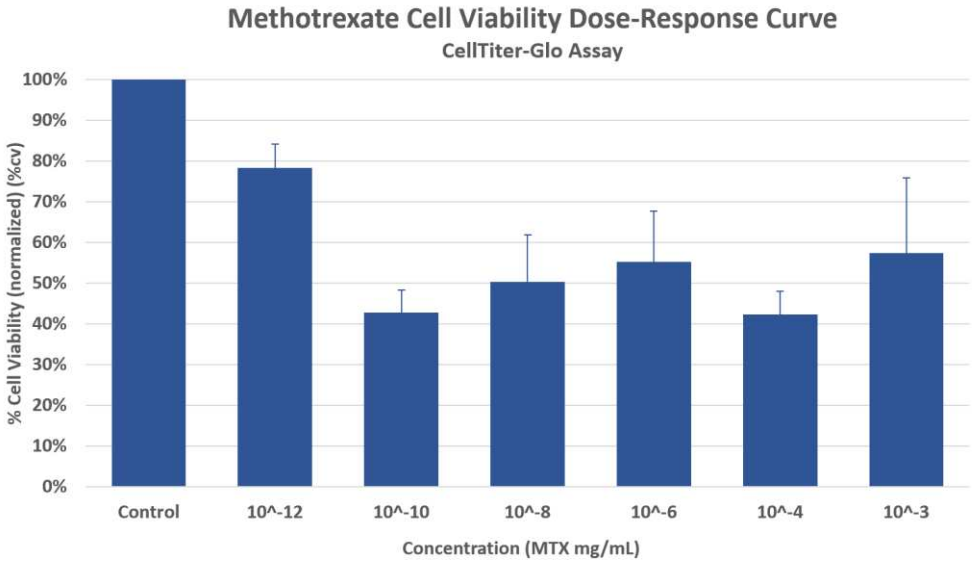

Figure 16. Normalized dose-response curve of OKF6 cells with six different concentrations of MTX. CellTiter-Glo assay was performed after 48 hours of exposure to treatments. Volumes plated were 100 µL of cells per well in a 96-well plate. An equivalent volume of CellTiter-Glo® 2.0 Reagent was dispensed into each well and luminescence was recorded 10 minutes after that. Error bars indicate the standard deviation of technical replicates (n=2) (Assay performed February 2023)

A second experiment was made seven months later to test if the effect of MTX had changed over time. As shown in the following graph (Figure 17) it was observed that even at the highest concentration tested, the cell viability did not decrease cell viability below 50%, unlike the results obtained in February. The results suggested that a 10^{-8} mg/mL concentration that had been used for past experiments was not working effectively anymore. The effect of this drug at these concentrations was expected to cause a greater growth inhibition [47]. The MTX in its solution presentation is handled in a transparent glass bottle at a 25 mg/mL concentration. It was stored at -4 °C and covered with parafilm laboratory film after every use.

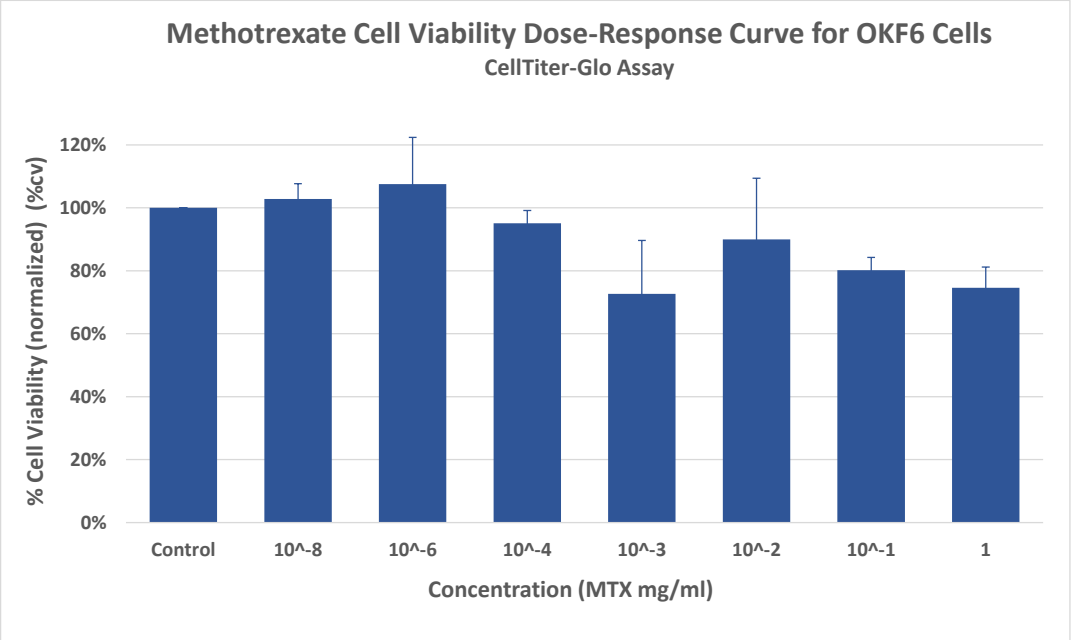

Figure 17. Normalized dose-response curves of OKF6 cells with seven different concentrations of MTX in solution presentation after 48 hours of treatment exposure. Adding treatment in a 10^{-3} mg/mL concentration decreased the cell viability a 27.35%, while 1 mg/mL decreased it by 25.4%. Error bars indicate the standard deviation of technical replicates (n=2) (Assay performed September 2023)

The data shown in Figure 18, differs from the graphs presented in previous MTX dose-response curves because the MTX dilutions were prepared from its powder presentation. The following graph shows the results of an MTX dose-response curve generated from the luminescence values from a CellTiter-Glo assay. The lowest cell viability recorded is observed after the application of 10 mg/mL of MTX. This concentration decreased it by 79.4%, while the lowest concentration tested, 10^{-8} mg/mL, decreased the cell viability by 34%. The chosen concentrations to continue working with were 10^{-6} and 10^{-1} mg/mL which decreased cell viability by 30.6% and 46.45% respectively. The final dosage between these two was chosen after assessing the effect that they exerted on the bacteria.

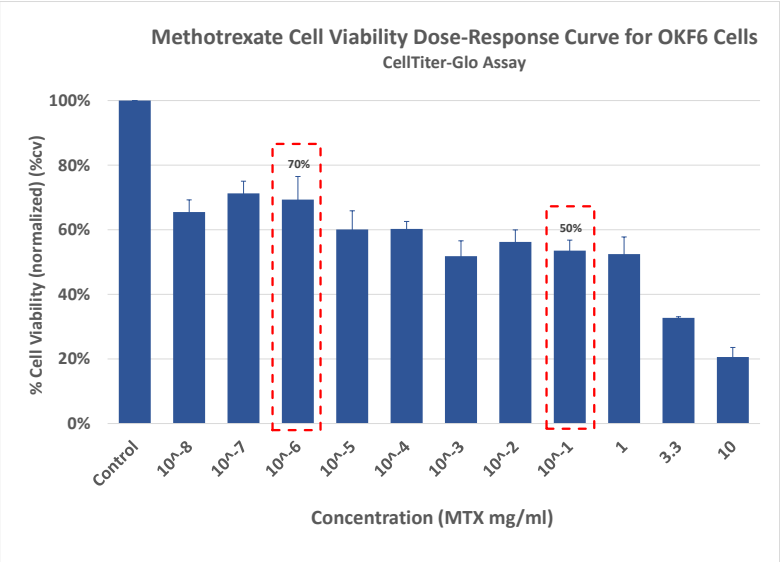

Figure 18. Normalized dose-response curve of OKF6 cells with eleven different concentrations of MTX analyzing luminescence obtained from the CellTiter-Glo assay. The cell viability assay was performed after 48 hours of exposure to treatments. Volumes plated were 100 µL of cells per well in a 96-well plate. An equivalent volume of CellTiter-Glo® 2.0 Reagent was dispensed into each well and luminescence was recorded 10 minutes after that. Error bars indicate the standard deviation of technical replicates (n=2) (Assay performed September 2023)

3.3. Characterization of Bacteria with Probiotic Potential

3.3.1. Growth curves and OD_{600} – CFU/mL equivalences for *L. brevis*

The characterization of the selected bacteria involved the establishment of the growth curve on specific conditions. Figure 19 shows the growth curve for *L. brevis*, the optical density was read approximately every 2 hours for over two days. The exponential phase finished approximately at the 35th hour, marking the beginning of the stationary phase. The exponential phase can be observed between the hour 15th and the 33rd, between

0.2 and 0.5 OD600 read at 600 nm.

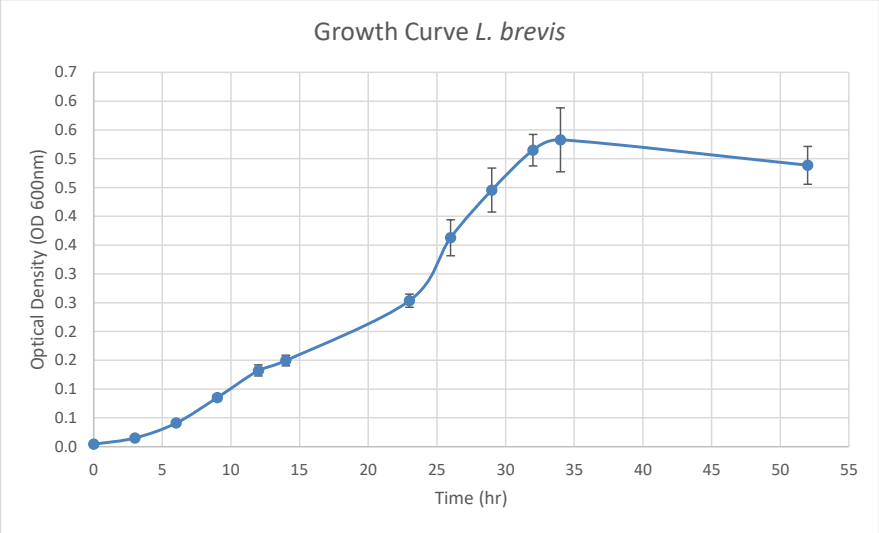

Figure 19. L. brevis growth curve. Growth conditions were established at 37°C, in constant orbital agitation at 200 rpm in MRS liquid broth. Optical density (OD) was read at 600nm in 12 time points. (n=1) Error bars indicate the standard deviation of technical replicates

The correlation graph between the optical density and the bacterial concentration in CFU/mL returned an R-squared value of 0.95 (Figure 20), suggesting that this model can accurately aid in the conversion of CFU/mL of this bacteria into OD_{600} and vice versa. A 0.6 OD_{600} corresponded to approximately 550 million CFU/mL, the highest concentration recorded, while the smallest value of the analyzed range was 98 million CFU/mL, equivalent to 0.1 OD_{600}.

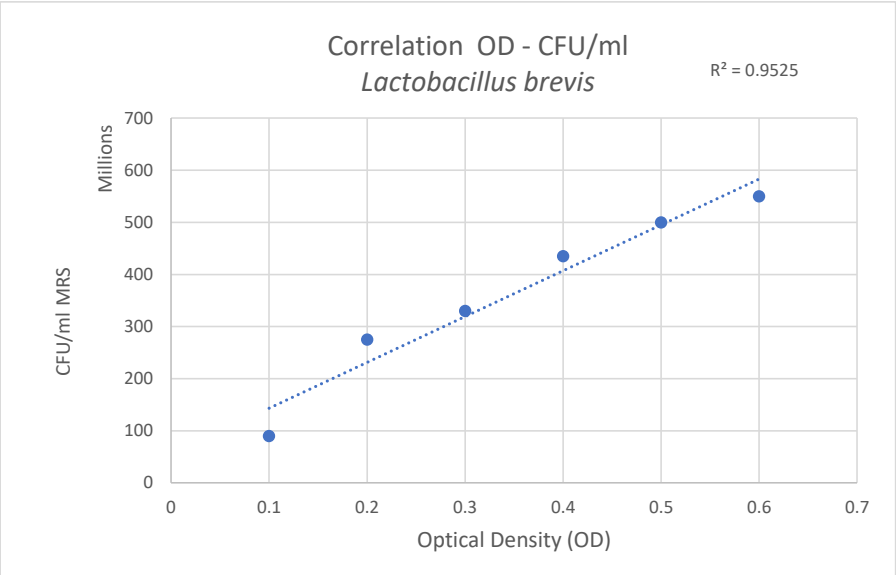

Figure 20. Correlation graph of the optical density (OD) read at 600nm and CFU/mL of L. brevis in MRS media was calculated using a spot plating method.

3.3.2. Growth curves and OD_{600} – CFU/mL equivalences for *S. salivarius*

The growth curve made for the characterization of *S. salivarius* is shown in Figure 21, the optical density was read every 2 hours until the 12-hour mark where the OD_{600} was read after 4 hours. The highest OD_{600} observed was 0.39 reached after 6h of the inoculation. After this point, the OD_{600} started dropping. At 16h an OD_{600} 0f 0.32 was recorded. Between the second hour after inoculation and hour 6, an exponential increase in OD_{600} can be observed which suggests the rage for the exponential phase.

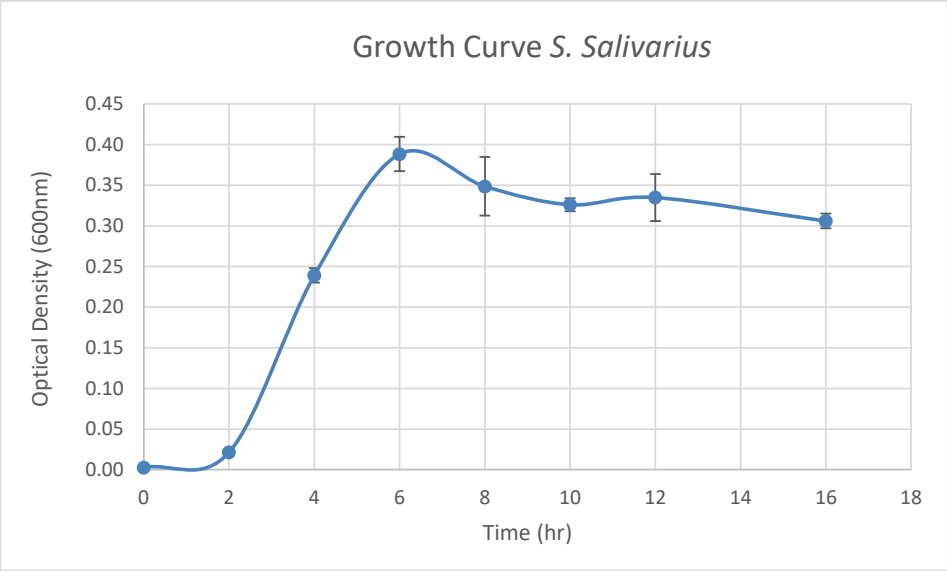

Figure 21. S. salivarius growth curve. Growth conditions were established at 37°C, constant orbital agitation of 200 rpm in BHI liquid broth. Optical density (OD_{600}) was read at 600nm every 2 hours in 6 time points. (n=1) Error bars indicate the standard deviation of the technical replicates.

The correlation graph between the optical density and the bacterial concentration of *S. salivarius* in CFU/mL returned an R-squared value of 0.94 (Figure 22), suggesting a significant correlation between the two evaluated variables. 0.5 OD_{600} corresponded to approximately 3300 million CFU/mL, the highest concentration evaluated, while the smallest value of the analyzed range was around 200 million CFU/mL, equivalent to 0.1 OD_{600}.

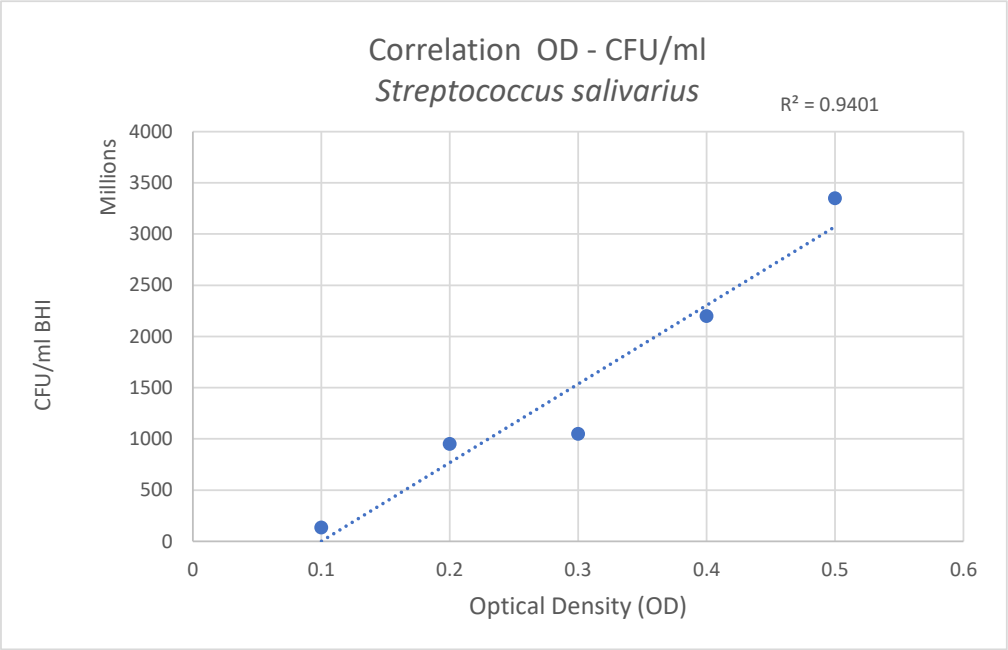

Figure 22. Correlation graph of the optical density (OD) read at 600nm and CFU/mL of S. salivarius in BHI media was calculated using spot plating method.

3.4. Assessment of Bacteria Compatibility with ATPS

3.4.1. Optimization of an ATPS for the Containment of Viable *L. brevis* for 48 Hours

The compatibility of *L. brevis* with the ATPS was first assessed by testing the adequate bacterial concentration that would allow the containment of the bacteria for 48 hours. This ATPS was prepared with both the DEX and the PEG-phases made with the broth of preference of this strain, MRS.

L. brevis remained contained within the DEX-phase of the ATPS when a 10% concentration of PEG was used for the ATPS. On the other hand, when a 5% concentration of PEG was used in conjunction with a 0.1 OD_{600} concentration, the bacteria was only contained for 48 hours. As shown in Figure 23, when the low

concentration of PEG (5%) was combined with a bacterial concentration of 0.3 and 0.5 OD_{600}, the bacteria grew into the PEG-phase, which appeared as black spots on the background of the phase contrast images. When a 10% concentration of PEG was used, the bacterial growth remained within the DEX-phase after 24 hours at the three concentrations that were tested.

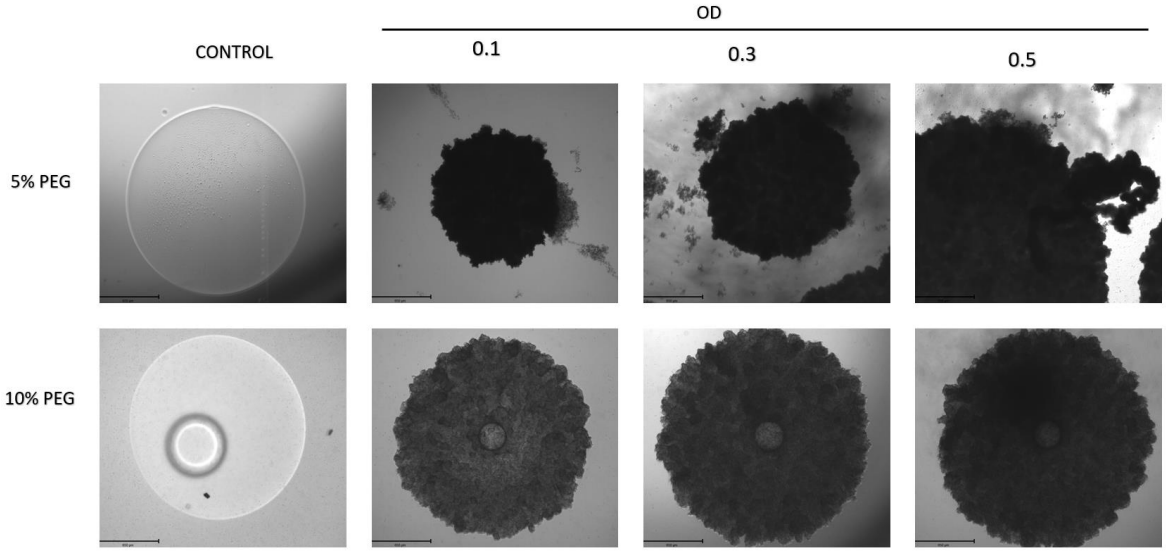

Figure 23. Phase contrast images of an aqueous two-phase system (ATPS) containing L. brevis in three different concentrations: 0.1, 0.3, and 0.5OD after 48h. The first row of images shows ATPS prepared with 5% PEG and 5% DEX and the second row with 10% PEG and 5% DEX. Both of the ATPS were prepared in MRS broth. Bacteria was incubated at 37°C with 5% CO_2 in a 48-well plate. ATPS prepared with 5% PEG shows a lack of bacterial containment beyond 48h (scale bar 650um).

The application of the ATPS on top of a cell culture requires the PEG-phase of the system to supply nutrition to mammalian cells, thus, the PEG-phase of the system requires an optimized formulation to allow this while allowing bacterial growth in the DEX-phase. *L. brevis* did not show any growth when the 10% PEG-phase was prepared with KSFM at any of the three tested bacterial concentrations: 0.1, 0.3, and 0.5 OD_{600} nor at any of the two tested PEG concentrations. As observed in Figure 24, the positive control where the PEG-phase is prepared with MRS, shows an increase in density, unlike the KSFM PEG treatment which shows no difference with the bacteria-free control.

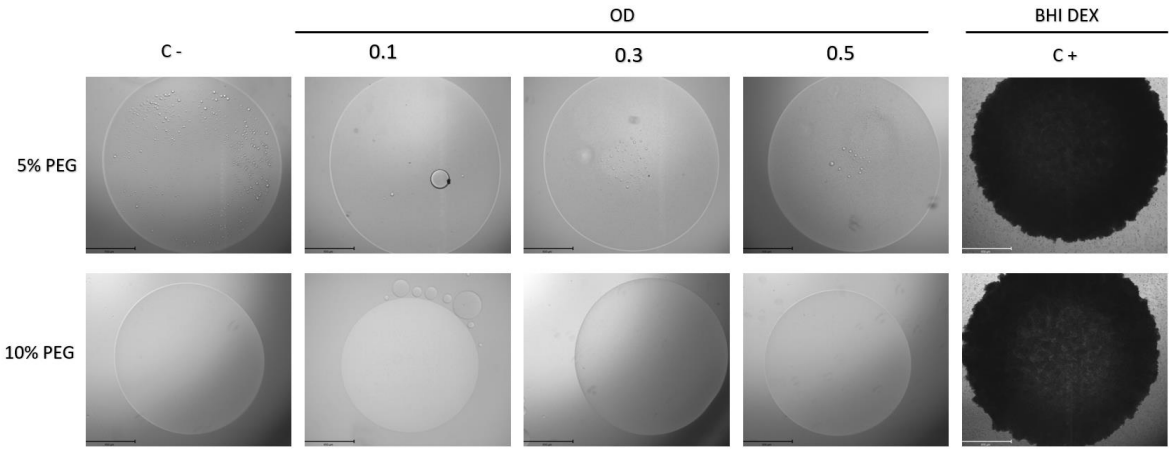

Figure 24. Phase contrast images of an aqueous two-phase system (ATPS) containing L. brevis in three different concentrations: 0.1, 0.3, and 0.5 OD_{600} after 48h. The ATPS was prepared with 5% and 10% PEG in keratinocyte serum-free media (KSFM) and positive control (C +) in MRS broth. 5% DEX droplets in MRS broth for all treatments. Bacteria was incubated at 37°C with 5% CO_2 in a 48-well plate. (scale bar 650um).

The optimized ATPS formulation prepared using 50% MRS and 50% KSFM for the PEG-phase demonstrated an increase in bacterial density contained within the droplet (Figure 25). Two different broth formulations were tested for the 5% DEX-phase, one prepared 50% MRS and 50% KSFM and the other one made entirely with MRS. No clear difference was observed between the different DEX formulations. Both of the ATPS formulations allowed bacterial growth within the DEX-phase beyond 48 hours.

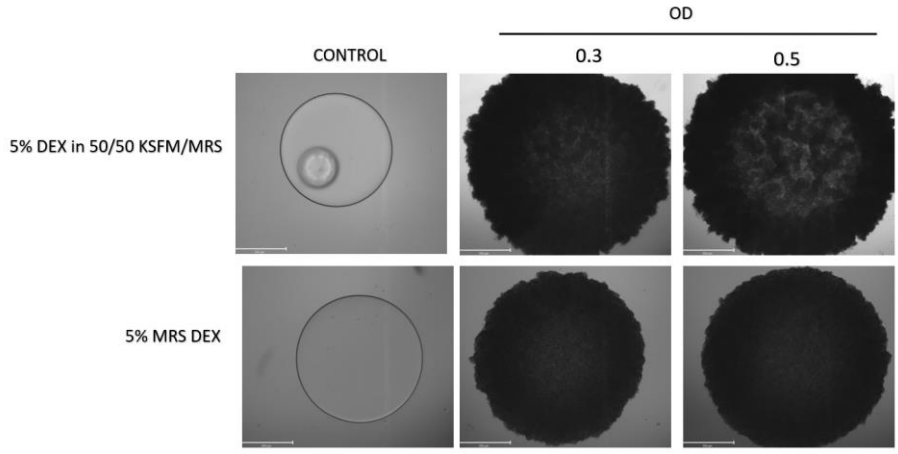

Figure 25. Phase contrast images of aqueous two-phase systems (ATPS) containing L. brevis in two different concentrations: 0.3 and 0.5OD after 24h. The first row of images shows ATPS prepared with 5% DEX in 50% MRS and 50% KSFM and the second row with 5% DEX just in MRS. Both ATPS have PEG-phase prepared in a 10% in 50/50 KSFM/MRS. Bacteria was incubated at 37°C with 5% CO_2 in a 48-well plate. (scale bar 650um).

ATPS prepared with 50% MRS and 50% KSFM, both the PEG and the DEX-phase, demonstrated a good and prolonged containment of *L. brevis* for 48 hours as shown in Figure 26. The three different concentrations that were analyzed resulted in good

containment in the three time points that were analyzed. Bacteria remained contained within the DEX droplet for 48 hours even in the highest concentration, 0.5 OD_{600}.

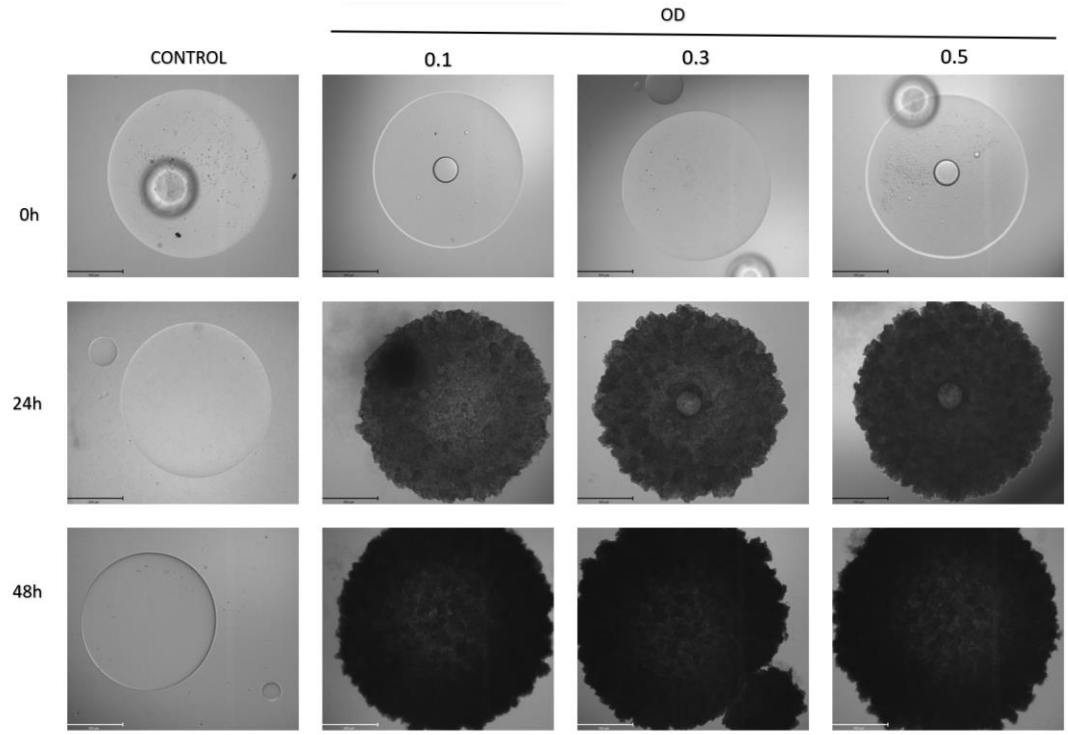

Figure 26. Phase contrast images of an aqueous two-phase system (ATPS) containing L. brevis in three different concentrations: 0.1, 0.3, and 0.5OD after 24 and 48h. ATPS prepared with 10% PEG and 5% DEX both phases were prepared in 50/50 MRS/KSFM broth. Bacteria was incubated at 37°C with 5% CO_2 in a 48-well plate. (scale bar 650um).

3.4.2. Assessment of *L. brevis* Viability After ATPS Containment for 72 Hours

The results obtained to validate the viability of *L. brevis* after 72 hours of containment in the ATPS indicated that the bacteria was still alive and capable of cell division after the indicated period. Figure 27 shows the results of the spot plating performed on two biological replicates of two assembled ATPS prepared with 50% MRS and 50% KSFM. As observed in the figure the control remained clear given the lack of bacterial growth while the two replicates show that neither the PEG nor the DEX affected the ability of the cells to proliferate. From this technique, the average concentration of the replicates gave an approximate $1.15x10^8$ CFU/mL.

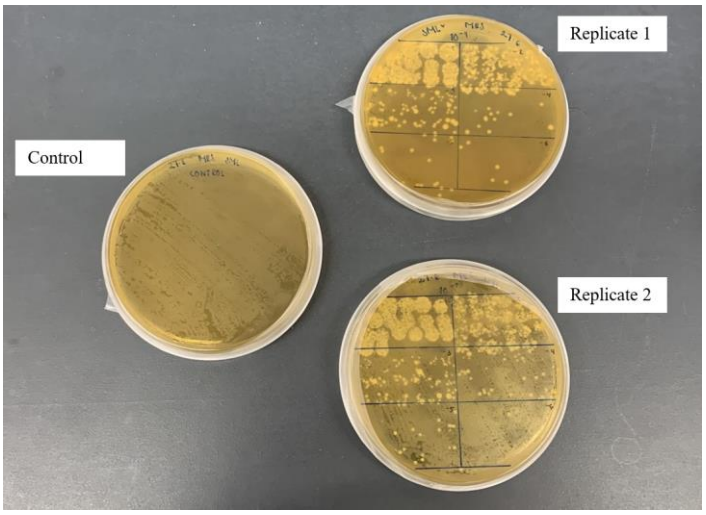

Figure 27. Spot plating in MRS agar of ATPS prepared with 10% PEG in 50/50 MRS/KSFM and 5% DEX in MRS after 72 hours of containment of L. brevis in 24-well plate inserts. A final concentration of $1.15x10^8$ CFU/mL was obtained from this technique.

3.4.3. Optimization of an ATPS for the Containment of Viable *S. salivarius* for 48 Hours

The compatibility of *S. salivarius* with the ATPS was first assessed by testing the adequate bacterial concentration that would allow the containment of the bacteria for 48 hours. This ATPS was prepared with both the DEX and PEG-phases made with the broth of preference of this strain, BHI. Figure 28 shows the containment of *S. salivarius* in four different concentrations evaluated every 24 hours. The increase in density within the droplet increases slightly between 24 and 48 hours but containment was achieved at all time points. All the concentrations of bacteria tested remained contained beyond 48 hours in an ATPS prepared with 10% PEG in BHI and 5% DEX in BHI as well.

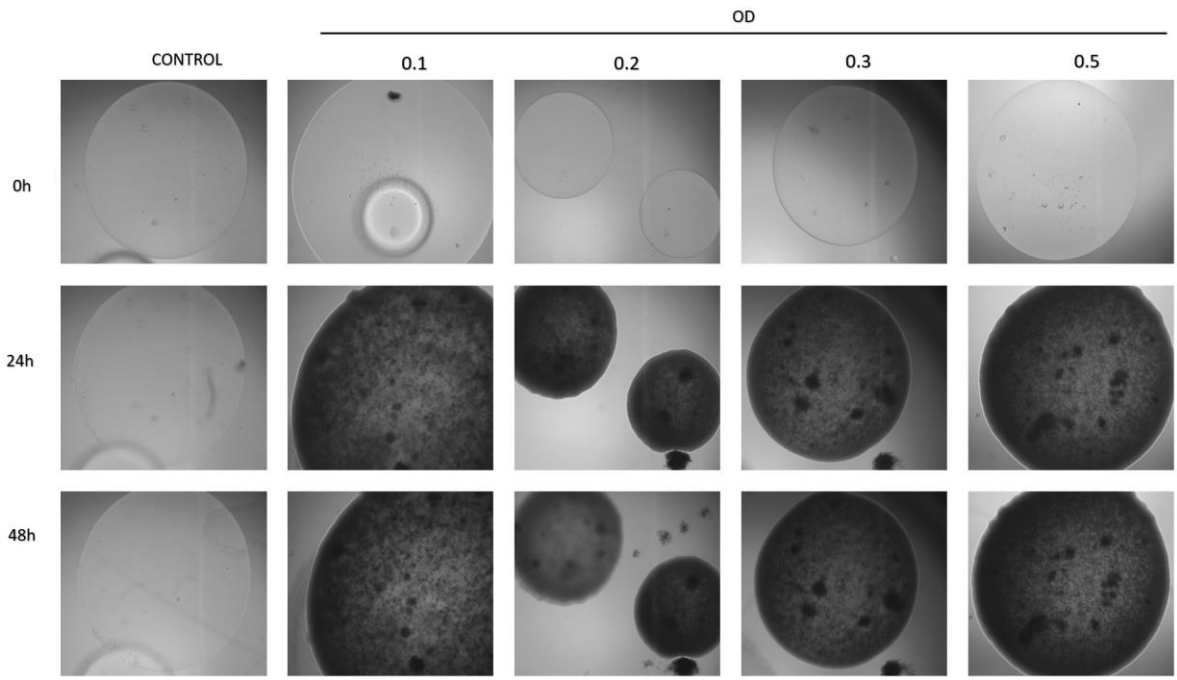

Figure 28. Phase contrast images of an aqueous two-phase system (ATPS) containing S. salivarius in four different concentrations: 0.1, 0.2, 0.3, and 0.5 OD_{600} after 24 and 48h of containment. The ATPS was prepared with 10% PEG and 5% DEX both phases prepared in BHI broth. Bacteria was incubated at 37°C with 5% CO_2 in a 48-well plate. Bacteria remained contained within the DEX droplet up to a concentration of 0.5 OD_{600} for 48h. (scale bar 650um)

S. salivarius remained contained within the DEX-phase of the ATPS when a 10% concentration of PEG was used for the ATPS. On the other hand, when a 5% concentration of PEG was used the bacteria was unable to remain contained even for 24h and using the lowest concentration tested, 0.1 OD_{600}. As shown in Figure 29, the first row of images that display the three tested bacterial concentrations show uneven borders around the DEX droplet, and bacteria growth is observed in the PEG-phase, which appears as black spots on the background of the phase contrast images. When a 10% concentration of PEG was used, the bacterial growth remained within the DEX-phase after 24 hours at the three concentrations that were tested, which allowed for testing the containment beyond 24 and 48 hours. The containment and growth resulted suitable with this same formulation, nevertheless, this ATPS formulation still was not optimized to allow mammalian cell growth in parallel to the microbial growth.

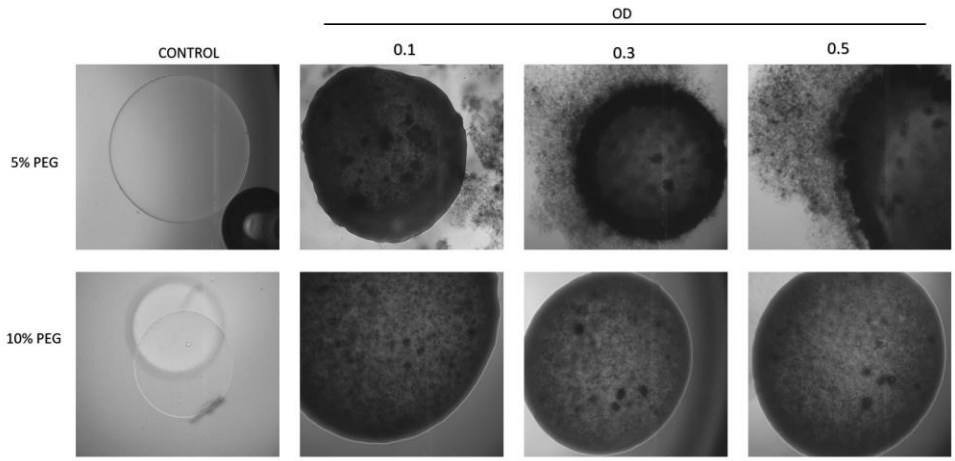

Figure 29. Phase contrast images of an aqueous two-phase system (ATPS) containing S. salivarius in three different concentrations: 0.1, 0.2, and 0.3 OD_{600} after 24 hours. The first row of images shows ATPS prepared with 5% PEG and 5% DEX and the second row with 10% PEG and 5% DEX. Both of the ATPS were prepared in BHI broth. Bacteria was incubated at 37°C with 5% CO_2 in a 48-well plate. ATPS prepared with 5% PEG shows a lack of bacterial containment beyond 48h (scale bar 650um).

As shown in Figure 30, the treatment that shows the least increase in density within the DEX droplet is the treatment that has the PEG-phase prepared with KSFM. However, bacteria remained viable, and containment was achieved, which were the two criteria established to meet this experiment. The ideal ATPS formulation must contain KSFM to feed the keratinocytes. As observed in Figure 30, an increase in density within the DEX droplet of the KSFM PEG treatment is observed from 0 to 72 hours despite being slighter than the other treatments.

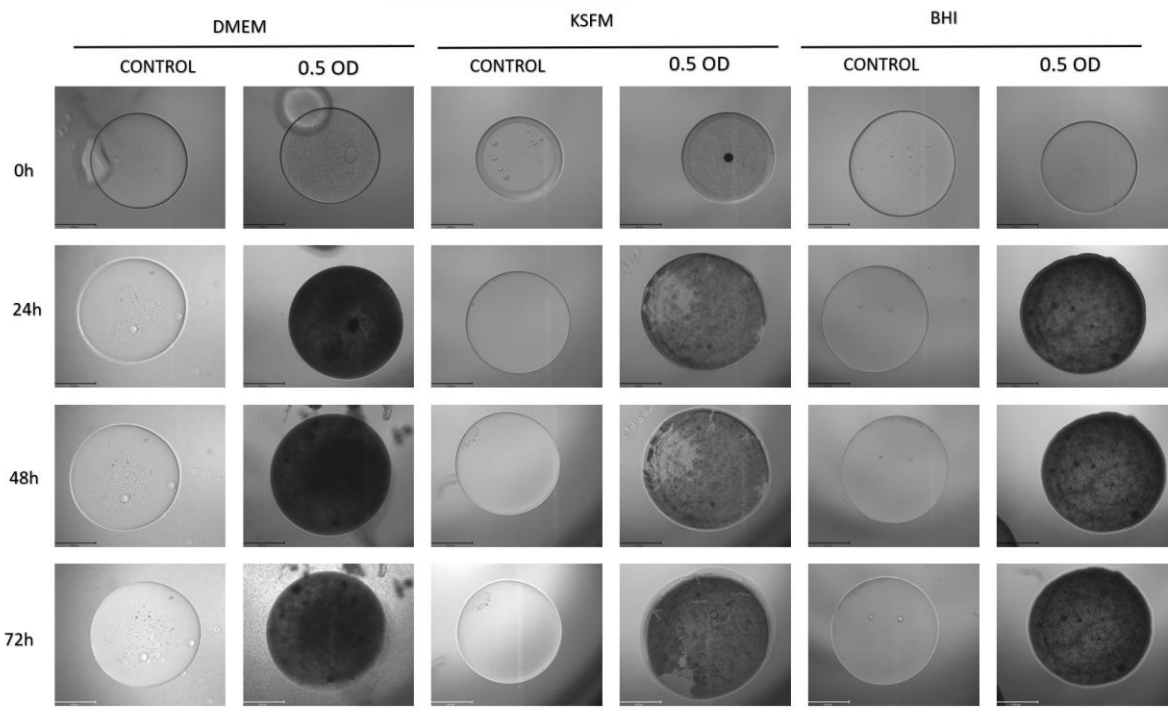

Figure 30. Phase contrast images of aqueous two-phase systems (ATPS) containing S. salivarius at a 0.5 OD_{600} concentration for 24, 48, and 72h. The first two columns of images from left to right show ATPS prepared with 10% PEG made with DMEM, then with KSFM, and then BHI broth, respectively. All DEX droplets are prepared with 5% DEX in BHI broth. Bacteria was incubated at 37°C with 5% CO_2 in a 48-well plate. ATPS prepared with 10% PEG in DMEM shows a lack of bacterial containment beyond 24h (scale bar 650um)

3.4.4. Assessment of *S. salivarius* Viability After ATPS Containment for 72 Hours

The results obtained to validate the viability of *S. salivarius* after 72 hours of containment in the ATPS indicated that the bacteria was still alive and capable of cell division after the indicated time. Figure 31 shows the results of the spot plating performed on two biological replicates of two assembled ATPS made with 10% PEG in KSFM and 5% DEX in BHI. As observed in the figure, the control remained clear given the lack of bacterial growth while the two treatments show that neither the PEG nor the DEX affected the ability of the cells to proliferate. From this technique, the average concentration of the replicates gave an approximate 700 million CFU/mL.

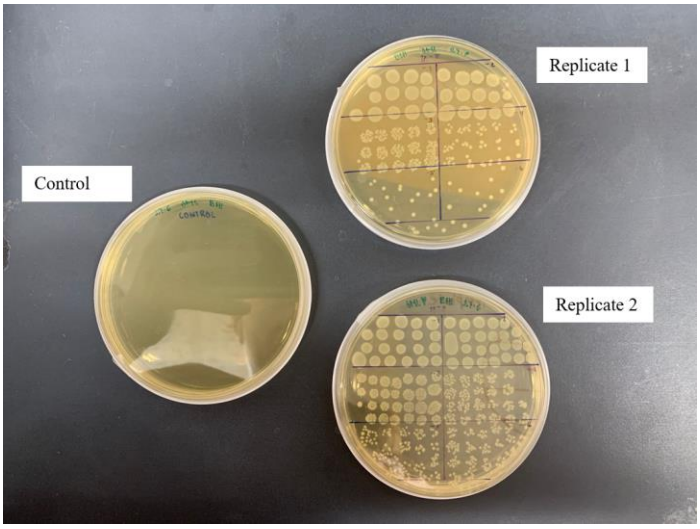

Figure 31. Spot plating in BHI agar of ATPS prepared with 10% PEG in KSFM and 5% DEX in BHI after 72 hours of containment of S. salivarius in 24-well plate inserts. A final concentration of ~700 million CFU/mL was obtained from this technique.

3.5. Evaluation of Bacteria Tolerance to Selected MTX Dosage

3.5.1. *L. brevis* exposure to MTX for 72 hours in ATPS

The effects of two different MTX concentrations in *L. brevis* are tested in Figure 32; 10^{-1}, and 10^{-6} mg/mL MTX. The figure shows eight phase contrast images showing bacteria growth or lack of it, according to the treatment or control. The first column shows the negative control (C-) without MTX or bacteria, suggesting a lack of external contamination. The second column shows the positive control (C+), showing the healthy growth over time of *L. brevis* within an ATPS. The third and fourth columns show *L. brevis* within an ATPS exposed to 10^{-1} and 10^{-6} mg/mL MTX, respectively. MTX was added to the basolateral compartment at time 0h at the same point in which the bacteria was seeded into the system. 10^{-1} mg/mL MTX seems to have inhibited bacterial growth by its resemblance in density to the control without bacteria. 10^{-6} mg/mL MTX appeared to have allowed the growth of *L. brevis* in the ATPS without any evident limitations, as compared to the MTX-free control. The effect of a third concentration of MTX was tested, 10^{-8} mg/mL of MTX. An increase in density was observed at this concentration within all the MRS DEX droplets containing *L. brevis* despite drug exposure. There are no signs of the MTX inhibiting bacterial growth in the ATPS using this MTX concentration (Figure 44).

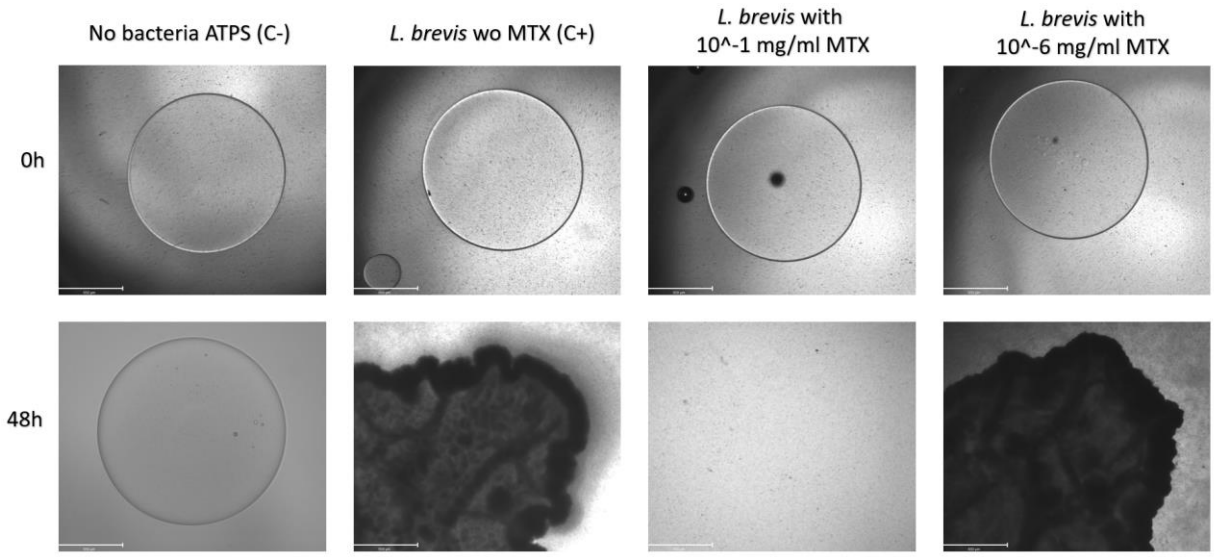

Figure 32. Phase contrast images of an aqueous two-phase system (ATPS) containing L. brevis at a 0.5 OD_{600} after 48 hours exposed to 10^{-1} and 10^{-6} mg/mL of MTX. ATPS prepared with 10% PEG on 50% MRS 50% KSFM and 5% DEX in MRS. Bacteria were incubated at 37°C with 5% CO_2 in a 24-well plate using 6.5 mm in diameter inserts (scale bar 650um).

To test the cell viability of bacteria after exposure to two different MTX concentrations, 10^{-1} and 10^{-6} mg/mL, the bacteria contained in the DEX-phase of the ATPS shown in Figure 33, were spot-plated in MRS agar dishes after 72 hours of being contained in the system and after being exposed to MTX the last 48 hours. The ATPS containing *L. brevis* that were exposed to 10^{-1} mg/mL of MTX did not show any CFU, which aligns with the low bacterial density observed with this concentration in Figure 32, these results were consistent for the three technical replicates. The concentration of 10^{-6} mg/mL MTX decreased the CFU/mL count compared to the ATPS plated without exposure to MTX (Figure 27). Nevertheless, viable bacteria cells can still be observed in the agar. A third concentration had been previously tested at 10^{-8} mg/mL MTX. It can be observed in Appendix B (Figure 45) that both technical replicates that were plated show prominent growth while the clear agar dish which contained the same ATPS without bacteria did not grow any colonies over the incubation time.

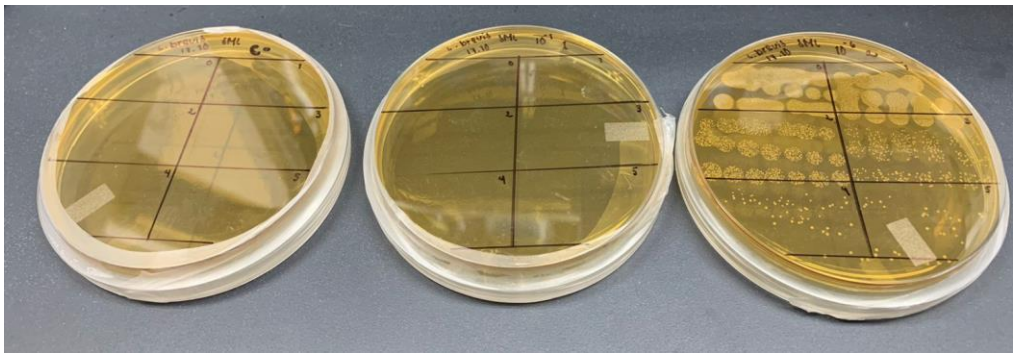

Figure 33. Spot plating of ATPS of L. brevis exposed to 10^{-1} and 10^{-6} mg/mL MTX in MRS agar dishes after 72 hours of containment. The first form left to right dish shows the negative control suggesting a lack of contamination, followed by L. brevis exposed to 10^{-1} mg/mL and then 10^{-6} mg/mL MTX. Bacteria viability is observed in the dish with bacteria exposed to 10^{-6} mg/mL MTX. No bacterial growth is observed when L. brevis is exposed to 10^{-1} mg/mL MTX.

3.5.2. *S. salivarius* exposure to MTX for 72 hours in ATPS

To assess the effect of the chosen MTX dosage in *S. salivarius* when it is contained in ATPS, a system was assembled using 10% PEG in KSFM and 5% DEX on BHI (Figure 34). *S. salivarius* was resuspended in the DEX-phase at a concentration of 0.5 OD_{600}. The following figure shows in the first column the ATPS without bacteria to prove the lack of contamination after 48 hours in the ATPS. The second column shows the DEX droplets containing *S. salivarius* without MTX to verify that the bacteria is viable without the effect of the chemotherapeutic. The third column shows a DEX droplet containing *S. salivarius* that has been exposed to 10^{-1} mg/mL of MTX. Bacteria density within the DEX is reduced compared to the positive control (C+) but higher than the negative control (C-) without any bacteria growth. The fourth column shows a DEX droplet containing *S. salivarius* that has been exposed to 10^{-6} mg/mL of MTX. Cell density approaches the one observed in the positive control (C+). The second row of photos shows the same DEX droplets as the first row but after 48 hours of starting the system. The results suggest bacterial growth is not completely inhibited by the application of MTX in the above-mentioned concentrations. Appendix C shows the effect of a third concentration, 10^{-8} mg/mL MTX, tested using MTX in solution. Bacterial growth did not appear to be inhibited by the MTX application in this concentration either (Figure 46).

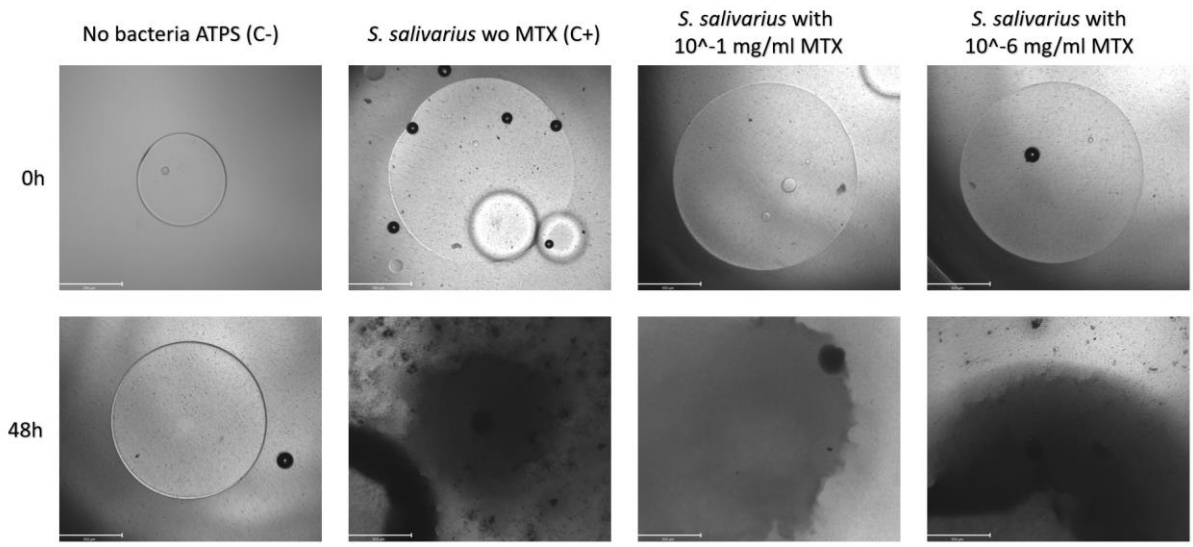

Figure 34. Phase contrast images of aqueous two-phase system (ATPS) containing S. salivarius at a 0.5 OD_{600} after 48 hours exposed to 10^{-1} and 10^{-6} mg/mL MTX. ATPS prepared with 10% PEG on KSFM and 5% DEX in BHI. Bacteria was incubated at 37°C with 5% CO_2 in a 48-well plate. (Scale bar 650 µm).

Figure 35 shows three BHI agar plates that were spot-plated from ATPS containing *S. salivarius* exposed to two different concentrations and one without any bacteria, to verify the lack of contamination. Colony forming units (CFU) are observed from both ATPS that contained bacteria despite exposure to MTX. Five ten-fold dilutions were made from the samples, between the second and third dish. A higher concentration of CFUs is observed in the lower concentration of MTX. The observed bacterial growth on the BHI agar corroborates the lack of bacterial inhibition exerted by the MTX at this concentration previously shown in Figure 34. The effect of a lower concentration of MTX is shown in Appendix D. A higher bacteria viability is observed as the concentration of MTX decreases. Nevertheless, the samples tested for this concentration were prepared using MTX in solution (Figure 47).

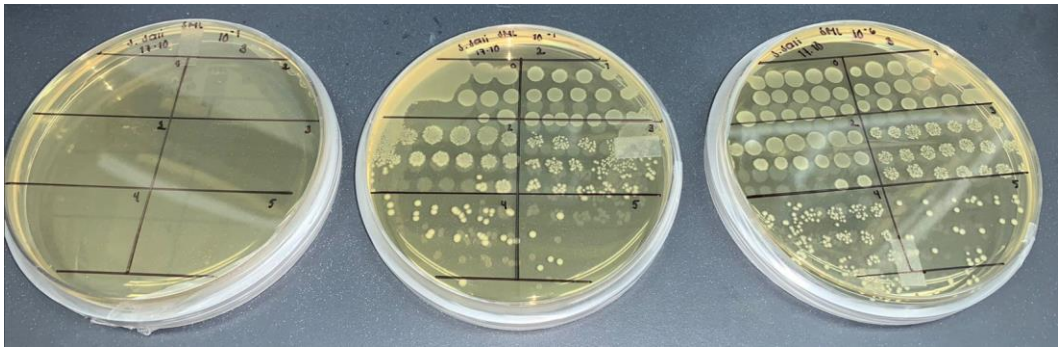

Figure 35. Spot plating of ATPS of S. salivarius exposed to 10^{-6} and 10^{-1} mg/mL MTX in BHI agar dishes. Bacteria viability is confirmed by the growth of colonies in the agar after 72 hours of MTX exposure. The

first form left to right dish shows the negative control suggesting a lack of contamination, followed by S. salivarius exposed to 10^{-1} mg/mL and then 10^{-6} mg/mL MTX.

3.5.3. *S. salivarius* and *L. brevis* Exposure to MTX for 24 Hours on Overnight Cultures

The effect of MTX on two different concentrations is shown in Figure 36. Three biological replicates with three technical replicates are shown for each treatment in the following figure. The MTX dilutions were prepared on MRS and BHI for *L. brevis* and *S. salivarius* respectively. The controls have the bacteria grown in their media of preference without MTX. The two tested MTX concentrations were 10^{-1} mg/mL and 10^{-6} mg/mL of MTX. 10^{-1} mg/mL of MTX decreased *L. brevis* cell viability by 99.67% and decreased *S. salivarius* cell viability by 53.2%. The results for 10^{-6} mg/mL suggest that this concentration reduces the cell viability of *S. salivarius* by less than 5% and decreases the cell viability of *L. brevis* by 28.7%.

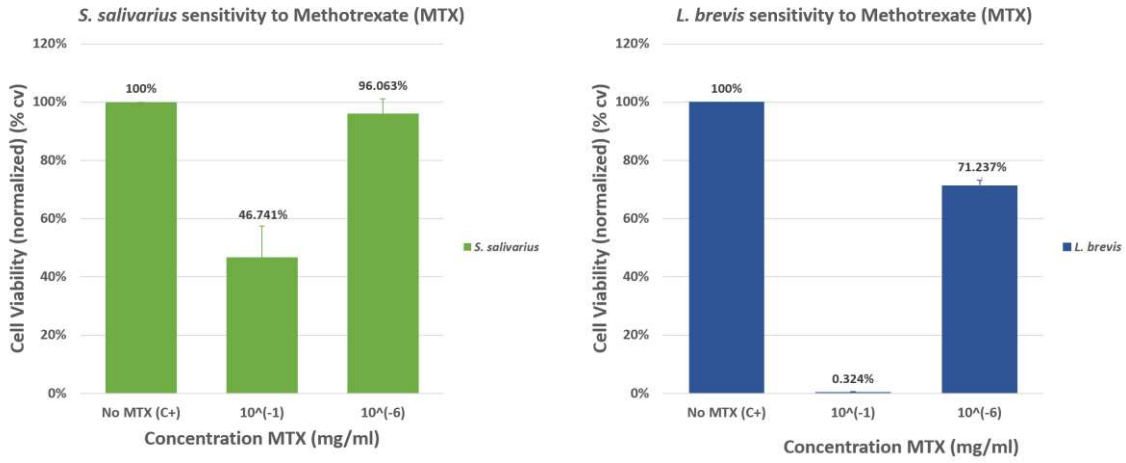

Figure 36. Effect of MTX on overnight cultures of L. brevis and S. salivarius. Three overnight cultures per treatment were left for incubation for 24h at 37°C. (n=3) Error bars indicate the standard deviation.

3.6. Assessment of Bacteria Effect on Healthy Monolayer of OKF6 Cells

The effect of *L. brevis* on a healthy monolayer of oral keratinocytes is shown in Figure 37. Live cells emit a red fluorescent signal. Viable cells are observed in the wells after 48h of exposure to *L. brevis.* The addition of bacteria to the ATPS does not seem to reduce the fluorescent signal received from the cells in contrast to the ATPS without bacteria. Two biological replicates with three technical replicates are shown for each

treatment in the following figure (Figure 38). The data suggests that *L. brevis* caused no change in cell viability when applied on top of the monolayer with respect to the ATPS without bacteria.

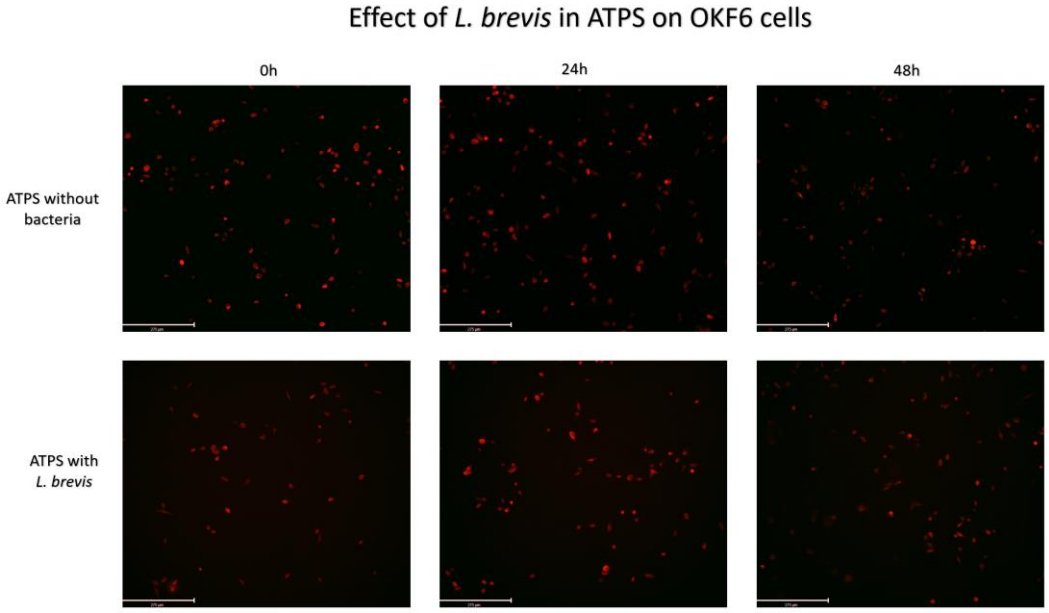

Figure 37. Effect of L. brevis on a healthy monolayer of OKF6. The keratinocytes are CellTracker-stained with CellTracker Orange CMRA, they were covered with a thin film of alginate hydrogel and had on top an ATPS prepared with 50/50 KSFM/MRS PEG and MRS DEX. assembled without bacteria (first row) and with L. brevis at a 0.5 OD_{600} concentration (scale bar 275).

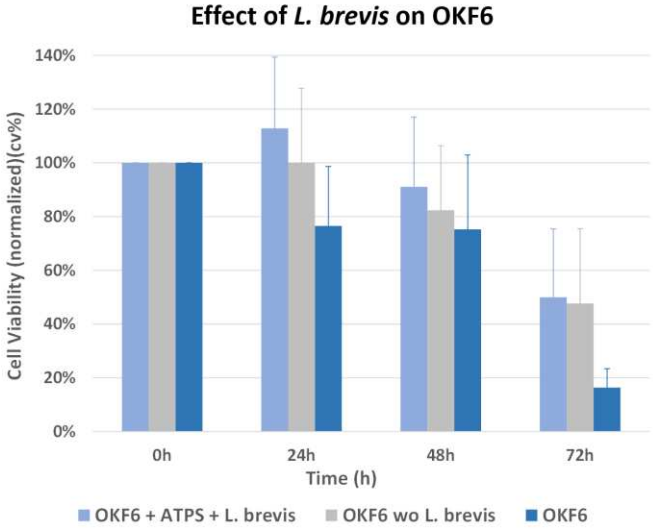

Figure 38. Normalized cell viability of oral keratinocytes exposed to L. brevis in an ATPS (light blue), exposed to the ATPS without bacteria (grey) and the cells alone (dark blue). Cell viability was obtained from the average of the cell count of five pictures taken from each of the three technical replicates at each time point. (n=2) Error bars indicate the standard deviation.

The effect of *S. salivarius* on a healthy monolayer of oral keratinocytes is shown in the following fluorescent images (Figure 39). Live cells are observed in the wells after 48h of exposure to *S. salivarius*. The presence of the bacteria in the ATPS does not seem to reduce the fluorescent signal received from the live cells in contrast to the ATPS without the bacteria. Two biological replicates with three technical replicates are shown for each treatment in Figure 40. The graph shows that the cell count of the OKF6 that were not exposed to any treatment, neither the ATPS without bacteria nor the one containing *S. salivarius,* decreased the most over time.

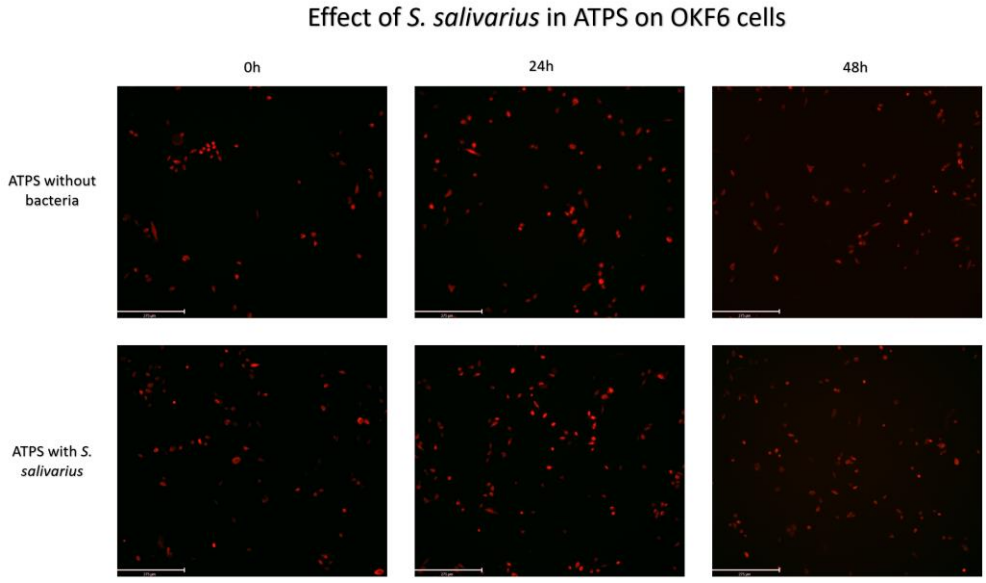

Figure 39. Effect of S. salivarius on a healthy monolayer of OKF6. The keratinocytes are CellTracker-stained with CellTracker Orange CMRA, they were covered with a thin film of alginate hydrogel and had on top an ATPS prepared with 50/50 KSFM PEG and BHI DEX. assembled without bacteria (first row) and with S. salivarius at a 0.5 OD_{600} concentration (scale bar 275). Error bars indicate the standard deviation

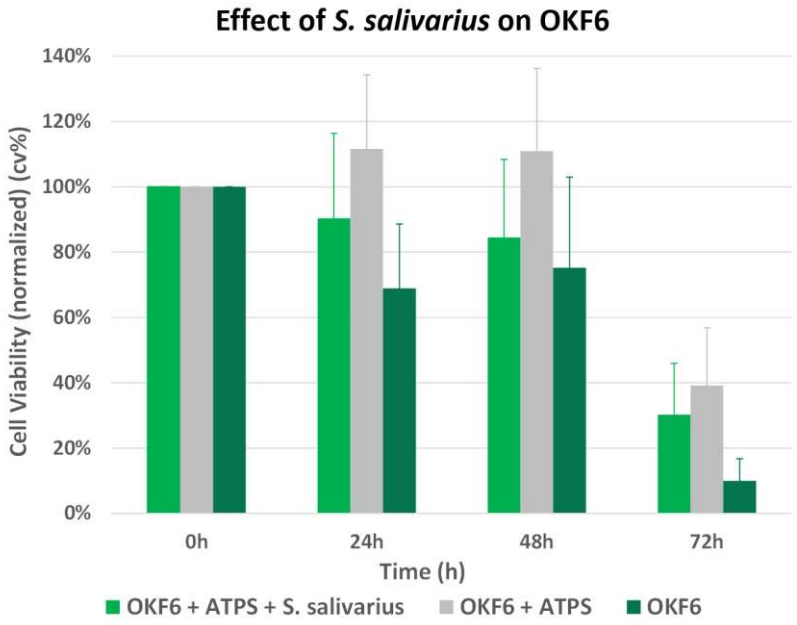

Figure 40. Normalized cell viability of oral keratinocytes exposed to S. salivarius in an ATPS (light green), exposed to the ATPS without bacteria (grey) and the cells alone (dark green). Cell viability was obtained from the average of the cell count of five pictures taken from each of the three technical replicates at each time point. (n=2) Error bars indicate the standard deviation.

3.7. Assessment of Bacteria Effect on a Monolayer of OKF6 Cells Exposed to MTX

The effect of the application of *L. brevis* and *S. salivarius* on oral keratinocytes 24 hours before exposure to MTX is shown in the following two graphs (Figure 41 and Figure 42).

The following graph shows the cell viability and the count of the oral keratinocytes when *L. brevis* was applied 24 hours before the addition of MTX. Three biological replicates with three technical replicates are shown for each treatment in the following figure. This graph shows no difference in the first 24 hours in the cell viability with and without bacteria. During this time, MTX had not been applied yet. Between the first three time points, 0, 24, and 48 hours, cell viability remains stable over time without difference when *L. brevis* is applied. At the 72-hour mark, a drop can be observed. On the other hand, a difference in cell viability is observed between hour zero and hour 48 when there are no bacteria applied in the ATPS. Nevertheless, at the 72-hour mark, there was a decrease in cell viability on the wells exposed to *L. brevis*, while the cell viability on the wells that did not have bacteria showed no change from the previous 24 hours. There is a

bigger difference in viability in the *L. brevis* treatment than in the one without bacteria when comparing the change in cell viability between the time of application of MTX (24h) and the last recorded time point (72h).

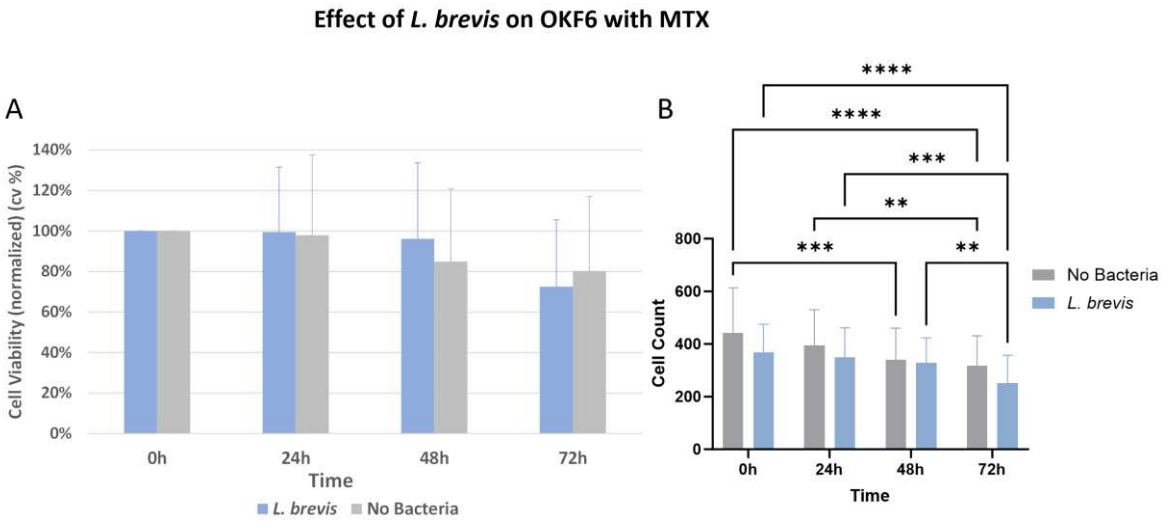

*Figure 41. Cell viability (A) and Cell count (B) of oral keratinocytes exposed to L. brevis before MTX application (blue) compared to oral keratinocytes not exposed to bacteria before MTX application (Grey). At time 0h bacteria was applied on top of OKF6 and at time 24h MTX was administered to the basal compartment of the inserts. The experiment was performed with three biological replicates and three technical replicates. Cell count was obtained from the average of five pictures taken from each technical replicate at each time point. P values were obtained using two-way ANOVA. *p < 0.05, **p < 0.01, ***p < 0.001, ****p < 0.0001 (n=3) Error bars indicate the standard deviation.*

The following graphs describe the behavior of a monolayer of OKF6 exposed to *S. salivarius* 24 hours prior to the application of MTX. Three biological replicates with three technical replicates are shown for each treatment in the following graphs. Figure 42 shows that 24 hours after the application of MTX, the cell count of the monolayer that did not contain bacteria decreased, while the cell count of the OKF6 exposed to *S. salivarius* appears to have remained stable without changes for the 24 hours following drug administration. By the 72h time point, the data suggests that the cell count of the wells with no bacteria had decreased in cell viability by 86% from the time 0h. While the cell viability decreased by 75% from the first cell count when *S. salivarius* was applied.

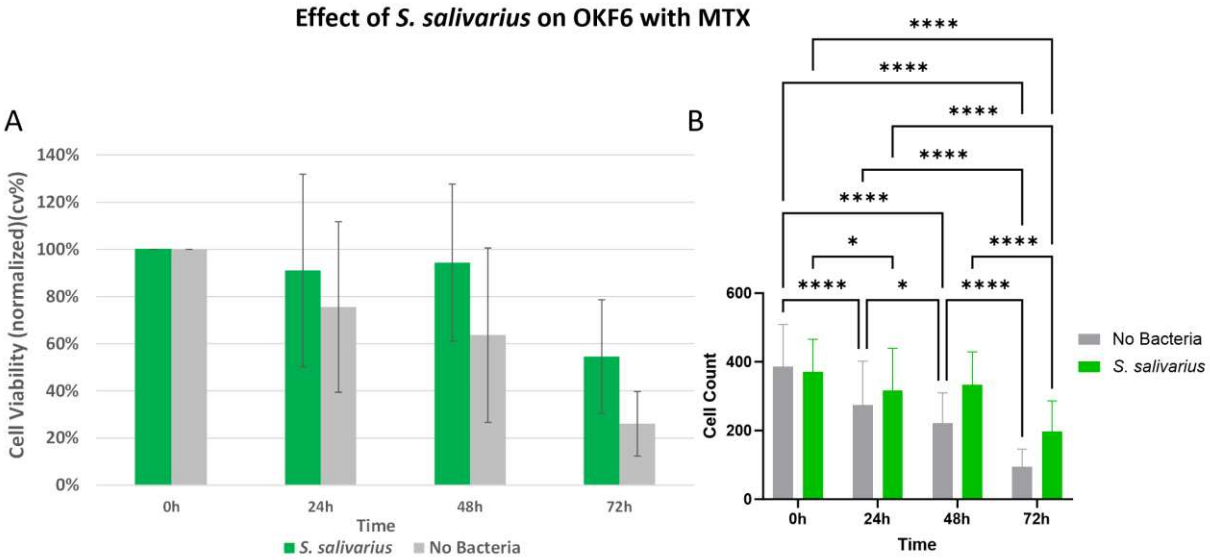

*Figure 42. Cell viability (A) and Cell count (B) of oral keratinocytes exposed to S. salivarius before MTX application (Green) compared to oral keratinocytes not exposed to bacteria before MTX application (Grey). At time 0h bacteria was applied and at time 24h MTX was administered to the basal compartment of the inserts. Three biological replicates, with 3 technical replicates. Cell count was obtained from the average of five pictures taken from each technical replicate at each time point. P values were obtained using two-way ANOVA. *p < 0.05, **p < 0.01, ***p < 0.001, ****p < 0.0001. (n=3). Error bars indicate the standard deviation.*

3.8. RNA Isolation from OKF6 Cells Exposed to Bacteria Before MTX Application

The first attempt to isolate mRNA from the OKF6 was made from the initial model, where a 24-well plate containing 12 inserts and a surface area of 0.33 cm^2. 9,000 OKF6 cells were seeded initially into each well, they were allowed to adhere for over 24 hours before starting treatment. Each treatment had six technical replicates, the cells from the six inserts were pulled together to perform the RNA isolation. The cells were stained with the CMRA CellTracker to observe if they were still attached to the membrane after the solubilization of the alginate hydrogel with EDTA. It was observed that a small number of cells remained attached but there were enough to proceed with the experiment (>200). After quantifying the RNA in the plate reader, no RNA was present in any of the tubes except for the samples from the cells treated with *S. salivarius*, which showed an RNA concentration of 1.529 x 10^{-3} mg/mL.

The second attempt involved the use of bigger inserts, the 6-well plates have a surface area of 4.67 cm^2, allowing the seeding of 146,000 cells per well. Each treatment had three technical replicates (three inserts). The cells from the three inserts, with the

same treatments, were pooled to perform the RNA isolation. This time the alginate hydrogel was not discarded after adding the EDTA. The gel with the EDTA, plus the cells and the trypsin were centrifuged and the supernatant was discarded. After the pellet was resuspended in PBS, 10 µL of the cell suspension was taken into the hemacytometer, where the presence of cells was corroborated. After quantifying the RNA in the plate reader, no RNA was present in any of the tubes except for the samples from the cells treated with *S. salivarius*, which showed an RNA concentration of 1.96 $x10^{-3}$ mg/mL.

CHAPTER 4. Discussion

4.1. Proposed *In Vitro* Model is Capable of Reflecting CIOM-Like Damage

4.1.1. CellTracker Reflects the Loss of OKF6 Cell Viability in a MTX Concentration Dependant Manner

The staining process of cells using the CellTracker™ involves incubating the cells with the fluorescent probes, which permeate through the cell membranes, these probes contain a chloromethyl or bromomethyl group that reacts with thiol groups, utilizing a glutathione S-transferase–mediated reaction. Since glutathione transferase in a ubiquitous enzyme and glutathione levels are high within the cell, the probes are transformed into cell-impermeant reaction products that can fluorescence for more than 72 hours, are well retained in living cells through several generations, and are transferred to daughter cells, but not to adjacent cells in a population [48].

To assess if the CellTracker could reflect the effect of MTX in the proposed *in vitro* model, a dose-response curve was established (Figure 9). It has been observed that MTX cytotoxicity depends on exposure time and concentration [49]. The results obtained in this experiment showed that MTX at a concentration of 10^{-10} mg/mL after 48 hours of exposure decreased cell viability by 18.3%, while a concentration of 10^{-4} mg/mL decreased it a 20.8% after only 24 hours.

The data obtained from the CellTracker dose-response curve performed in this study indicated a decrease in cell viability of 41%, 69%, and 95%, after 24, 48, and 72 hours of exposure to MTX in a 10^{-3} mg/mL MTX concentration. The effects of MTX in the monolayer were expected to be more detrimental. Compared to the literature, the effects of MTX in concentrations as high as 10^{-3} mg/mL MTX exceed the MTX plasma concentrations recorded for intermediate-dose and even high-dose MTX therapy for leukemia pediatric patients [50], [51], [52], [53]. Nevertheless, this data was obtained from studies where the dosage regimen involved prolonged exposure to MTX. The following scenarios were considered as possible explanations as to the high MTX concentration required to caused the desired decrease in cell viability in the OKF6 in this study. The first one revolves around the fact that MTX strongly inhibits proliferative keratinocytes even at low concentrations but has no cytotoxic effect on non-proliferative cells [54]. Thus, cells that the MTX had not targeted due to being non-proliferative, could have started dividing or remained untargeted and displaying the signal of the tracker. An alternative theory suggests that the drug's effectiveness may be lacking in the

keratinocytes. An *in silico* study suggested that when free MTX is at low concentrations but intracellular dihydrofolate is high, displacement of bound MTX by dihydrofolate plays an important role in reversing the toxic effects of this agent [55]. The possibility of these cells expressing high levels of dihydrofolate due to the upregulation of its gene or due to regions with increased dihydrofolate gene cannot be discarded. It has been observed in previous studies that some cell lines exhibit increased dihydrofolate reductase levels and chromosomal regions with increased DHFR genes [56]. This would suggest a mechanism for MTX resistance is present. It has also been reported in the literature, that rabbit keratinocytes can show resistance to MTX, possibly through a defective MTX transport into the cell or altered affinity of DHFR for MTX [57] [58]. Hence, the potential for cells to develop resistance to the drug must not be entirely discounted. However, some studies suggest otherwise, it has also been observed that MTX has anti-proliferative and apoptotic effects on keratinocytes [3], [59].

4.1.2. CellTracker Reflects Cell Death Caused by *P. aeruginosa* (PA CF18)

The use of *Pseudomonas aeruginosa* CF18 (PA CF18) aimed to demonstrate the ability of the system to reflect cell death from a microorganism contained in an ATPS on top of the oral keratinocytes. This to ensure if that if the tested probiotics damaged the cells, the model would not fail to show it. The CellTracker CMRA dye paired with a microscopy software is an effective tool to track and monitor proliferation of stained cells [60], it has also been used to represent different types of tumor cells and calculate the percent yield of each cell line with automated microscopy tools [61]. This was achieved as the fluorescent signal from the live cells decreased after 48h of exposure to this strain. PA CF18 was chosen given its cytotoxicity towards mammalian cells [62], [63], [64]. Nevertheless, the damage reflected by the CellTracker is believed to be caused by multiple factors. The lack of containment of this bacteria in the ATPS could have led to a decrease of nutrients available for the mammalian cells, given that the bacteria can grow in tissue culture media and its growth is fostered in the incubation conditions of the cell culture [65].

4.1.3. CellTracker Reflects Cell Death Caused by 5% DMSO

The addition of DMSO tested the ability of the CellTracker to reflect the onset of cytotoxicity. DMSO is capable of inducing cell death through apoptosis, mitochondrial impairment, or oxidative damage, due to reactive oxygen species production [66], [67].

These mechanisms - oxidative stress damage, mitochondrial impairment, and induced apoptosis - are also known effects of MTX that impact mammalian cells [68] [69] [70]. Thus, this experiment tested the ability of the CellTracker to reflect cell damage through mechanisms known to be exerted by MTX. Figure 12 shows that, after only 90 minutes of exposure to 5% DMSO, the fluorescent signal initially observed from the viable cells decreases in intensity reflecting the cell death.

4.2. *S. salivarius* and *L. brevis* are Compatible with an ATPS Suitable for OKF6 Cells

Different concentrations of bacteria were resuspended in the DEX-phase before its application in the PEG-phase of the ATPS. The purpose of adjusting the bacterial load was to assess an adequate bacterial density that would have an effect in the monolayer, but that would not spread across the whole culture, causing a depletion of nutrients to the mammalian cells in the first 48 hours. The size of the droplet had to be consistent when testing the containment for each given bacterial concentration and ATPS formulation. In droplets where the DEX volume was partitioned at the moment of assembling the ATPS into two smaller DEX droplets rather than a big one, as it happened in Figure 28, it was more likely for the bacteria to migrate into the PEG phase and break the containment. Both bacteria remained contained when added in a 0.5 $OD_{600.}$ The concentration of PEG that allowed the containment of both bacteria for 48 hours was 10% rather than 5%. Bacteria were able to escape the DEX-phase when the PEG concentration was at the lower concentration, likely due to the reduced viscosity of the polymeric solution and interfacial tension. This tension is proportional to the polymer concentration of the system; as the PEG concentration increased, the interfacial tension increased [71]. Interfacial tension occurs at the boundary of two immiscible solutions due to the imbalance of intermolecular forces [72]. Smaller droplets of DEX likely had the bacteria rupturing containment more often due to the reduced surface tension that came with having a smaller droplet and thus a smaller interfacial surface area.

An important factor to consider when optimizing an ATPS for specific microbes is the ability of the strain to hydrolyze the DEX. Although no evidence was found of *S. salivarius* or *L. brevis* secreting dextranases that could reduce the molecular weight of the DEX and thus disrupt the equilibrium of the ATPS, other species of *Lactobacillus* and *Streptococcus* have been reported to have dextranase activity [73]. In this study, the containment of these bacteria was successfully achieved and this aspect did not appear to

be a factor.

The previously mentioned concentrations of polymers used for the ATPS in this study represent an approximation of what the precise polymeric concentration is after filtration. The molecular weight cut-off (MWCO) of a membrane is defined as the molecular weight at which 90% of the macromolecular solute is rejected by the membrane [74]. A pore size between 0.1- 10 μm has an MWCO greater than 100 kDa [75], this means that the 0.22 μm diameter filter that was used in this study is not expected to have removed the 50 kDa DEX molecule nor the 35 kDa PEG molecules from the filtrate in considerable amounts. Membrane fouling is a process by which particles or solute macromolecules are deposited or adsorbed onto the membrane pores or a membrane surface by physical and chemical interactions or mechanical action, which results in smaller or blocked membrane pores [76] which could potentially explain the slow filtration process that extended proportional the volume of filtrate. Although the filtered volume did not exceed the limit of the filter, it cannot be discarded that some polymer molecules may have adsorbed to the membrane reducing their final concentration in the filtrate.

After allowing bacterial growth within some of the DEX droplets it was noticed in the phase contrast images that the center of these droplets appeared to have a lighter shading in the center compared to its surroundings (Figure 24, Figure 25). A darker color spot in a phase contrast image indicates a higher density as the light passing through the specimen is diffracted by it [77]. The lighter shading in the middle of some of the droplets compared to the borders suggests that the boundaries between the two phases of the ATPS had higher bacterial density. To this observation, a possible explanation is that the interface between the solutions is acting as a barrier retarding the diffusive transport from one phase to another, and causing the particles to get trapped in the potential-energy minimum in the interphase [78]. In this scenario, the bacteria may be attracted to this boundary or are simply able to grow with more ease around it. The principle of minimum total potential energy establishes that a structure or body shall be displaced to a position that minimizes the total potential energy [79].

The ATPS formulation was adjusted for each strain. While *S. salivarius* demonstrated an ability to grow in the ATPS when the PEG-phase was prepared with different mammalian culture media, *L. brevis* was incapable of growth when the PEG-phase was prepared with KSFM. *L. brevis* has been demonstrated to have specific iron requirements because it plays a role in the pyrimidine and purine metabolism of

lactobacilli [80]. Most bacteria can produce nucleotides *de novo*, while others, including some lactic acid bacteria, require the addition of either purines or pyrimidines to the growth medium [81]. Thus, the possibility of iron and the lack of availability of precursors in the media being a limiting factor for bacteria growth was considered. Keratinocyte SFM (KSFM) contains iron at low concentrations [82], and its availability may not have been sufficient for the model system. Another possibility that may have prevented *L. brevis* growth when the PEG-phase was made with KSFM, was the low content of dextrose and peptone in the ATPS. These two ingredients supply *L. brevis* with nitrogen, carbon, and other elements necessary for growth, which is why MRS, the preferred broth of *L. brevis,* contains high concentrations; 20 g/l of Dextrose and 10 g/l of Peptone [83].

The fact that *L. brevis* would not grow in the ATPS when the PEG-phase was made with the media that support mammalian cell growth, imposed a challenge for the co-culture of these two. Even though reducing the content of KSFM and increasing the percentage of MRS media in the PEG-phase would likely render the media not ideal for the keratinocytes, preparing the PEG with 50% MRS and 50% KSFM allowed the growth of the bacteria in the DEX-phase and did not appear to damage the OKF6.

To evaluate if the containment of the strains within the ATPS was affecting bacteria viability after 48 hours, the ATPS containing *L. brevis* and the one containing *S. salivarius* were spot-plated in MRS and BHI agar respectively. Multiple colonies of each strain were observed in each agar. Bacterial plating is one of the most common methods to assess bacteria viability and quantify if needed. The results from this experiment demonstrated that the bacterial cells inside the ATPS were alive through colony-forming unit (CFU) assessment. This method was selected because only viable bacteria are observed it excludes dead bacteria and debris [84].

4.3. Multiple Cell Viability Assays are Necessary to Assess MTX Dosage

High variability between assays has been reported in the literature when developing drug dose-response curves. Studies suggest that the mechanism of action of the drugs often influences the assay results [85]. This inherent variation between assays emphasizes the significance of using more than one assay to validate the results when screening for compounds that have antiproliferative activity [86]. The following sections discuss the results of the assays used to determine the MTX dosage for this study.

An important point concerning the availability of MTX in the culture is the fact that the apical compartment of the insert containing the ATPS is filled up mainly with PEG

in KSFM, this media does not contain MTX, thus, when the drug is administered through the basal compartment at the desired concentration, the drug is concentration is slightly reduced over time due to diffusion.

4.3.1. Live/Dead Assay

The first assay to select the adequate MTX dosage was a Live/dead assay. Parameters such as plasma membrane integrity, mitochondrial membrane potential, and intracellular esterase activity, can collectively be used to differentiate live and dead cell populations, to determine cell viability, and to screen for compound cytotoxicity [87]. These parameters form the basis for the Live/Dead cell viability assay. This technique uses two fluorescent reagents, a live cell esterase substrate, and a cell-impermeable DNA binding dye to stain live and dead cells in two different colors within a sample population. Live cells were stained with calcein acetoxymethyl (AM), while dead cells were labeled using a cell-impermeable DNA binding dye in this case Ethidium Homodimer-1. Calcein AM is a non-fluorescent esterase substrate that diffuses across unharmed cell membranes and permeates into live cells. Once inside, non-specific intracellular esterases hydrolyze the substrate into a fluorescent byproduct that stays trapped within the cell. The fluorescence signal emitted by the substrate indicates live cells with esterase activity and an intact membrane. The cell-impermeable DNA binding dye, which binds selectively and with a high affinity to DNA, can only penetrate the damaged membranes of dead cells and will fluoresce upon binding to nucleic acids. Healthy live cells with intact cell membranes, prevent the dye from entering the cell.

Because the determination of cell viability is dependent on these properties, cytotoxic events that damage the cells through different mechanisms and do not affect these parameters, cannot be accurately assessed using this assay. Cell membrane permeation, mitochondrial impairment, as well as damage to the plasma membrane, are effects that have been reported in the literature following MTX administration in diverse cell lines [88] [89] [68] [69] [70]. Thus, the Live/Dead assay was very likely to reflect the effect of this drug. It must be noted that some of these effects are observed until the late apoptotic stages of the damaged cell. This could mean that for the assay to reflect damage, prolonged exposure to the drug or a higher concentration could be required, compared to what was tested for this study. Nevertheless, the main limitation observed with this assay was the cell loss, which reduced the accuracy of the live-to-dead cells ratio, and the fact that it cannot be differentiated if the cells were lost during the treatment or if they were

never present in the area being captured.

Lack of cell adherence due to the effects of MTX has been reported in previous studies [90], [91], additionally, the required PBS washes to remove the ATPS containing the bacteria and the alginate hydrogel, may have led to a low yield of cells remaining for the assay. This might have also affected the results of other cell viability assays. In the Live/Dead assay, it was suspected that mainly dead cells were discarded in this process, as the red fluorescent signal received was low to non-existent. Nevertheless, the lack of cells does not necessarily mean that there were no dead cells or that no live cells were lost as well. This led to the conclusion that this assay may have not been ideal for the determination of the adequate MTX dosage.

During the Live/Dead assay performed in this study, the red fluorescent signal from the ethidium homodimer-1 generated a weak and almost undetectable signal. It has been reported in the literature that this compound displays a weak signal which has prompted the development of improved alternatives for this dye, such as the Ethidium homodimer III [92]. However, the fact that for some samples the dye could not be detected at all, suggests that the cell membrane of the keratinocytes may have still been intact for hours despite the damage induced by the MTX following the application of the drug.

4.3.2. AlamarBlue (AB) Assay

A second assay was tested to determine a sufficient chemotherapy dosage. The Alamar Blue (AB) assay is based on the ability of metabolically active cells to convert a redox dye, resazurin, into a fluorescent end product, resorufin [93]. This assay was selected because it is a widely studied, reproducible, and high-throughput method [94]. The graphs obtained from the MTX dose-response curve using this assay reported a consistent 15% decrease in cell viability for all concentrations tested.

Two possible scenarios were considered. It has been reported in the literature that the AB assay alone is not suitable for the evaluation of the inhibition of keratinocyte proliferation *in vitro* due to potential underestimation of damage when testing the effect of different drugs [47]. Also, cell culture media [93] and anti-oxidant drugs [95] have been reported to interfere with the AB Assay. The possibility of the drug interfering with the assay chemistry was considered. This may be a potential explanation for why the assay reported similar fluorescence after the application of different concentrations of MTX, the drug may have reduced the resazurin rather than the reductases within viable cells. The fact that the wells with the cells were washed before adding the AB reagent,

implies a modification in the original protocol that could have also led to biased results.

4.3.3. CellTiter-Glo Assay

The last assay used to determine MTX concentration was the CellTiter-Glo® Luminescent Cell Viability Assay. It relies on the measurement of intracellular ATP using firefly luciferase. The ATP detection reagent contains a detergent to lyse the cells, ATPase inhibitors to stabilize the ATP released from the ruptured cells, luciferin as a substrate, and a stable form of luciferase to catalyze the reaction that generates photons of light. When cells lose membrane integrity, they lose the ability to synthesize ATP, and endogenous ATPases rapidly break down any remaining ATP from the cytoplasm [96]. This provides the basis for the most commonly used cell viability assays. Consequently, ATP has been widely accepted as a marker of viable cells.

ATP assays are specific and sensitive techniques to measure cell viability. They have the advantage that they do not require the incubation of a population of viable cells to convert a substrate, such as resazurin, into a colored compound. The ATP assay chemistry can typically detect fewer than 10 cells per well. Its sensitivity is dependent on the reproducibility of pipetting replicate samples rather than a result of the assay chemistry [97].

The results from an initial CellTiter-Glo assay using MTX in its solution form suggested that a concentration of 10^{-8} mg/mL decreased cell viability by 49.59%, this was the concentration that approached the most to 50% cell viability. This would be the most ideal concentration to apply for 48 hours to induce CIOM-like damage and allow to study changes in cellular response caused by the presence of microbes (Figure 16).

Nevertheless, a second experiment testing the effect of MTX concentrations on OKF6 viability using the CellTiter-Glo assay was conducted six months later, the results suggested that the efficacy of the drug had decreased over time. The decrease in cell viability caused by the MTX had consistently diminished for all concentrations. The chemical stability of MTX has been found to be influenced not only by thermal and photolytic effects but also by the permeability of the container to water vapor and pH [98] [99]. The drug in solution was contained in a glass bottle at 4 °C. The lid was sealed with laboratory film after every use. However, it was observed that the yellow solution was present in the laboratory film which could suggest evaporation. Additionally, previous studies have reported that after being exposed to a UV light source, MTX was found to be significantly deteriorated, and in order to prevent photolytic degradation shielding the

drug from direct exposure to a light source was necessary [99]. The bottle containing the drug was transparent and was kept inside its box inside the fridge. No yellow precipitate was observed in the vial, which according to previous studies is a physical manifestation of MTX photolysis [98].

Given the evidence that the efficacy of the drug may have been affected, previous experiments made with the MTX in solution were repeated and the selection of the chemotherapy dosage was reassessed. For this experiment, the drug was aliquoted from a powder and the stock and working solutions were prepared on the day of the experiment. The data from this experiment (Figure 18) reflected that a concentration between 10^{-3} and 1 mg/mL would decrease the cell viability by 50%. However, this range of concentrations exceeds the MTX plasma concentrations recorded in the literature for intermediate-dose and even high-dose MTX therapy for leukemia pediatric patients [50], [51], [52], [53]. Nevertheless, this data was obtained from studies where the dosage regimen involved prolonged exposure to MTX. In these studies, treatments involved the administration of either one-tenth or one-third of the total drug dose, through rapid infusion over 30 min, and the remainder through continuous infusion over 24 hours or even 42 hours. In the present study, the culture was exposed to the drug at time zero without further infusions. A constant infusion of the drug in patients involves a constant supply of free MTX. Therefore, even if the plasma levels of MTX observed in patients are lower than the concentrations that the CellTiter-Glo assay reported that would induce a ~50% decrease in cell viability, the cell death induced in the cells is believed to be related to the free-MTX with respect to the cells that take up the drug.

Since the MTX concentrations that appeared to have induced a 50% decrease in cell viability appeared to be higher than what had been reported in the literature for MTX plasma concentrations in patients [50], [51], [52], [53] and it has also been observed that the concentration of MTX able to induce half-maximal cell viability (IC50) in immortalized human keratinocytes is 5.95 x10^{-3} mg/mL [100]. A lower concentration was also selected to be tested. A concentration that induced a decrease in cell viability by 70% and another one that reduced it by 50% were chosen, 10^{-6}, and 10^{-1} mg/mL respectively (Figure 18). Bacteria susceptibility to these concentrations was tested. These concentrations appeared to have different means from one another in the dose-response curve while still affecting cell viability in a way that the effects of the probiotics could be noticed in case there were any.

4.4. MTX Shows Antimicrobial Activity

Two MTX concentrations were added to the overnight cultures, 10^{-1}, and 10^{-6} mg/mL. 10^{-1} mg/mL of MTX decreased viability of *L. brevis* by 99.67% and decreased by 53.2% cell viability of *S. salivarius*. The results for 10^{-6} mg/mL suggested that this concentration reduced the cell viability of *S. salivarius* by less than 5% and decreased the cell viability of *L. brevis* by 28.7%.

Nevertheless, opposed findings have reported that *L. brevis* shows resistance to MTX in the concentrations of 10^{-3}, 10^{-2}, 10^{-1}, and 1 mg/mL, using the Kirby-Bauer disc diffusion test [101]. A second experiment was conducted where the bacteria were exposed to the drug in a 10^{-6} and 10^{-1} mg/mL concentration through the basal compartment of an insert, while the strains were contained in an ATPS on the apical side. The results of this experiment corroborated the susceptibility to the drug. There were no CFU after plating the ATPS exposed to 10^{-1} mg/mL MTX and reduced colonies concerning the control were observed for the 10^{-6} mg/mL treatment (Figure 33). Phase contrast images of the ATPS exposed to MTX were taken every 42 until the 72-hour mark when *L. brevis* was plated, no increase in density was observed for concentration 10^{-1} mg/mL (Figure 33). *S. salivarius* showed resistance, as an increase in density in the phase contrast pictures was observed for both concentrations (Figure 34). Additionally, there were colonies in the agar when the ATPS was plated, although they were reduced with respect to the control (Figure 35).

MTX is a folate analog that inhibits the activity of dihydrofolate reductase (DHFR), which is its major target. It catalyzes the NADPH-dependent reduction of dihydrofolate to tetrahydrofolate [102]. Reduced folates are substrates in purine, pyrimidine, and amino acid biosynthesis. Inhibition of DHFR activity initially results in reduced amino acid synthesis as well as reduced purine, and pyrimidine synthesis and thus inhibition of replication and ultimately cell death [103] [43]. DHFR is conserved across all domains of life and MTX can directly bind DHFR from multiple bacteria [104]. This could explain the shifts in gut and oral microbiota that MTX patients present [8], [9], [41], [42].

High-throughput screening studies of human gut bacterial isolates have identified multiple MTX-susceptible bacteria [104]. However, it has been shown that drug susceptibility varies across strains [104]. In this study, *S. salivarius* appeared to be less susceptible to MTX than *L. brevis*. The underlying determinants of variability in MTX susceptibility towards bacteria remain to be investigated. Additionally, they are very

likely multifactorial and may involve one or more of the following: drug influx and efflux [103], drug metabolism [105], and compensatory pathways (i.e., *de novo* synthesis of folic acid) [106].

With regards to potential bacterial resistance to MTX, resistance mechanisms to trimethoprim have been observed in bacteria, which is the MTX microbial counterpart. Thus, the possibility of S. salivarius showing resistance mechanisms to MTX cannot be discarded. The cause of the species-dependent antimicrobial activity of MTX may be due to similar mechanisms of action than the ones of trimethoprim. These comprise impaired permeability, intrinsic or acquired insensitive DHFR, compensatory increased production of target enzymes, or the expression of efflux pumps [43], [103].

4.5. Bacteria Does Not Damage Healthy Cell Culture of OKF6

Once the ability of CellTracker to reflect cell damage was evaluated, the cells were coated with a layer of alginate hydrogel and *L. brevis* and *S. salivarius* were added in an ATPS on top. The bacteria were left for a total of 48 hours and fluorescent live images of the cells underneath the DEX droplet were taken at time 0, 24, and 48 hours. The fluorescent signal was still observed after 48 hours of exposure to the bacteria and the ATPS, suggesting that the bacteria was not exerting any damage that would affect the retainment of the fluorescent probes within the cell and thus, cell viability. For some replicates it was observed that the bacteria escaped the DEX-phase and invaded the PEG-phase, nevertheless, cell signal intensity was not reduced.

The effect of *L. brevis* and *S. salivarius* was tested by analyzing the effects of each bacteria contained in an ATPS on the keratinocytes, in contrast to the effects of the ATPS without bacteria and no ATPS at all. The results showed little difference in cell viability of the OKF6 between the treatment with the ATPS with the bacteria and the ATPS without the bacteria. This suggested that the bacteria contained in the ATPS was not damaging the cells. The cell viability of the cells that were not exposed to the ATPS at all showed the most pronounced and rapid decrease in cell viability. It is hypothesized that the keratinocytes that were not exposed to an ATPS reached full confluency in the first 48 hours, unlike the other treatments which led to a more significant drop in cell viability in the last 24 hours of the experiment as reflected in the graphs (Figure 38 and Figure 39). This is likely due to nutrient depletion.

Given that it has been suggested in the literature that polyethylene glycol (PEG) may have cytotoxic effects on mammalian cells, the effect of the ATPS without the

bacteria was assessed. No decrease in cell viability was observed when the ATPS was added on top of the OKF6 in contrast to the cells without the system, nor to the cells exposed to ATPS with bacteria.

The cytotoxic effects of PEG on mammalian cells have been observed to occur in a concentration-dependent manner but are also related to the molecular weight of the molecule. Moreover, cell types also played a role in the results of PEG cytotoxicity studies. The mechanism of PEG-mediated cell death is primarily due to its ability to disrupt the cellular membrane, but it has also been suggested that the generation of reactive oxygen species (ROS) could also be a possible mechanism of cytotoxicity [107]. In healthy conditions, the intracellular level of ROS is balanced through cell antioxidant mechanisms, but it can dramatically increase under environmental stress, leading to cell apoptosis. The generation of ROS is often considered one of the most possible reasons for cytotoxicity for many biomedical materials [107]. Glutathione (GSH) is an important antioxidant in mammalian cells. It has been reported that the incubation of cells with PEG, can lead to a decline in GSH levels. Thus, the decrease in GSH could have broken intracellular redox equilibrium. This could also be thought of as one of the possible mechanisms of cytotoxicity of PEG [107].

To reduce the potential cytotoxic effect that the PEG may exert in the mammalian cells, an alginate hydrogel was added to act as a buffer between the OKF6 cells and the PEG-phase of the ATPS to enhance cell viability after prolonged exposure to the polymeric solution. The use of this hydrogel was chosen given its effectiveness in mitigating potential damage to cells from a polymeric solution. The use of this hydrogel was chosen due to its ability to mitigate damage from the ATPS. Alginate hydrogels are widely used in biomedical applications, the compatibility of this gel with the proposed model relies on its ability to allow the mobilization of small molecules throughout it [108]. Small molecules such as signaling molecules from bacteria and cells have been used to study microbes' behavior within a hydrogel-like environment [109] suggesting the bacteria used in this study would not show unwanted interactions. The effectiveness of the hydrogel was previously investigated and confirmed by another lab member, they also observed that some strains grew into the hydrogel. It has been reported in the literature that the major producers of alginate lyases are bacteria, and it has been observed that even bacteria that are not capable of using alginate as a carbon source are capable of expressing alginate lyases that catalyze the degradation of alginate [110]. Although no information was found in the literature reporting *L. brevis* or *S. salivarius* being capable

of secreting alginate lyases, the migration of the strains into the hydrogel reported by previous lab members could have been caused by the secretion of these enzymes.

4.6. Effect of *S. salivarius* and *L. brevis* on Oral Keratinocytes Exposed of MTX

4.6.1. Effect of *L. brevis* on OKF6 cells with MTX

Exposing a monolayer of oral keratinocytes to *L. brevis* prior to the application of MTX, appeared to have preserved cell viability from damage induced by the drug the first 24 hours after adding the drug to the system. During this period, no statistical difference was observed in cell count, unlike the wells that were not exposed to the bacteria. Two possible scenarios were considered: the bacteria could have exerted protective mechanisms, or the CellTracker could have been unable to accurately reflect the effect of the bacteria on the cell viability.

Given the extensive literature suggesting *L. brevis'* potential application to manage diverse health conditions [34], [35], [111], [112], [113], the possibility that the reduced MTX-mediated cytotoxicity in the presence of *L. brevis* was caused by the protective mechanisms of the bacteria, was considered. It has been reported that strains of *L. brevis*, produce high levels of arginine deiminase and sphingomyelinase. Human cells can convert arginine into nitric oxide by the actions of nitric oxide synthase. Arginine deiminase of bacterial origin competes with nitric oxide synthase, downregulating its conversion to nitric oxide, leading to the reduced secretion of inflammatory markers [26], [27], [111], [112]. Moreover, bacterial sphingomyelinase, which has also been recorded to be produced by *L. brevis*, can hydrolyze the platelet-activating factor (PAF), a strong inflammatory cytokine, that has been reported for its role in tissue injury [26], and it is known to be associated with oral mucositis during radiation therapy [27]. The secretion of arginine deiminase and sphingomyelinase by *L. brevis* could have led the OKF6 to tolerate to some extent the MTX, and thus maintain cell viability for a longer period.

Strains of *L. brevis* have also been reported to exhibit high expression of glutathione peroxidase which results in higher resistance of the cell toward oxidative damage by scavenging reactive oxygen species [114]. Given that the generation of ROS and pro-inflammatory cytokines are hallmarks of the clinical phenotype of oral mucositis [12], [115], a decrease in oxidative species or the regulation of inflammatory molecules, may have been mechanisms through which the bacteria prevented cell damage. Thus, *L.*

brevis may have exerted protective mechanisms that regulated molecular signaling pathways in OKF6 that led to a reduction in cell death after exposure to MTX.

The second scenario evaluates the possibility that the CellTracker was not able to accurately reflect the effect of the bacteria on the cell viability. The data (Figure 39) may be just showing the overall lack of effect in the cells, with high variability in the cell count and a lack of accuracy with a certain tendency to a decrease in cell viability exclusively exerted by the MTX. Still, previous experiments using *P. aeruginosa* and DMSO suggested that the CellTracker can accurately reflect cell damage, not to mention the dose-response curve generated with the CellTracker, which reflected MTX damage in a concentration-dependent manner. This helped to reduce the likelihood of this scenario, but it cannot be entirely discarded.

However, at the 72-hour mark, a decrease in cell viability was observed in cells exposed to *L. brevis*, while the cell count in the wells that did not have bacteria showed no significant change during that same period. As shown in previous findings, (Section 4.4) the growth of *L. brevis* within the DEX droplet appeared to have slowed down significantly at the 24-hour time point where MTX was administered. The results suggested that *L. brevis* has a high susceptibility to MTX. The controls of the ATPS where the bacteria were not exposed to MTX, resulted in consistent bacteria growth within the DEX-phase (Figure 49). Thus, a lack of effect exerted by *L. brevis* could be a result of the lack of bacterial growth or bacteria viability. No conflicting studies were found suggesting potential detrimental effects of *L. brevis*. Nonetheless, the possibility that the bacteria did not show a protective effect towards the keratinocytes is not disregarded.

4.6.2. Effect of *S. salivarius* on OKF6 cells with MTX

Exposing a monolayer of oral keratinocytes to *S. salivarius* 24 hours prior to the application of MTX, appeared to have maintained the cell viability without changes for the 24 hours following drug administration. While the cell count of the monolayer that did not contain bacteria showed a significant decrease. Furthermore, the data suggests that the cell viability continued to decrease significantly following the 24-hour mark when *S. salivarius* was not applied. On the other hand, cells exposed to the bacteria showed a significant drop in cell viability until after 48 hours of drug exposure. The possibility of *S. salivarius* exerting a protective mechanism towards the keratinocytes was considered. MTX-induced oxidative stress has been extensively studied in the literature in diverse cell lines [115], [116], [117] this indicates that oxidative species may be a cause of cell

damage in this study. *S. salivarius* probiotic protective effect could be related to the reduction of ROS accumulation through their free radical scavenging ability, reducing lipid peroxidation or/and its ability to chelate metal ions [118]. Lipid peroxidation arises from a series of reactions between free radicals and lipids. The products of lipid peroxidation play an important role in cellular injury, due to their ability to increase membrane permeability, and damage proteins, nucleic acids, and other biological macromolecules resulting in pathological events [119]. On the other hand, chelating agents can act against stress due to their ability to mask the effect of metal ions, such as iron ions, which are involved in oxidative processes and participate in hydroxyl radical formation [118] which has been reported to be the main cause of oxidative damage *in vivo* due to its strong reactivity and oxidizing capacity [120].

Nevertheless, both treatments, with and without *S. salivarius*, showed a decrease in cell count of similar magnitude after 72 hours. At this time point, the data suggests that the cell count of the wells with no bacteria had decreased in cell viability by 86% from the time 0h. While the cell viability decreased by 75% from the first cell count when *S. salivarius* was applied. Even though, no studies were found explaining the potentially harmful mechanisms of *S. salivarius* towards the cells, a few cases of *S. salivarius* bacteremia have been recorded [121], [122]. Additionally, information about *S. salivarius* bacteremia is uncommon. *S. salivarius* is rarely isolated from blood: only 5–15% of blood culture isolates of viridans streptococci are *S. salivarius*. The viridans group streptococci (VGS) is generally considered to be of low pathogenic potential in immunocompetent individuals. However, in certain patient populations, VGS can cause invasive diseases, such as endocarditis, intra-abdominal infection, and shock. Nevertheless, among the viridans group streptococci, *S. salivarius* showed one of the highest susceptibility to penicillin [123]. In addition, *S. salivarius* is usually considered a contaminant or an unclear cause of these infections [121]. Moreover, most viridans streptococcal infections have been associated with limited morbidity [124]. Given the existence of literature suggesting a potential association of *S. salivarius* infections, the possibility that the decrease in cell viability at 72 hours may be caused by the increase in bacteria density cannot be entirely discarded. At this time point, a considerable increase in bacteria density was observed (Figure 50) where the containment in the DEX droplet was ruptured, as shown in Appendix F.

The reason why *S. salivarius* appeared to have grown better on top of the alginate hydrogel and with the application of MTX in this experiment, remains unclear. It was

observed that the geometry of the DEX droplets had uneven borders given the irregular surface of the alginate hydrogel covering the monolayer. This could have altered the interfacial tension of the ATPS, an increased interfacial contact area of the phases enhances mass transfer [125], [125], which could have allowed easier bacterial escape from the ATPS.

4.7. Only Samples Treated with *S. salivarius* Allowed RNA Isolation

To assess shifts in molecular markers for inflammation and oxidative stress through a polymerase chain reaction (PCR), the RNA from the treated cells had to be initially isolated and quantified. No RNA was obtained for all treatments except for cells treated with *S. salivarius* prior to the application of MTX. The model needed to be adapted and limitations of the system needed to be identified. Multiple aspects could have led to the lack of genetic material.

The initial hypothesis was that given the surface area, the maximum number of cells that were seeded could not have been sufficient to extract their RNA and quantify it. During the 48 hours of exposure to MTX, it was expected that the cell count would decrease by a minimum of 30.6%, as it was reported by the CellTiter-Glo assay. Considering that the experiment had been performed in 6.5 mm in diameter inserts, where each insert had 9,000 cells initially, and the cells were pulled from six identical insert conditions, 16,500 cells would have been lost just by the exposure to MTX. Additionally, the PBS washes could have very likely detached some cells or removed the cells that had their adherence ability affected by MTX [67][68]. The stress induced by the addition of the ATPS, and the seeding process probably also caused cell death to some extent. The small amount of RNA could have also been lost in the handling steps where the labware consumable products, such as pipette tips, centrifuge tubes, and even the plate which are generally molded from polypropylene, could have non-specifically adsorb to the genetic material [126]. The possibility that the number of cells in the system overall was not enough for this experiment appeared to be the most probable explanation.

Another scenario evaluates the possibility of the RNA binding non-specifically to the membrane of the inserts when the lysis buffer was added directly into the monolayer adhered to the insert. As previously mentioned, it has been observed that some consumable products, like plastics used in labware, can bind to genetic material [126]. Nevertheless, the 6-well inserts had a polycarbonate membrane. No information could be found in the literature suggesting non-specific DNA or RNA binding to this material. This

was supported by the fact that microfluidic chips designed for DNA and RNA purification have been made out of polycarbonate [127]. Additionally, low DNA binding products are also made of polycarbonate [128]. The same was observed with the membrane of the 6.5 mm inserts which were made of polyethylene terephthalate (PET). No information could be found in the literature suggesting non-specific binding of PET to genetic material, also, microdevices for DNA purification have been designed using this material. The possibility of the digestion products filtering into the basal compartment of the insert was discarded because no media was observed below the 6.5 mm inserts and for the 6-well plates, the media from the basal compartment was collected with the rest of the cells.

The possibility that the RNA was degraded was contemplated. The RNA isolation protocol required the use of reagents that have been associated with RNA degradation. The process of removing the hydrogel could have potentially led to the activation of stress-inducible intracellular RNases and subsequent degradation of RNA in affected cells [129]. Additionally, the presence of prokaryotic RNases from *L. brevis* and *S. salivarius* could have degraded the RNA.

Protocols for RNA isolation suggest that cells grown in a monolayer may be prepared for RNA extraction by direct lysis in a cell culture vessel or trypsinized and collected as a cell pellet before lysis. Other manufacturers of RNA isolation reagents indicate performing direct cell lysis without advising for or against trypsinization. Trypsin reagents available on the market are almost exclusively derived from porcine or bovine pancreas. Studies have demonstrated the presence of contaminating RNases in the trypsin reagents [130]. Thus, RNases coming from these reagents may have led to RNA degradation. A possible solution to reduce this effect would be the use of an animal-origin-free recombinant trypsin replacement, such as TrypLE™ Express Enzyme [131].

Another important consideration is that RNases are ubiquitous. They are present in all eukaryotes and prokaryotes. The possibility of RNases contamination from *S. salivarius* or *L. brevis* should be emphasized. Although PBS washes were performed following the removal of the ATPS containing the bacteria, it cannot be confirmed that there were no residual bacteria in the remaining cell suspension. This presents a potential threat of RNA degradation even before starting the RNA extraction [130].

Nevertheless, the fact that the only treatment that yielded RNA was from the cells treated with *S. salivarius* did not entirely corroborate this scenario. The reasons remain unclear. As reflected by the results of the CellTracker (Section 4.6.2), the possibility of *S. salivarius* exerting a protective mechanism that yielded a higher number of healthy

cells available for RNA extraction is a possibility.

CHAPTER 5. Conclusions

5.1. Limitations and Future Directions

The ability of this bacteria to regulate the microbiota of the host has been observed to be one of the main probiotic mechanisms of *L. brevis*. This involves the inhibition of opportunistic pathogens and dysbiosis that could lead to the progression of CIOM [34], [132]. However, this study model has not been optimized to allow interactions between more than one microorganism. In future studies, different strains of bacteria could be contained in different DEX droplets within the ATPS and be added over the OKF6. This would allow them to determine the inhibitory mechanisms of *L. brevis,* and to determine its ability to maintain the cell viability of the OKF6. Thus, a limitation of this study is that it does not currently allow to reflect one of the most broadly studied mechanisms that have been suggested for these bacteria. However, not all bacteria are suitable to be contained in an ATPS. An important consideration when optimizing an ATPS for a strain is to evaluate the ability of the bacteria to degrade the DEX. A bacteria capable of hydrolyzing this polymer would not be able to be contained easily.

For future directions, it would be necessary to analyze the potential cytotoxicity or the inflammatory potential of the endotoxins of the DEX to assess if using another grade of DEX would be necessary for this model.

Another limitation found in this study is that the administration of MTX does not replicate the administration regimen observed in patients. The availability of free MTX over time does not reproduce a clinical setup where there is an initial prolonged infusion, and then the administration is constant but reduced the following hours. This constant supply of the drug at lower concentrations could have led to increased damage in the epithelium in contrast to one single infusion of the drug at a higher dilution, which was the arrangement for this study. Additionally, the fact that the MTX dose did not consider the volume of media in the apical compartment of the insert could have altered the concentration to which the keratinocytes were exposed.

The results obtained concerning the conserved cell viability of the OKF6 with the application of *S. salivarius* after MTX application, and the fact that the only samples that allowed RNA recovery were the ones treated with this same strain, could suggest that the bacteria prevented cell loss after MTX application, this could have allowed a higher cell yield and allowed for the recovery of the genetic material. Assessing the effects in the up or downregulation of inflammation genes as well as in genes involved in oxidative stress

in the keratinocytes of this model, are important factors to assess in future studies. A group of genes are proposed for this matter and their primers are shown in Table 1.

To achieve this, it is suggested the system be adapted to allow RNA isolation. A first step towards this could be using PET membrane inserts in the 6-well inserts rather than polycarbonate. This membrane is transparent and allows for visualization of cells with fluorescent microscopy when they are stained. This would ensure that the cells remained in the membrane after the PBS washes, which are fundamental to removing both, potential prokaryotic RNases, and the trypsin, which would degrade the genetic material. Furthermore, corroborating the presence of cells after solubilizing the hydrogel and after the first centrifugation steps using an hemacytometer, could also provide useful insights to understand in which step are the cells being lost, or if the lack of RNA is due to degradation.

For future work, another possible solution to assess molecular markers in this model would be the use of an enzyme-linked immunosorbent (ELISA) assay. This technique would take advantage of the conformation of the model where the conditioning media could be obtained from the basal compartment without having to remove the ATPS and the hydrogel. This would reduce the chances of having prokaryotic RNases or having to use trypsin. Nevertheless, the number of cells could also lead to negative results due to low analyte concentrations. Additionally, analytical interferences due to the bacterial ATPS cannot be entirely discarded. Among other things, the specificity of the assay is dependent on the composition of the sample antigen and its matrix [133]. To validate this assay in this setup the detection of interference may require the use of an alternate assay.

The established model shows potential to be adapted into a 3D model where the protective mechanisms of *L. brevis* and *S. salivarius* proposed in this study could be tested in an organotypic system. This would allow the study of bacteria's ability to avoid epithelium thinning or loss of basement membrane components caused by chemotherapy. To achieve this, an oral epithelium model could be assembled in an insert using human dermal fibroblasts and human basal keratinocytes. The addition of an engineered ATPS used in this study could be added in the apical side over the epithelium, while the MTX in the proposed concentration could be administered through the basal compartment. As shown in Appendix G, this organotypic model started being developed in parallel to the 2D model established in the presented research. It was possible to establish an organotypic culture where the cells proliferated, one on top of each other allowing multiple layers of keratinocytes to stratify towards the surface. The stratification layers

appeared to be even through the model. Furthermore, the presence of desmosomes between the cells was observed (Figure 51). This suggested that the model was successfully assembled and could be ready to test the effects of chemotherapy and bacteria.

5.2. Conclusions

The established *in vitro* co-culture model successfully demonstrated cell damage by the effects of MTX. Additionally, the compatibility of *S. salivarius* and *L. brevis* with an ATPS was tested, and a system was optimized for each one of them positively maintaining them contained and viable for 48 hours within the DEX-phase. The effects of the co-culture of these bacteria in the ATPS with a monolayer of oral keratinocytes were assessed. From the results, it was established that the bacteria did not compromise the overall health of the monolayer.

The findings presented in this study suggest that an *in vitro* model to culture oral keratinocytes while exposing them to *S. salivarius* or *L. brevis* and MTX, could be a feasible model to assess the protective mechanism of probiotics in CIOM.

The application of *S. salivarius* to a monolayer of OKF6 prior to administration of MTX appeared to have prevented a decrease in cell viability in comparison to the bacteria-free control. The possibility that this strain reduced ROS accumulation through its free radical scavenging ability or/and its ability to chelate metal ions, is contemplated as a potential explanation.

Exposing a monolayer of oral keratinocytes to *L. brevis* before the application of MTX, appeared to have prevented a decrease in cell viability induced by the chemotherapeutic agent the first 24 hours after adding the drug to the system. The possibility that *L. brevis* could have exerted a protective mechanism in the system was evaluated. The immunomodulation ability of *L. brevis* and its ability to decrease oxidative stress in mammalian cells has been widely studied in the literature. Thus, *L. brevis* may have exerted protective mechanisms that regulated molecular signaling pathways in OKF6 that led to a reduction in cell death after exposure to MTX.

Contrary to that theory, it is possible that the data may have failed to show the effect of the two bacteria. To validate the results shown in this study, the use of an alternate assay is imperative.

The susceptibility of MTX to both bacteria was tested. *L. brevis* appeared to be more susceptible to MTX than *S. salivarius.* Lactobacilli species were found to be one of

the most prevalent probiotics suggested for chemotherapy side effects [26], [27], [28]. However, most of the literature found for probiotic susceptibility to MTX focused on Streptococci species [7], [104], [134], [135]. There is a strong likelihood that this is the case because articles that have reported changes in the oral microbiota induced by chemotherapeutic agents often show species of Streptococcus of the viridans group in blood cultures. The prevalence of this species in patients undergoing chemotherapy, coupled with its tendency to cause bacteremia in cancer patients, could contribute to a more extensive literature base on the topic.

Given the susceptibility that the studied bacteria presented towards MTX in this study, it is suggested the possibility that chemotherapy patients taking probiotics, could be experiencing low to non-existent protective effects from the bacteria due to the antimicrobial effects of the drug. Consequently, before physicians suggest the use of probiotics to treat or prevent side effects of chemotherapy, they should take into consideration the susceptibility of the different probiotics to the patients' chemotherapeutic agent and the regimen that they are prescribed. However, further studies to test the susceptibility of the different probiotics are also required.

L. brevis has been extensively studied as a potential treatment to reduce mucositis in chemotherapy patients. However, the results of this study suggest that this strain has a high susceptibility to MTX. This opens up the possibility that patients who are undergoing MTX treatment and who are taking *L. brevis* to reduce the side effects of chemotherapy, may not be benefiting from the potential probiotic effects of this bacteria. This could even contribute to the lack of resolution that many clinical trials have shown in the literature [26], [136], [137], [138].

It is important to note that additional factors to the MTX and the tested probiotics in the system could also have an effect on the cell viability of the keratinocytes. Dextran is a commercially available bacterial polysaccharide. Its production at the industrial level occurs through the fermentation of a sucrose-rich medium [139]. Almost all Gram-negative bacteria produce endotoxins, which are cell wall components of bacteria with multiple biological activities [140]. They are attached to about 75% of the bacterial outer cell membrane and they are released during cultivation and cell lysis into the cell culture [141]. Given the bacterial nature of DEX, the presence of endotoxins in the DEX is dependent on the purification grade of the final product. This study used technical grade DEX, which has been reported to contain endotoxin levels greater than 0.04 pg/mL [140]. Given that endotoxin has been demonstrated to be an inflammatory stimulus for

keratinocytes [142], this must be taken into consideration when analyzing the behavior of the OKF6 in this model or when testing for molecular markers of inflammation.

Another factor that may have affected the growth of the OKF6 is the possible degradation of growth factors and supplements added to the KSFM due to the proteolytic activity of the probiotics. The proteolytic activity of *L. brevis* could have a role in this matter, as this strain is widely used in the food industry due to its ability to break down proteic precursors and generate soluble peptides, free amino acids, and other smaller molecule compounds. The purification and application of protease secreted by *L. brevis* have multiple applications in the industry [143].

This research showed limitations, some of which have prompted future directions for the project. To further study the effect of probiotics in the proposed representative model of CIOM, the MTX dosage could be adjusted, to have longer infusion periods and make the model more representative of CIOM. The chosen bacteria is known to be able to regulate dysbiosis. Future work should focus on the co-culture of different species at the same time, to study the effects in the epithelium, which is something that this system allows.

Given that the extraction of genetic material presented obstacles, a proposed solution is the use of an ELISA assay. This would allow for the sampling of the conditioning media of the cells for molecular markers from the basal compartment in this proposed model, without disrupting the ATPS. Future investigations could also aim to test the effects of probiotics on histopathological features of CIOM using an organotypic model.

References

[1] Z. Cheng, M. Li, R. Dey, and Y. Chen, 'Nanomaterials for cancer therapy: current progress and perspectives', *Journal of Hematology & Oncology*, vol. 14, no. 1, p. 85, May 2021, doi: 10.1186/s13045-021-01096-0.

[2] M. T. Amjad, A. Chidharla, and A. Kasi, 'Cancer Chemotherapy', in *StatPearls*, Treasure Island (FL): StatPearls Publishing, 2022. Accessed: Nov. 27, 2022. [Online]. Available: http://www.ncbi.nlm.nih.gov/books/NBK564367/

[3] M. F. Medellín-Luna *et al.*, 'Methotrexate reduces keratinocyte proliferation, migration and induces apoptosis in HaCaT keratinocytes in vitro and reduces wound closure in Skh1 mice in vivo', *Journal of Tissue Viability*, vol. 30, no. 1, pp. 51–58, Feb. 2021, doi: 10.1016/j.jtv.2020.10.004.

[4] V. Maksimovic *et al.*, 'Molecular mechanism of action and pharmacokinetic properties of methotrexate', *Mol Biol Rep*, vol. 47, no. 6, pp. 4699–4708, Jun. 2020, doi: 10.1007/s11033-020-05481-9.

[5] A. M. Stringer and R. M. Logan, 'The role of oral flora in the development of chemotherapy-induced oral mucositis', *Journal of Oral Pathology & Medicine*, vol. 44, no. 2, pp. 81–87, 2015, doi: 10.1111/jop.12152.

[6] E. Mutluay Yayla, N. Izgu, L. Ozdemir, S. Aslan Erdem, and M. Kartal, 'Sage tea-thyme-peppermint hydrosol oral rinse reduces chemotherapy-induced oral mucositis: A randomized controlled pilot study', *Complementary Therapies in Medicine*, vol. 27, pp. 58–64, 2016, doi: 10.1016/j.ctim.2016.05.010.

[7] K. R. V. Villafuerte, C. de J. H. Martinez, F. T. Dantas, H. H. A. Carrara, F. J. C. dos Reis, and D. B. Palioto, 'The impact of chemotherapeutic treatment on the oral microbiota of patients with cancer: a systematic review', *Oral Surgery, Oral Medicine, Oral Pathology and Oral Radiology*, vol. 125, no. 6, pp. 552–566, Jun. 2018, doi: 10.1016/j.oooo.2018.02.008.

[8] B. Vanhoecke, T. De Ryck, A. Stringer, T. Van de Wiele, and D. Keefe, 'Microbiota and their role in the pathogenesis of oral mucositis', *Oral Diseases*, vol. 21, no. 1, pp. 17–30, 2015, doi: 10.1111/odi.12224.

[9] N. Subramaniam and A. Muthukrishnan, 'Oral mucositis and microbial colonization in oral cancer patients undergoing radiotherapy and chemotherapy: A prospective analysis in a tertiary care dental hospital', *Journal of Investigative and Clinical Dentistry*, vol. 10, no. 4, p. e12454, 2019, doi: 10.1111/jicd.12454.

[10] 'Mucositis From Cancer Treatment: Care Instructions'. Accessed: Sep. 26, 2023. [Online]. Available: https://myhealth.alberta.ca:443/Health/aftercareinformation/pages/conditions.aspx?hwid=a

ck5321

[11] J. E. Raber-Durlacher, S. Elad, and A. Barasch, ‘Oral mucositis’, *Oral Oncology*, vol. 46, no. 6, pp. 452–456, Jun. 2010, doi: 10.1016/j.oraloncology.2010.03.012.

[12] S. T. Sonis, ‘The pathobiology of mucositis’, *Nat Rev Cancer*, vol. 4, no. 4, Art. no. 4, Apr. 2004, doi: 10.1038/nrc1318.

[13] S. Kuba *et al.*, ‘EFFICACY AND SAFETY OF A DEXAMETHASONE-BASED MOUTHWASH TO PREVENT CHEMOTHERAPY-INDUCED STOMATITIS IN WOMEN WITH BREAST CANCER: A MULTICENTRE, OPEN-LABEL, RANDOMISED PHASE 2 STUDY’, *Journal of Evidence-Based Dental Practice*, vol. 23, no. 3, p. 101896, Sep. 2023, doi: 10.1016/j.jebdp.2023.101896.

[14] da Silva Ferreira A R *et al.*, ‘Development of a self-limiting model of methotrexate-induced mucositis reinforces butyrate as a potential therapy’, *Scientific Reports (Nature Publisher Group)*, vol. 11, no. 1, 2021, doi: 10.1038/s41598-021-02308-w.

[15] M. A. Skeff *et al.*, ‘S-nitrosoglutathione accelerates recovery from 5-fluorouracil-induced oral mucositis’, *PloS one*, vol. 9, no. 12, pp. e113378–e113378, 2014, doi: 10.1371/journal.pone.0113378.

[16] I. N. Vergara Sasada, L. José Gregianin, and M. Cristina Munerato, ‘Oral health and stomatological complications in pediatric cancer patients’, *Oral Health Care*, vol. 1, no. 1, 2016, doi: 10.15761/OHC.1000102.

[17] M. Dwidar, B. M. Leung, T. Yaguchi, S. Takayama, and R. J. Mitchell, ‘Patterning Bacterial Communities on Epithelial Cells’, *PLoS One*, vol. 8, no. 6, p. e67165, Jun. 2013, doi: 10.1371/journal.pone.0067165.

[18] T. Sobue, M. Bertolini, A. Thompson, D. E. Peterson, P. I. Diaz, and A. Dongari-Bagtzoglou, ‘Chemotherapy-induced oral mucositis and associated infections in a novel organotypic model’, *Molecular oral microbiology*, vol. 33, no. 3, pp. 212–223, 2018, doi: 10.1111/omi.12214.

[19] E. Driehuis *et al.*, ‘Oral Mucosal Organoids as a Potential Platform for Personalized Cancer Therapy’, *Cancer Discovery*, vol. 9, no. 7, pp. 852–871, Jul. 2019, doi: 10.1158/2159-8290.CD-18-1522.

[20] E. Driehuis *et al.*, ‘Patient-derived oral mucosa organoids as an in vitro model for methotrexate induced toxicity in pediatric acute lymphoblastic leukemia’, *PLOS ONE*, vol. 15, no. 5, p. e0231588, May 2020, doi: 10.1371/journal.pone.0231588.

[21] A. Dalponte, ‘Human primary cells and immortal cell lines: differences and advantages’, PromoCell. Accessed: Jan. 04, 2024. [Online]. Available: https://promocell.com/in-the-lab/human-primary-cells-and-immortal-cell-lines/

[22] J. M. Bowen, R. J. Gibson, and D. M. K. Keefe, ‘Animal Models of Mucositis: Implications for Therapy’, *The Journal of Supportive Oncology*, vol. 9, no. 5, pp. 161–

168, Sep. 2011, doi: 10.1016/j.suponc.2011.04.009.

[23] J. Huang *et al.*, 'Experimental Chemotherapy-Induced Mucositis: A Scoping Review Guiding the Design of Suitable Preclinical Models', *International Journal of Molecular Sciences*, vol. 23, no. 23, Art. no. 23, Jan. 2022, doi: 10.3390/ijms232315434.

[24] J. Schrezenmeir and M. de Vrese, 'Probiotics, prebiotics, and synbiotics—approaching a definition', *The American Journal of Clinical Nutrition*, vol. 73, no. 2, pp. 361s–364s, Feb. 2001, doi: 10.1093/ajcn/73.2.361s.

[25] N. Gupta, J. Ferreira, C. H. L. Hong, and K. S. Tan, 'Lactobacillus reuteri DSM 17938 and ATCC PTA 5289 ameliorates chemotherapy-induced oral mucositis', *Sci Rep*, vol. 10, no. 1, Art. no. 1, Oct. 2020, doi: 10.1038/s41598-020-73292-w.

[26] A. Sharma *et al.*, 'Lactobacillus brevis CD2 lozenges prevent oral mucositis in patients undergoing high dose chemotherapy followed by haematopoietic stem cell transplantation', *ESMO Open*, vol. 1, no. 6, p. e000138, Feb. 2017, doi: 10.1136/esmoopen-2016-000138.

[27] A. Sharma, G. K. Rath, S. P. Chaudhary, A. Thakar, B. K. Mohanti, and S. Bahadur, 'Lactobacillus brevis CD2 lozenges reduce radiation- and chemotherapy-induced mucositis in patients with head and neck cancer: a randomized double-blind placebo-controlled study', *Eur J Cancer*, vol. 48, no. 6, pp. 875–881, Apr. 2012, doi: 10.1016/j.ejca.2011.06.010.

[28] V. DE Sanctis *et al.*, 'Lactobacillus brevis CD2 for Prevention of Oral Mucositis in Patients With Head and Neck Tumors: A Multicentric Randomized Study', *Anticancer research*, vol. 39, no. 4, pp. 1935–1942, 2019, doi: 10.21873/anticanres.13303.

[29] A. Ingendoh-Tsakmakidis, J. Eberhard, C. S. Falk, M. Stiesch, and A. Winkel, 'In Vitro Effects of Streptococcus oralis Biofilm on Peri-Implant Soft Tissue Cells', *Cells*, vol. 9, no. 5, p. 1226, 2020, doi: 10.3390/cells9051226.

[30] Y. Wang *et al.*, 'Probiotic Streptococcus salivarius K12 Alleviates Radiation-Induced Oral Mucositis in Mice', *Frontiers in immunology*, vol. 12, pp. 684824–684824, 2021, doi: 10.3389/fimmu.2021.684824.

[31] Y.-C. Liu, C.-R. Wu, and T.-W. Huang, 'Preventive Effect of Probiotics on Oral Mucositis Induced by Cancer Treatment: A Systematic Review and Meta-Analysis', *International Journal of Molecular Sciences*, vol. 23, no. 21, Art. no. 21, Jan. 2022, doi: 10.3390/ijms232113268.

[32] F. Sotoudegan, M. Daniali, S. Hassani, S. Nikfar, and M. Abdollahi, 'Reappraisal of probiotics' safety in human', *Food and Chemical Toxicology*, vol. 129, pp. 22–29, Jul. 2019, doi: 10.1016/j.fct.2019.04.032.

[33] J. Suez, N. Zmora, E. Segal, and E. Elinav, 'The pros, cons, and many unknowns of probiotics', *Nat Med*, vol. 25, no. 5, Art. no. 5, May 2019, doi: 10.1038/s41591-019-0439-

x.

[34] F. Fang, J. Xu, Q. Li, X. Xia, and G. Du, ‘Characterization of a Lactobacillus brevis strain with potential oral probiotic properties’, *BMC Microbiology*, vol. 18, 2018, doi: 10.1186/s12866-018-1369-3.

[35] T. Maekawa and G. Hajishengallis, ‘Topical treatment with probiotic Lactobacillus brevis CD2 inhibits experimental periodontal inflammation and bone loss’, *Journal of Periodontal Research*, vol. 49, no. 6, pp. 785–791, 2014, doi: 10.1111/jre.12164.

[36] P. H. A. of Canada, ‘Pathogen Safety Data Sheets: Infectious Substances – Streptococcus salivarius’. Accessed: Nov. 20, 2023. [Online]. Available: https://www.canada.ca/en/public-health/services/laboratory-biosafety-biosecurity/pathogen-safety-data-sheets-risk-assessment/streptococcus-salivarius.html

[37] L. Masdea, E. M. Kulik, I. Hauser-Gerspach, A. M. Ramseier, A. Filippi, and T. Waltimo, ‘Antimicrobial activity of Streptococcus salivarius K12 on bacteria involved in oral malodour’, *Arch Oral Biol*, vol. 57, no. 8, pp. 1041–1047, Aug. 2012, doi: 10.1016/j.archoralbio.2012.02.011.

[38] M. T. Murray and J. Nowicki, ‘220 - Streptococcal Pharyngitis’, in *Textbook of Natural Medicine (Fifth Edition)*, J. E. Pizzorno and M. T. Murray, Eds., St. Louis (MO): Churchill Livingstone, 2020, pp. 1814-1816.e1. doi: 10.1016/B978-0-323-43044-9.00220-X.

[39] F. Di Pierro *et al.*, ‘Effect of administration of Streptococcus salivarius K12 on the occurrence of streptococcal pharyngo-tonsillitis, scarlet fever and acute otitis media in 3 years old children’, *Eur Rev Med Pharmacol Sci*, vol. 20, no. 21, pp. 4601–4606, Nov. 2016.

[40] K. Srikham, W. Daengprok, P. Niamsup, and M. Thirabunyanon, ‘Characterization of Streptococcus salivarius as New Probiotics Derived From Human Breast Milk and Their Potential on Proliferative Inhibition of Liver and Breast Cancer Cells and Antioxidant Activity’, *Front Microbiol*, vol. 12, p. 797445, Dec. 2021, doi: 10.3389/fmicb.2021.797445.

[41] Y. Ye *et al.*, ‘Oral bacterial community dynamics in paediatric patients with malignancies in relation to chemotherapy-related oral mucositis: a prospective study’, *Clinical Microbiology and Infection*, vol. 19, no. 12, pp. E559–E567, 2013, doi: 10.1111/1469-0691.12287.

[42] J. J. Napeñas *et al.*, ‘Molecular methodology to assess the impact of cancer chemotherapy on the oral bacterial flora: a pilot study’, *Oral Surgery, Oral Medicine, Oral Pathology, Oral Radiology, and Endodontology*, vol. 109, no. 4, pp. 554–560, Apr. 2010, doi: 10.1016/j.tripleo.2009.11.015.

[43] M. Kussmann, M. Obermueller, K. Spettel, S. Winkler, and D. Aletaha, ‘In vitro

evaluation of disease-modifying antirheumatic drugs against rheumatoid arthritis associated pathogens of the oral microflora', *RMD Open*, vol. 7, no. 3, p. e001737, Sep. 2021, doi: 10.1136/rmdopen-2021-001737.

[44] Y. Wang *et al.*, 'Oral Health, Caries Risk Profiles, and Oral Microbiome of Pediatric Patients with Leukemia Submitted to Chemotherapy', *Biomed Res Int*, vol. 2021, p. 6637503, Jan. 2021, doi: 10.1155/2021/6637503.

[45] J. P. Frampton, J. B. White, A. T. Abraham, and S. Takayama, 'Cell Co-culture Patterning Using Aqueous Two-phase Systems', *J Vis Exp*, no. 73, p. 50304, Mar. 2013, doi: 10.3791/50304.

[46] J. Wang, M. Woo, and C. Yan, 'Spot Plating Assay for the Determination of Survival and Plating Efficiency of Escherichia coli in sub-MIC Levels of Antibiotics', vol. 1, 2017.

[47] S. E. George, R. J. Anderson, A. Cunningham, M. Donaldson, and P. W. Groundwater, 'Evaluation of a Range of Anti-Proliferative Assays for the Preclinical Screening of Anti-Psoriatic Drugs: A Comparison of Colorimetric and Fluorimetric Assays with the Thymidine Incorporation Assay', *ASSAY and Drug Development Technologies*, vol. 8, no. 3, pp. 384–395, Jun. 2010, doi: 10.1089/adt.2009.0224.

[48] 'CellTracker™ Orange CMRA Dye'. Accessed: Nov. 20, 2023. [Online]. Available: https://www.thermofisher.com/order/catalog/product/C34551

[49] S. Maehara, '[In vitro cytotoxicity of methotrexate]', *Nihon Seikeigeka Gakkai Zasshi*, vol. 58, no. 7, pp. 677–684, Jul. 1984.

[50] Y. Liu *et al.*, 'Association of ABCC2 −24C>T Polymorphism with High-Dose Methotrexate Plasma Concentrations and Toxicities in Childhood Acute Lymphoblastic Leukemia', *PLoS ONE*, vol. 9, no. 1, p. e82681, Jan. 2014, doi: 10.1371/journal.pone.0082681.

[51] F. Albertioni, C. Rask, H. Schroeder, and C. Peterson, 'Monitoring of methotrexate and 7-hydroxy-methotrexate in saliva from children with acute lymphoblastic leukemia receiving high-dose consolidation treatment: relation to oral mucositis', *Anti-Cancer Drugs*, vol. 8, no. 2, p. 119, Feb. 1997.

[52] E. Ishii *et al.*, 'Oral mucositis and salivary methotrexate concentration in intermediate-dose methotrexate therapy for children with acute lymphoblastic leukemia', *Medical and Pediatric Oncology*, vol. 17, no. 5–6, pp. 429–432, 1989, doi: 10.1002/mpo.2950170514.

[53] A. Oliff, W. A. Bleyer, and D. G. Poplack, 'Methotrexate-induced oral mucositis and salivary methotrexate concentrations', *Cancer Chemother. Pharmacol.*, vol. 2, no. 3, pp. 225–226, Sep. 1979, doi: 10.1007/BF00258300.

[54] J. J. Su-Chin Liu and M. Karasek, 'Isolation and Growth of Adult Human Epidermal Keratinocytes in Cell Culture', *Journal of Investigative Dermatology*, vol. 71, no. 2, pp. 157–164, Aug. 1978, doi: 10.1111/1523-1747.ep12546943.

[55] P. T. R. Rajagopalan, Z. Zhang, L. McCourt, M. Dwyer, S. J. Benkovic, and G. G. Hammes, 'Interaction of dihydrofolate reductase with methotrexate: Ensemble and single-molecule kinetics', *Proc Natl Acad Sci U S A*, vol. 99, no. 21, pp. 13481–13486, Oct. 2002, doi: 10.1073/pnas.172501499.

[56] J. Nunberg and R. Kaufman, 'Amplified dihydrofolate reductase genes are localized to a homogeneously staining region of a single chromosome in a methotrexate-resistant Chinese hamster ovary cell line.' Accessed: Nov. 15, 2023. [Online]. Available: https://www.pnas.org/doi/10.1073/pnas.75.11.5553

[57] R. A. Harper and B. A. Flaxman, 'Relative resistance to methothexate by proliferating normal rabbit epidermal cells in vitro', *In Vitro*, vol. 17, no. 5, pp. 393–396, May 1981, doi: 10.1007/BF02626738.

[58] H. Zeng, Z.-S. Chen, M. G. Belinsky, P. A. Rea, and G. D. Kruh, 'Transport of Methotrexate (MTX) and Folates by Multidrug Resistance Protein (MRP) 3 and MRP1: Effect of Polyglutamylation on MTX Transport1', *Cancer Research*, vol. 61, no. 19, pp. 7225–7232, Oct. 2001.

[59] T. Elango, A. Thirupathi, S. Subramanian, P. Ethiraj, H. Dayalan, and P. Gnanaraj, 'Methotrexate treatment provokes apoptosis of proliferating keratinocyte in psoriasis patients', *Clin Exp Med*, vol. 17, no. 3, pp. 371–381, Aug. 2017, doi: 10.1007/s10238-016-0431-4.

[60] C. Barrera-Avalos *et al.*, 'P2X7 receptor is essential for cross-dressing of bone marrow-derived dendritic cells', *iScience*, vol. 24, no. 12, p. 103520, Dec. 2021, doi: 10.1016/j.isci.2021.103520.

[61] N. M. Karabacak *et al.*, 'Microfluidic, marker-free isolation of circulating tumor cells from blood samples', *Nat Protoc*, vol. 9, no. 3, pp. 694–710, Mar. 2014, doi: 10.1038/nprot.2014.044.

[62] G. Soberón-Chávez, F. Lépine, and E. Déziel, 'Production of rhamnolipids by Pseudomonas aeruginosa', *Appl Microbiol Biotechnol*, vol. 68, no. 6, pp. 718–725, Oct. 2005, doi: 10.1007/s00253-005-0150-3.

[63] H. Mikkelsen, R. McMullan, and A. Filloux, 'The Pseudomonas aeruginosa Reference Strain PA14 Displays Increased Virulence Due to a Mutation in ladS', *PLoS One*, vol. 6, no. 12, p. e29113, Dec. 2011, doi: 10.1371/journal.pone.0029113.

[64] J. Morlon-Guyot, J. Méré, A. Bonhoure, and B. Beaumelle, 'Processing of Pseudomonas aeruginosa Exotoxin A Is Dispensable for Cell Intoxication', *Infect Immun*, vol. 77, no. 7, pp. 3090–3099, Jul. 2009, doi: 10.1128/IAI.01390-08.

[65] K. Wolf, '[8] Laboratory management of cell cultures', in *Methods in Enzymology*, vol. 58, in Cell Culture, vol. 58. , Academic Press, 1979, pp. 116–119. doi: 10.1016/S0076-6879(79)58129-4.

[66] C. Yuan *et al.*, 'Dimethyl Sulfoxide Damages Mitochondrial Integrity and Membrane Potential in Cultured Astrocytes', *PLOS ONE*, vol. 9, no. 9, p. e107447, Sep. 2014, doi: 10.1371/journal.pone.0107447.

[67] M. T. Château, C. Ginestier-Verne, J. Chiesa, R. Caravano, and J. P. Bureau, 'Dimethyl sulfoxide-induced apoptosis in human leukemic U937 cells', *Anal Cell Pathol*, vol. 10, no. 2, pp. 75–84, Mar. 1996.

[68] A. Salimi, R. Pirhadi, Z. Jamali, M. Ramazani, B. Yousefsani, and J. Pourahmad, 'Mitochondrial and lysosomal protective agents ameliorate cytotoxicity and oxidative stress induced by cyclophosphamide and methotrexate in human blood lymphocytes', *Hum Exp Toxicol*, vol. 38, no. 11, pp. 1266–1274, Nov. 2019, doi: 10.1177/0960327119871096.

[69] H. Tabassum, S. Parvez, S. T. Pasha, B. D. Banerjee, and S. Raisuddin, 'Protective effect of lipoic acid against methotrexate-induced oxidative stress in liver mitochondria', *Food and Chemical Toxicology*, vol. 48, no. 7, pp. 1973–1979, Jul. 2010, doi: 10.1016/j.fct.2010.04.047.

[70] N. Yamamoto, L. C. V. Lopes, A. P. Campello, and M. L. W. Klüppel, 'Methotrexate: Studies on cellular metabolism. II—Effects on mitochondrial oxidative metabolism and ion transport', *Cell Biochemistry and Function*, vol. 7, no. 2, pp. 129–134, 1989, doi: 10.1002/cbf.290070208.

[71] J. Kim, H. Shin, J. Kim, J. Kim, and J. Park, 'Isolation of High-Purity Extracellular Vesicles by Extracting Proteins Using Aqueous Two-Phase System', *PLoS One*, vol. 10, no. 6, p. e0129760, Jun. 2015, doi: 10.1371/journal.pone.0129760.

[72] K. Mishima, K. Matsuyama, M. Ezawa, Y. Taruta, S. Takarabe, and M. Nagatani, 'Interfacial tension of aqueous two-phase systems containing poly(ethylene glycol) and dipotassium hydrogenphosphate', *Journal of Chromatography B: Biomedical Sciences and Applications*, vol. 711, no. 1, pp. 313–318, Jun. 1998, doi: 10.1016/S0378-4347(97)00660-9.

[73] E. Khalikova, P. Susi, and T. Korpela, 'Microbial Dextran-Hydrolyzing Enzymes: Fundamentals and Applications', *Microbiol Mol Biol Rev*, vol. 69, no. 2, pp. 306–325, Jun. 2005, doi: 10.1128/MMBR.69.2.306-325.2005.

[74] R. Singh, 'Chapter 1 - Introduction to Membrane Technology', in *Membrane Technology and Engineering for Water Purification (Second Edition)*, R. Singh, Ed., Oxford: Butterworth-Heinemann, 2015, pp. 1–80. doi: 10.1016/B978-0-444-63362-0.00001-X.

[75] Lenntech B.V., 'Molecular weight cutoff (MWCO)', Lenntech. Accessed: Jan. 25, 2024. [Online]. Available: https://www.lenntech.com/services/mwco.htm

[76] L. Liu, X.-B. Luo, L. Ding, and S.-L. Luo, '4 - Application of Nanotechnology in the Removal of Heavy Metal From Water', in *Nanomaterials for the Removal of*

Pollutantsand Resource Reutilization, X. Luo and F. Deng, Eds., in Micro and Nano Technologies. , Elsevier, 2019, pp. 83–147. doi: 10.1016/B978-0-12-814837-2.00004-4.

[77] A. Ji *et al.*, 'Quantitative phase contrast imaging with a nonlocal angle-selective metasurface', *Nat Commun*, vol. 13, no. 1, Art. no. 1, Dec. 2022, doi: 10.1038/s41467-022-34197-6.

[78] G. Münchow, F. Schönfeld, S. Hardt, and K. Graf, 'Protein Diffusion Across the Interface in Aqueous Two-Phase Systems', *Langmuir*, vol. 24, no. 16, pp. 8547–8553, Aug. 2008, doi: 10.1021/la800956j.

[79] J. E. Akin, 'Chapter 7 - Variational methods', in *Finite Element Analysis with Error Estimators*, J. E. Akin, Ed., Oxford: Butterworth-Heinemann, 2005, pp. 178–214. doi: 10.1016/B978-075066722-7/50038-2.

[80] M. Elli, R. Zink, A. Rytz, R. Reniero, and L. Morelli, 'Iron requirement of Lactobacillus spp. in completely chemically defined growth media', *Journal of Applied Microbiology*, vol. 88, no. 4, pp. 695–703, Apr. 2000, doi: 10.1046/j.1365-2672.2000.01013.x.

[81] M. Kilstrup, K. Hammer, P. Ruhdal Jensen, and J. Martinussen, 'Nucleotide metabolism and its control in lactic acid bacteria', *FEMS Microbiology Reviews*, vol. 29, no. 3, pp. 555–590, Aug. 2005, doi: 10.1016/j.fmrre.2005.04.006.

[82] W.-C. Li, K. L. Ralphs, J. M. W. Slack, and D. Tosh, 'Keratinocyte serum-free medium maintains long-term liver gene expression and function in cultured rat hepatocytes by preventing the loss of liver-enriched transcription factors', *Int J Biochem Cell Biol*, vol. 39, no. 3, pp. 541–554, 2007, doi: 10.1016/j.biocel.2006.10.017.

[83] FisherScientific, 'BD Difco™ Lactobacilli MRS Broth'. Accessed: Nov. 17, 2023. [Online]. Available: https://www.fishersci.ca/shop/products/bd-difco-dehydrated-culture-media-lactobacilli-mrs-broth-3/p-4869073

[84] R. Hazan, Y.-A. Que, D. Maura, and L. G. Rahme, 'A method for high throughput determination of viable bacteria cell counts in 96-well plates', *BMC Microbiology*, vol. 12, no. 1, p. 259, Nov. 2012, doi: 10.1186/1471-2180-12-259.

[85] A. V. Marionnet, G. Lizard, Y. Chardonnet, and D. Schmitt, 'Comparative evaluation of the antiproliferative effect of cyclosporin A and γ-interferon on normal and HPV-transformed keratinocytes by cell counting, MTT assay and tritiated thymidine incorporation', *Cell Biol Toxicol*, vol. 13, no. 2, pp. 115–123, Feb. 1997, doi: 10.1023/B:CBTO.0000010396.88482.54.

[86] N. Kumar, R. Afjei, T. F. Massoud, and R. Paulmurugan, 'Comparison of cell-based assays to quantify treatment effects of anticancer drugs identifies a new application for Bodipy-L-cystine to measure apoptosis', *Sci Rep*, vol. 8, no. 1, Art. no. 1, Nov. 2018, doi: 10.1038/s41598-018-34696-x.

[87] 'Live or Dead Cell Viability Assays | AAT Bioquest'. Accessed: Nov. 18, 2023. [Online].

Available: https://www.aatbio.com/catalog/live-or-dead-cell-assays

[88] E. Falcieri, A. Cataldi, A. di Baldassarre, lole Robuffo, and S. Miscia, 'Morphological Patterns and DNA Polymerase Regulation in Apoptotic HL60 Cells', *Cell Structure and Function*, vol. 21, no. 3, pp. 213–220, 1996, doi: 10.1247/csf.21.213.

[89] F. M. Sirotnak and R. C. Donsbach, 'Differential cell permeability and the basis for selective activity of methotrexate during therapy of the L1210 leukemia', *Cancer Res*, vol. 33, no. 6, pp. 1290–1294, Jun. 1973.

[90] C. J. Ciesielski, J. Mei, and L. A. Piccinini, 'Effects of cyclosporine A and methotrexate on CD18 expression in recipients of rat cardiac allografts', *Transplant Immunology*, vol. 6, no. 2, pp. 122–133, Jun. 1998, doi: 10.1016/S0966-3274(98)80027-0.

[91] C. J. Ciesielski, J. J. Pflug, J. Mei, and L. A. Piccinini, 'Methotrexate regulates ICAM-1 expression in recipients of rat cardiac allografts', *Transplant Immunology*, vol. 6, no. 2, pp. 111–121, Jun. 1998, doi: 10.1016/S0966-3274(98)80026-9.

[92] P. A. H. Nguyen, E. R. Clark, S. Ananthakrishnan, K. Lenz, and H. E. Canavan, 'How to select the appropriate method(s) of cytotoxicity analysis of mammalian cells at biointerfaces: A tutorial', *Biointerphases*, vol. 15, no. 3, p. 031201, Jun. 2020, doi: 10.1116/6.0000136.

[93] S. Munshi, R. C. Twining, and R. Dahl, 'Alamar blue reagent interacts with cell-culture media giving different fluorescence over time: Potential for false positives', *Journal of Pharmacological and Toxicological Methods*, vol. 70, no. 2, pp. 195–198, Sep. 2014, doi: 10.1016/j.vascn.2014.06.005.

[94] H. K. Hamalainen-Laanaya and M. S. Orloff, 'Analysis of cell viability using time-dependent increase in fluorescence intensity', *Analytical Biochemistry*, vol. 429, no. 1, pp. 32–38, Oct. 2012, doi: 10.1016/j.ab.2012.07.006.

[95] M. N. Dinh, M. Hitomi, Z. A. Al-Turaihi, and J. G. Scott, 'Alamar Blue assay optimization to minimize drug interference and inter-assay viability', *bioRxiv*, p. 2023.03.16.532999, Mar. 2023, doi: 10.1101/2023.03.16.532999.

[96] 'CellTiter-Glo® Luminescent Cell Viability Assay'. Accessed: Nov. 19, 2023. [Online]. Available: https://www.promega.ca/products/cell-health-assays/cell-viability-and-cytotoxicity-assays/celltiter_glo-luminescent-cell-viability-assay/

[97] T. L. Riss *et al.*, 'Cell Viability Assays', in *Assay Guidance Manual*, S. Markossian, A. Grossman, K. Brimacombe, M. Arkin, D. Auld, C. Austin, J. Baell, T. D. Y. Chung, N. P. Coussens, J. L. Dahlin, V. Devanarayan, T. L. Foley, M. Glicksman, K. Gorshkov, J. V. Haas, M. D. Hall, S. Hoare, J. Inglese, P. W. Iversen, S. C. Kales, M. Lal-Nag, Z. Li, J. McGee, O. McManus, T. Riss, P. Saradjian, G. S. Sittampalam, M. Tarselli, O. J. Trask, Y. Wang, J. R. Weidner, M. J. Wildey, K. Wilson, M. Xia, and X. Xu, Eds., Bethesda (MD): Eli Lilly & Company and the National Center for Advancing Translational

Sciences, 2004. Accessed: Nov. 19, 2023. [Online]. Available: http://www.ncbi.nlm.nih.gov/books/NBK144065/

[98] M. P. Wright and J. M. Newton, 'Stability of methotrexate injection in prefilled, plastic disposable syringes', *International Journal of Pharmaceutics*, vol. 45, no. 3, pp. 237–244, Aug. 1988, doi: 10.1016/0378-5173(88)90293-1.

[99] B. R. Giri, H. S. Yang, I.-S. Song, H.-G. Choi, J. H. Cho, and D. W. Kim, 'Alternative Methotrexate Oral Formulation: Enhanced Aqueous Solubility, Bioavailability, Photostability, and Permeability', *Pharmaceutics*, vol. 14, no. 10, Art. no. 10, Oct. 2022, doi: 10.3390/pharmaceutics14102073.

[100] T. Arokia Femina, V. Barghavi, K. Archana, N. G. Swethaa, and R. Maddaly, 'Non-uniformity in in vitro drug-induced cytotoxicity as evidenced by differences in IC50 values – implications and way forward', *Journal of Pharmacological and Toxicological Methods*, vol. 119, p. 107238, Jan. 2023, doi: 10.1016/j.vascn.2022.107238.

[101] I. A. Ratnikova, N. N. Gavrilova, K. Bayakyshova, Z. Zh. Turlybaeva, L. A. Kosheleva, and N. M. Utegenova, 'Antitumor Activity of Probiotic Bacteria and the Bacterial Association in the Tumor Growth Model and in Cell Culture', *Biol Bull Russ Acad Sci*, vol. 45, no. 2, pp. 155–159, Mar. 2018, doi: 10.1134/S1062359018020103.

[102] 'Alteration of Streptococcus pneumoniae membrane properties by the folate analog methotrexate'. Accessed: Nov. 20, 2023. [Online]. Available: https://journals.asm.org/doi/epdf/10.1128/jb.160.3.849-853.1984

[103] S. J. Kopytek, J. C. Dyer, G. S. Knapp, and J. C. Hu, 'Resistance to methotrexate due to AcrAB-dependent export from Escherichia coli', *Antimicrob Agents Chemother*, vol. 44, no. 11, pp. 3210–3212, Nov. 2000, doi: 10.1128/AAC.44.11.3210-3212.2000.

[104] R. R. Nayak *et al.*, 'Methotrexate impacts conserved pathways in diverse human gut bacteria leading to decreased host immune activation', *Cell Host Microbe*, vol. 29, no. 3, pp. 362-377.e11, Mar. 2021, doi: 10.1016/j.chom.2020.12.008.

[105] D. M. Valerino, D. G. Johns, D. S. Zaharko, and V. T. Oliverio, 'Studies of the metabolism of methotrexate by intestinal flora—I: Identification and study of biological properties of the metabolite 4-amino-4-deoxy-N10-methylpteroic acid', *Biochemical Pharmacology*, vol. 21, no. 6, pp. 821–831, Mar. 1972, doi: 10.1016/0006-2952(72)90125-6.

[106] R. C. Wood, R. Ferone, and G. H. Hitchings, 'The relationship of cellular permeability to the degree of inhibition by amethopterin and pyrimethamine in several species of bacteria', *Biochemical Pharmacology*, vol. 6, no. 3, pp. 113–124, May 1961, doi: 10.1016/0006-2952(61)90155-1.

[107] G. Liu *et al.*, 'Cytotoxicity study of polyethylene glycol derivatives', *RSC Adv.*, vol. 7, no. 30, pp. 18252–18259, 2017, doi: 10.1039/C7RA00861A.

[108] D. P. Pacheco *et al.*, 'Disassembling the complexity of mucus barriers to develop a fast screening tool for early drug discovery', *J. Mater. Chem. B*, vol. 7, no. 32, pp. 4940–4952, Aug. 2019, doi: 10.1039/C9TB00957D.

[109] C. Taylor, J. P. Pearson, K. I. Draget, P. W. Dettmar, and O. Smidsrød, 'Rheological characterisation of mixed gels of mucin and alginate', *Carbohydrate Polymers*, vol. 59, no. 2, pp. 189–195, Jan. 2005, doi: 10.1016/j.carbpol.2004.09.009.

[110] L. Zhang, X. Li, X. Zhang, Y. Li, and L. Wang, 'Bacterial alginate metabolism: an important pathway for bioconversion of brown algae', *Biotechnology for Biofuels*, vol. 14, no. 1, p. 158, Jul. 2021, doi: 10.1186/s13068-021-02007-8.

[111] J.-K. Lee, S.-J. Kim, S.-H. Ko, A. Ouwehand, and D. Ma, 'Modulation of the host response by probiotic Lactobacillus brevis CD2 in experimental gingivitis', *Oral Diseases*, vol. 21, no. 6, pp. 705–712, 2015, doi: 10.1111/odi.12332.

[112] D. D. Riccia *et al.*, 'Anti-inflammatory effects of Lactobacillus brevis (CD2) on periodontal disease', *Oral Diseases*, vol. 13, no. 4, pp. 376–385, 2007, doi: 10.1111/j.1601-0825.2006.01291.x.

[113] L. Tasli, C. Mat, C. De Simone, and H. Yazici, 'Lactobacilli lozenges in the management of oral ulcers of Behçet's syndrome', *Clin Exp Rheumatol*, vol. 24, no. 5 Suppl 42, pp. S83-6, Sep. 2006.

[114] H. S. Kim *et al.*, 'In vitro Antioxidative Properties of Lactobacilli', *Asian-Australasian Journal of Animal Sciences*, vol. 19, no. 2, pp. 262–265, Dec. 2005.

[115] Y. Miyazono, F. Gao, and T. Horie, 'Oxidative stress contributes to methotrexate-induced small intestinal toxicity in rats', *Scandinavian Journal of Gastroenterology*, vol. 39, no. 11, pp. 1119–1127, Jan. 2004, doi: 10.1080/00365520410003605.

[116] M. H. Somi *et al.*, 'Protective role of lipoic acid on methotrexate induced intestinal damage in rabbit model', *Indian J Gastroenterol*, vol. 30, no. 1, pp. 38–40, Feb. 2011, doi: 10.1007/s12664-011-0090-z.

[117] D. Ley *et al.*, 'Methotrexate Reduces DNA Integrity in Sperm From Men With Inflammatory Bowel Disease', *Gastroenterology*, vol. 154, no. 8, pp. 2064-2067.e3, Jun. 2018, doi: 10.1053/j.gastro.2018.02.025.

[118] K. Riane, H. Ouled-Haddar, M. Alyane, M. Sifour, C. Espinosa, and M. Angeles Esteban, 'Assessment of Streptococcus Salivarius sp Thermophilus Antioxidant Efficiency and its Role in Reducing Paracetamol Hepatotoxicity', *Iranian Journal of Biotechnology*, vol. 17, no. 4, pp. 58–66, Dec. 2019, doi: 10.30498/ijb.2019.91761.

[119] K. Mukherjee, 'Free Radical Scavenging Activities of Date Palm (Phoenix sylvestris) Fruit Extracts', *Nat Prod Chem Res 2014*, vol. 2, no. 6, 2014, doi: 10.4172/2329-6836.1000151.

[120] Y. Wang *et al.*, 'Antioxidant Properties of Probiotic Bacteria', *Nutrients*, vol. 9, no. 5, p.

521, May 2017, doi: 10.3390/nu9050521.

[121] J. C. Corredoira *et al.*, 'Clinical characteristics and significance of Streptococcus salivarius bacteremia and Streptococcus bovis bacteremia: a prospective 16-year study', *Eur J Clin Microbiol Infect Dis*, vol. 24, no. 4, pp. 250–255, Apr. 2005, doi: 10.1007/s10096-005-1314-x.

[122] K. L. Ruoff, S. I. Miller, C. V. Garner, M. J. Ferraro, and S. B. Calderwood, 'Bacteremia with Streptococcus bovis and Streptococcus salivarius: clinical correlates of more accurate identification of isolates', *Journal of Clinical Microbiology*, vol. 27, no. 2, pp. 305–308, Feb. 1989, doi: 10.1128/jcm.27.2.305-308.1989.

[123] C. D. Doern and C.-A. D. Burnham, 'It's Not Easy Being Green: the Viridans Group Streptococci, with a Focus on Pediatric Clinical Manifestations', *J Clin Microbiol*, vol. 48, no. 11, pp. 3829–3835, Nov. 2010, doi: 10.1128/JCM.01563-10.

[124] J. Carratalá, F. Alcaide, A. Fernández-Sevilla, X. Corbella, J. Liñares, and F. Gudiol, 'Bacteremia Due to Viridans Streptococci That Are Highly Resistant to Penicillin: Increase Among Neutropenic Patients with Cancer', *Clinical Infectious Diseases*, vol. 20, no. 5, pp. 1169–1173, May 1995, doi: 10.1093/clinids/20.5.1169.

[125] R. Hatti-Kaul, Ed., *Aqueous two-phase systems: methods and protocols*. in Methods in biotechnology, no. 11. Totowa, N.J: Humana Press, 2000.

[126] C. M. Weikart, A. M. Klibanov, A. P. Breeland, A. H. Taha, B. R. Maurer, and S. P. Martin, 'Plasma-Treated Microplates with Enhanced Protein Recoveries and Minimized Extractables', *SLAS Technol*, vol. 22, no. 1, pp. 98–105, Feb. 2017, doi: 10.1177/2211068216666258.

[127] M. A. Witek, M. L. Hupert, D. S.-W. Park, K. Fears, M. C. Murphy, and S. A. Soper, '96-Well Polycarbonate-Based Microfluidic Titer Plate for High-Throughput Purification of DNA and RNA', *Anal Chem*, vol. 80, no. 9, pp. 3483–3491, May 2008, doi: 10.1021/ac8002352.

[128] Azenta Life Sciences, 'Low DNA Binding Products'. Accessed: Nov. 22, 2023. [Online]. Available: https://n-genetics.com/files/co/Documents/productcatalog/4titude_13970.pdf

[129] A. W. Nicholson, 'Function, mechanism and regulation of bacterial ribonucleases', *FEMS Microbiology Reviews*, vol. 23, no. 3, pp. 371–390, Jun. 1999, doi: 10.1111/j.1574-6976.1999.tb00405.x.

[130] P. Vrtačnik, Š. Kos, S. A. Bustin, J. Marc, and B. Ostanek, 'Influence of trypsinization and alternative procedures for cell preparation before RNA extraction on RNA integrity', *Anal Biochem*, vol. 463, pp. 38–44, Oct. 2014, doi: 10.1016/j.ab.2014.06.017.

[131] Gibco ThermoFisher, 'TrypLE™ Express Enzyme (1X), no phenol red'. Accessed: Nov. 23, 2023. [Online]. Available: https://www.thermofisher.com/order/catalog/product/12604013

[132] Y.-W. Kim *et al.*, 'Lactobacillus brevis Strains from Fermented Aloe vera Survive Gastroduodenal Environment and Suppress Common Food Borne Enteropathogens', *PLOS ONE*, vol. 9, no. 3, p. e90866, Mar. 2014, doi: 10.1371/journal.pone.0090866.

[133] J. Tate and G. Ward, 'Interferences in Immunoassay', *Clin Biochem Rev*, vol. 25, no. 2, pp. 105–120, May 2004.

[134] J. M. Hamilton-Miller, 'Antimicrobial activity of 21 anti-neoplastic agents', *Br J Cancer*, vol. 49, no. 3, Art. no. 3, Mar. 1984, doi: 10.1038/bjc.1984.58.

[135] D. Metcalfe and W. T. Hughes, 'Effects of methotrexate on group a beta hemolytic streptococci and streptococcal infection', *Cancer*, vol. 30, no. 2, pp. 588–593, 1972, doi: 10.1002/1097-0142(197208)30:2<588::AID-CNCR2820300240>3.0.CO;2-V.

[136] C. Xia *et al.*, 'A Phase II Randomized Clinical Trial and Mechanistic Studies Using Improved Probiotics to Prevent Oral Mucositis Induced by Concurrent Radiotherapy and Chemotherapy in Nasopharyngeal Carcinoma', *Frontiers in immunology*, vol. 12, pp. 618150–618150, 2021, doi: 10.3389/fimmu.2021.618150.

[137] Z. Shu, P. Li, B. Yu, S. Huang, and Y. Chen, 'The effectiveness of probiotics in prevention and treatment of cancer therapy-induced oral mucositis: A systematic review and meta-analysis', *Oral Oncology*, vol. 102, p. 104559, Mar. 2020, doi: 10.1016/j.oraloncology.2019.104559.

[138] C. Jiang *et al.*, 'A randomized, double-blind, placebo-controlled trial of probiotics to reduce the severity of oral mucositis induced by chemoradiotherapy for patients with nasopharyngeal carcinoma', *Cancer*, vol. 125, no. 7, pp. 1081–1090, 2019, doi: 10.1002/cncr.31907.

[139] A. Jumma Kareem and J. Abdul Sattar Salman, 'Production of Dextran from Locally Lactobacillus Spp. Isolates', *Rep Biochem Mol Biol*, vol. 8, no. 3, pp. 287–300, Oct. 2019.

[140] G. Takahashi, K. Inada, K. Sato, and Y. Inoue, 'A dextran-based warming method for preparing leukocyte-rich plasma and its clinical application for endotoxin assay', *Biotechniques*, vol. 68, no. 6, pp. 300–304, Jun. 2020, doi: 10.2144/btn-2020-0005.

[141] A. Hoffmann, K. Pacios, R. Mühlemann, R. Daumke, B. Frank, and F. Kalman, 'Application of a novel chemical assay for the quantification of endotoxins in bacterial bioreactor samples', *Journal of Chromatography B*, vol. 1228, p. 123839, Aug. 2023, doi: 10.1016/j.jchromb.2023.123839.

[142] T. Sugita, C.-C. Huang, and M. Abramson, 'Effect of endotoxin on keratin production of keratinocytes in vitro', *American Journal of Otolaryngology*, vol. 7, no. 1, pp. 42–46, Jan. 1986, doi: 10.1016/S0196-0709(86)80033-3.

[143] F. Sun, Q. Li, H. Liu, B. Kong, and Q. Liu, 'Purification and biochemical characteristics of the protease from Lactobacillus brevis R4 isolated from Harbin dry sausages', *LWT*, vol. 113, p. 108287, Oct. 2019, doi: 10.1016/j.lwt.2019.108287.

Appendix A

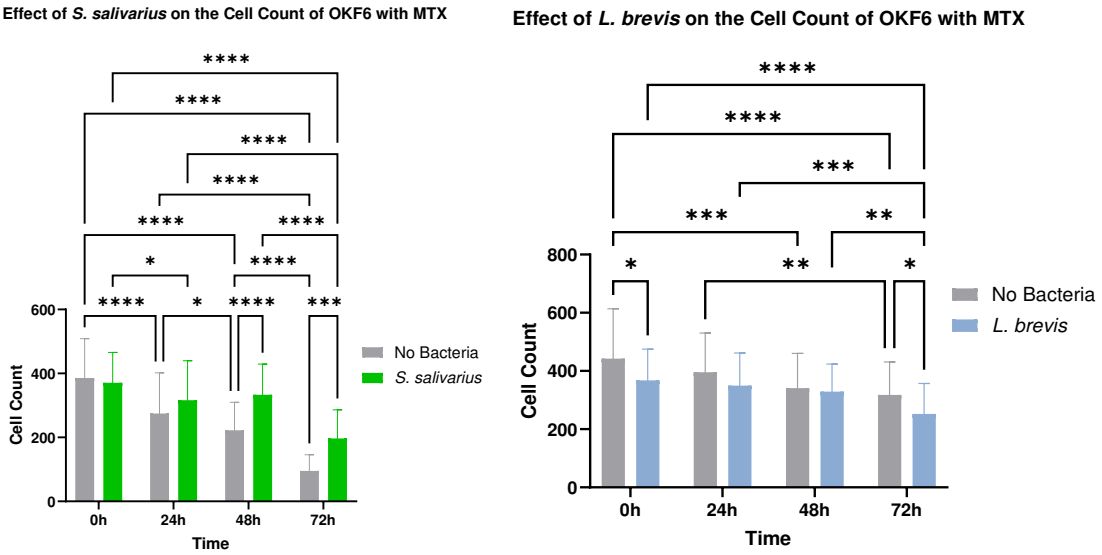

*Figure 43. Oral keratinocytes exposed to S. salivarius (green) or L. brevis (blue) 24 hours before MTX application. P values were obtained using two-way ANOVA. *p < 0.05, **p < 0.01, ***p < 0.001, ****p < 0.000. n=3. Error bars indicate standard deviation.*

Appendix B

An increase in density was observed within the MRS DEX droplets containing *L. brevis* after exposure to 10^{-8} mg/mL of MTX. As observed in Figure 44, bacteria containment was achieved until the 48h time point. The dark spots did not spread into the PEG phase. MTX was added to the basal compartment at time 0h at the same point in which the bacteria was seeded into the system. There are no signs of the MTX inhibiting bacterial growth in the ATPS using this MTX concentration.

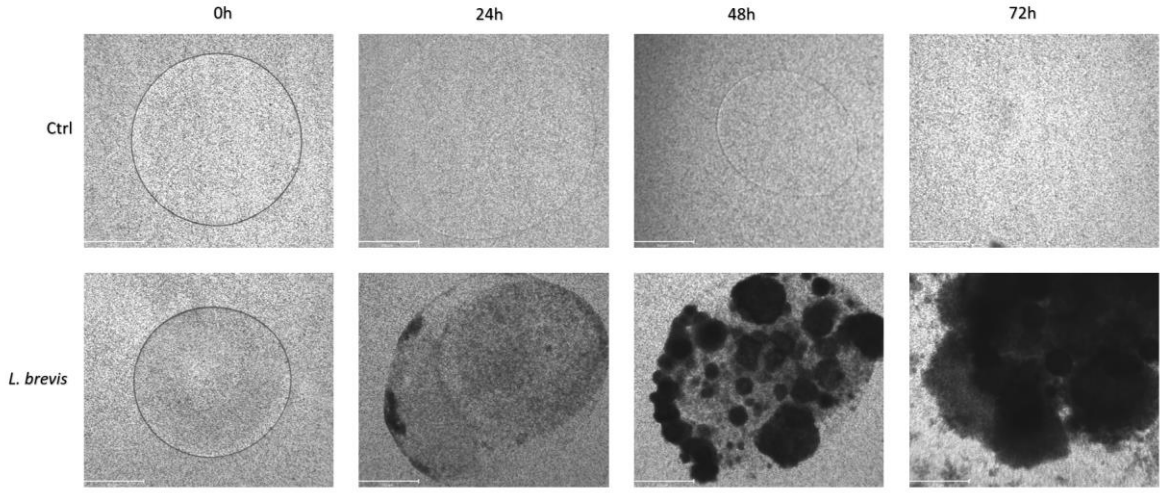

Figure 44. Phase contrast images of an aqueous two-phase system (ATPS) containing L. brevis at 0.5 OD_{600} after 24, 48, and 72h exposed to 10^{-8} mg/mL of MTX. ATPS prepared with 10% PEG on 50% MRS 50% KSFM and 5% DEX in MRS. Bacteria were incubated at 37°C with 5% CO_2 in a 24-well plate using 6mm in diameter inserts (scale bar 650um).

Appendix C

After 72 hours of allowing *L. brevis* to grow in a contained manner within an ATPS prepared with 10% PEG in 50% MRS 50% KSFM, and 5% DEX in MRS, and after exposing the bacteria to 10^{-8} mg/mL MTX for the last 48 hours, the lack of bacterial growth inhibition was confirmed through the plating of the colonies. Figure 45 demonstrates the viability of the bacteria through a spot-plating technique, which allowed for the quantification and validation of the ability of the cells to form colonies. It can be observed that both biological replicates that were plated showed prominent growth while the clear agar dish which contained the same ATPS without bacteria did not grow any colonies over the 48 hours that the dishes were incubated.

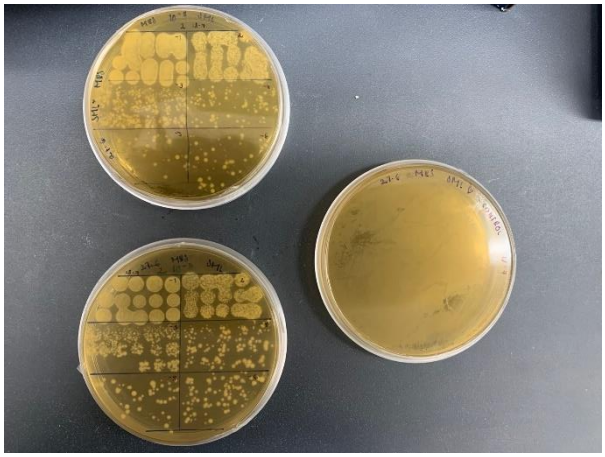

Figure 45. Spot plating of ATPS of L. brevis exposed to 10^{-8} mg/mL MTX in MRS agar dishes. Bacteria viability is confirmed by the growth of colonies in the agar after 72h of MTX exposure. An average concentration of 353 million CFU/mL was obtained from this technique.

Appendix D

Figure 46 shows the phase contrast images of an ATPS assembled with *S. salivarius* at four different time points. The shown ATPS was assembled with 10% PEG in KSFM and 5% DEX on BHI. The system was exposed to 10^{-8} mg/mL of MTX at the same time point of inoculation (0h). After 72 hours, it can be observed that there is an increase in density within the DEX droplet from time point 24h to 48h. Bacterial growth does not appear to be inhibited by the MTX application.

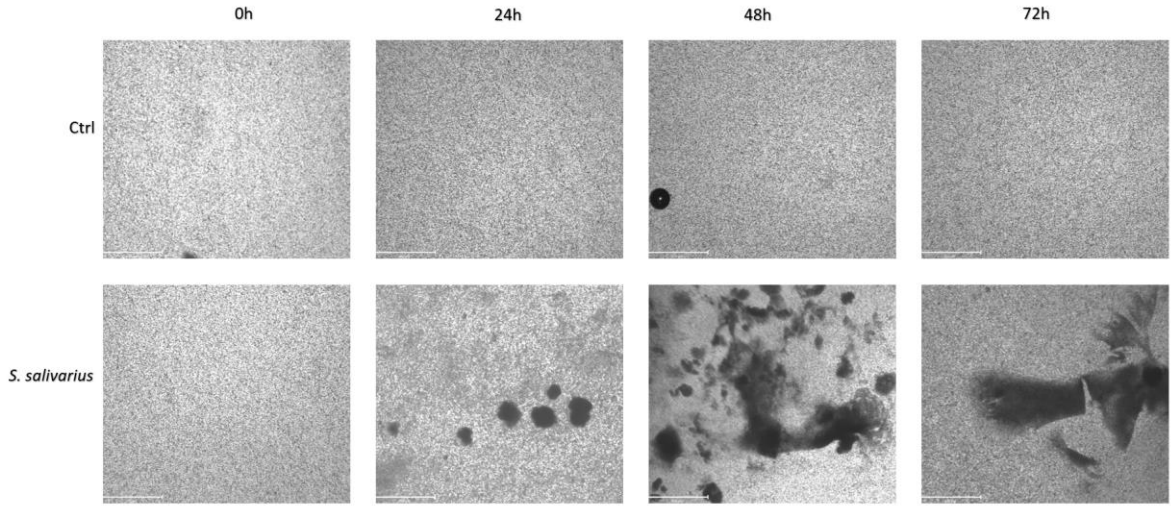

Figure 46. Phase contrast images of an aqueous two-phase system (ATPS) containing S. salivarius at 0.5 OD_{600} after 24, 48, and 72h exposed to 10^{-8} mg/mL MTX. ATPS prepared with 10% PEG on KSFM and 5% DEX in BHI. Bacteria was incubated at 37 °C with 5% CO_2 in a 48-well plate. (Scale bar 650um).

Appendix E

Figure 47 shows the spot plating of two ATPS containing *S. salivarius*. The formation of isolated colonies can be observed in both biological replicates in dilutions below 10^{-5}. The bacteria shown in the following picture was contained in an ATPS for 72 hours and exposed to 10^{-8} mg/mL of MTX for the same period. The observed bacterial growth on the BHI agar corroborates the lack of bacterial inhibition exerted by the MTX when diluted down to 10^{-8} mg/mL in KSFM.

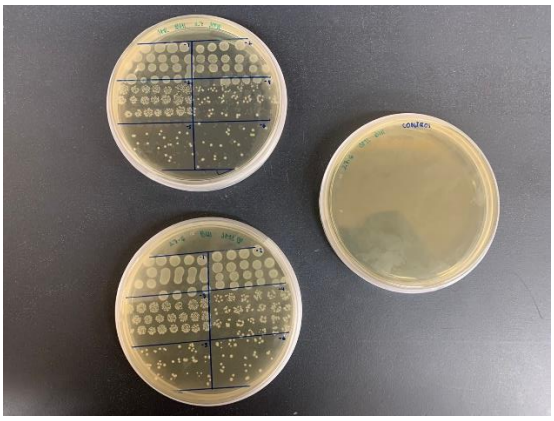

Figure 47. Spot plating of ATPS of S. salivarius exposed to 10^{-8} mg/mL MTX in BHI agar dishes. Bacteria viability is confirmed by the growth of colonies in the agar after 72h of MTX exposure. An average concentration of 1150 million CFU/mL was obtained from this technique.

Appendix F

To corroborate the lack of significant bacterial inhibition exerted by the MTX, the effect of the drug is analyzed in Figure 48. Three biological replicates with three technical replicates are shown for each treatment. After inoculating *L. brevis* of MRS broth and *S. salivarius* on BHI in broth with MTX at a 10^{-8} mg/mL concentration, no significant difference is observed in contrast to the respective control without MTX.

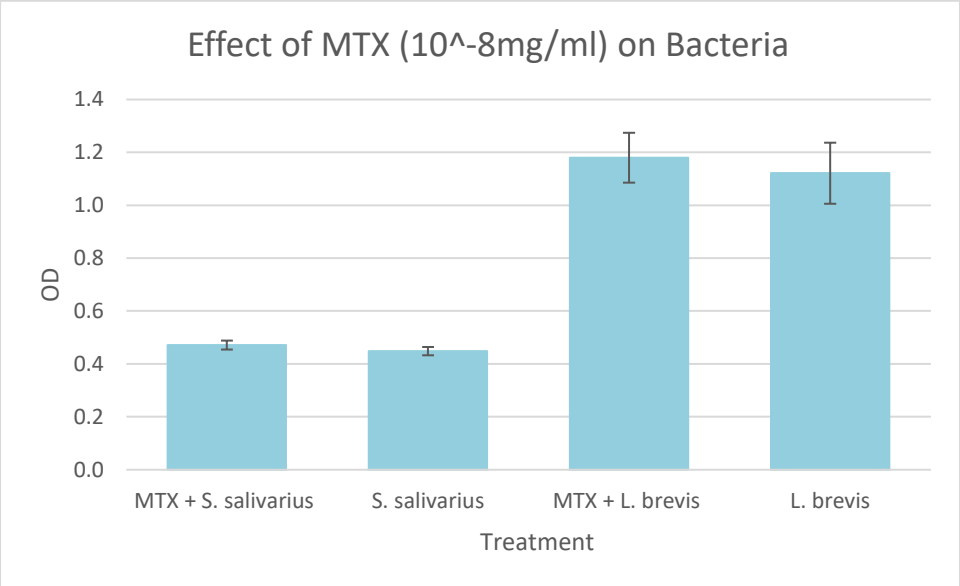

Figure 48. Effect of MTX on overnight cultures of L. brevis and S. salivarius. Three overnight cultures were left for incubation for 24 hours with MTX in a 10^{-8} mg/mL concentration. Each treatment was performed with three biological replicates, each with three technical replicates. No significant difference is observed between treatments of the same bacteria. n=3

Appendix G

The following graphs show the growth of *L. brevis* and *S. salivarius* over a monolayer of OKF6 covered by an alginate hydrogel. *L. brevis* appeared to have slowed down its growth after the application of MTX (24h) (Figure 49). *S. salivarius* was able to grow on top of the hydrogel that covered the OKF6 for 72 hours. The containment of the bacteria appears to have been ruptured after 24 hours (Figure 50).

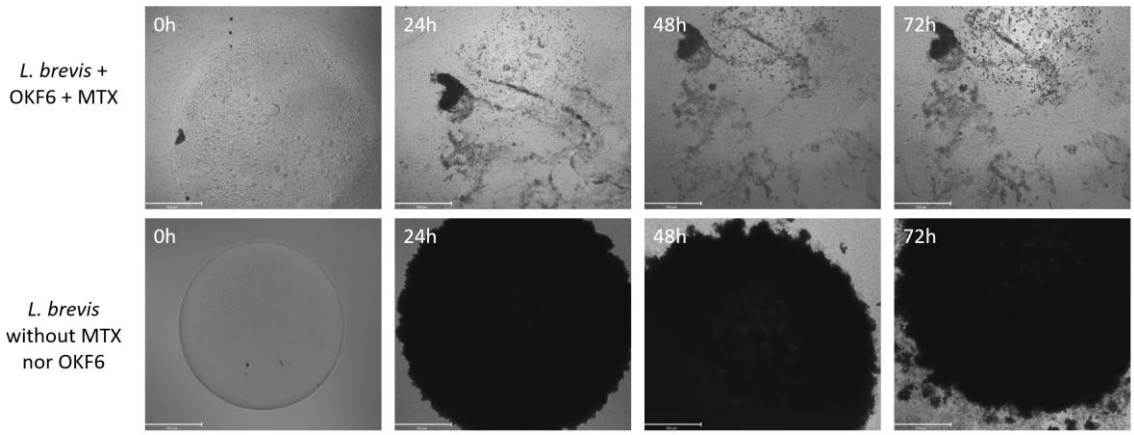

Figure 49.Phase contrast images showing L. brevis growth on top of a monolayer of OKF6 exposed to MTX and control of L. brevis without cells or MTX underneath. Bacteria were incubated at 37°C with 5% CO_2 in a 24-well plate using 6mm in diameter inserts (scale bar 650um).

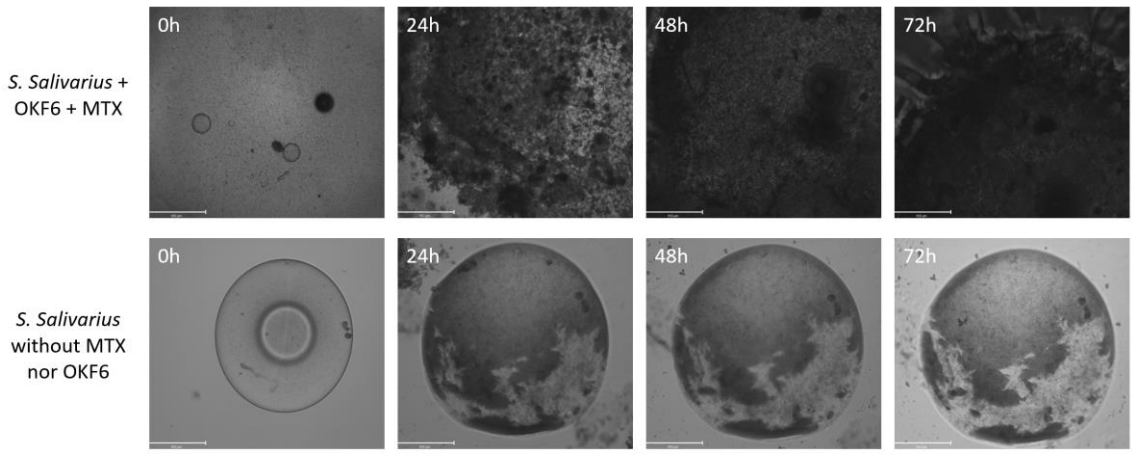

Figure 50. Phase contrast images showing S. salivarius growth on top of a monolayer of OKF6 exposed to MTX and control of S. salivarius without cells or MTX. Bacteria were incubated at 37°C with 5% CO_2 in a 24-well plate using 6mm in diameter inserts (scale bar 650um).

Appendix H

Figure 51 shows the histology slices of one of the six epithelium tissues that were grown as controls without MTX or Bacteria. After fixing the engineered model and staining it with Haematoxylin and Eosin, an even stratified layer of keratinocytes was observed. It is also noticeable that the cells grew one on top of each other allowing the multiple layers of keratinocytes to stratify towards the surface. The presence of desmosomes between the cells was observed using a greater magnification, this provides the tissue with strong adhesion between cells and allows them to withstand mechanical stress.

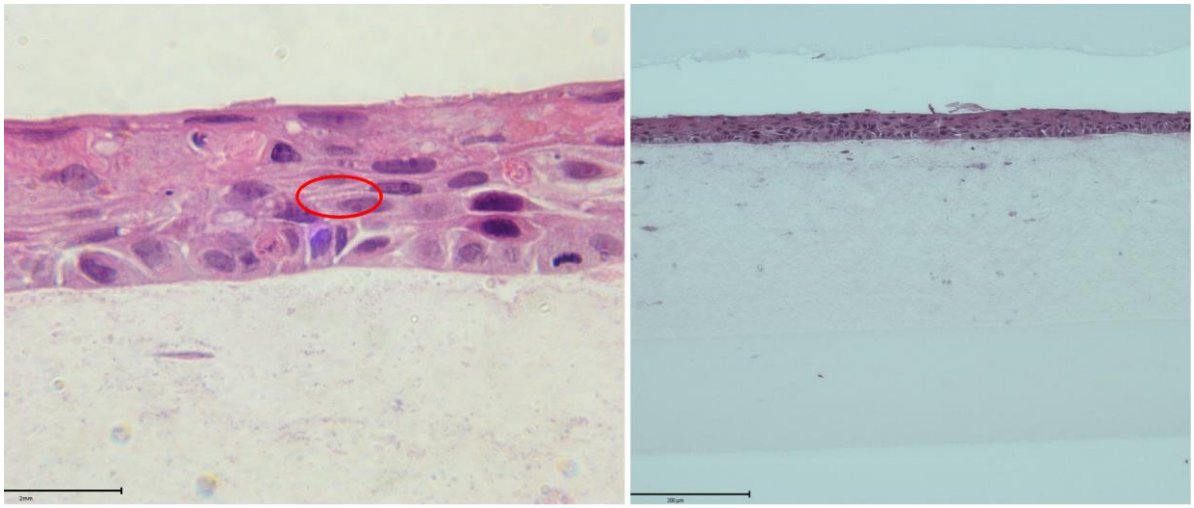

Figure 51. Histology sample stained with Haematoxylin and Eosin (H&E) showing desmosomes present between keratinocytes of stratified epithelium. The red circle on the left indicates the presence of desmosomal attachment between two cells (scale bar 2 mm). The image on the right shows the H&E staining of the sample sample displaying consistent and even stratification layers (scale bar 200 µm).

Appendix I

Table 1. Primer information for oxidative and inflammation markers.

Category	Gene	Abbreviation	Forward Primer	Reverse Primer	Amplicon size	Trancripts	Citation
Housekeeping genes	Beta-2-microglobulin	B2M	ACCCCCACTGAAAAAGATGA	CAACCATGCCTTACTTTATC	590	NM_004048.4	https://doi.org/10.1159/000027650
	Succinate dehydrogenase complex, subunit A, flavoprotein	SDHA2	CGGGTCCAATCCATCGCATAAG	TATATGCCTGTAGGGTGGAACTGAA	180	NM_004168, XM_011514073.3, XM_011514072.3, XM_054353043.1	https://doi.org/10.1111/febs.16413
	Tyrosine 3-monooxygenase/tryptophan 5-monooxygenase activation protein zeta	YWHAZ	GAAAAGTTCTTGATCCCCAATGC	TGTGACTGGTCCACAATTCCTT	134	NM_001135701.2,	10.1038/s41419-023-05951-5
Oxidative Stress	Heme oxygenase 1 (HMOX1)	HO-1 (HMOX1)	AGGAGGAGATTGAGCGCCAC	GCTTCACATAGCGCTGCATG	165	NM_002133	https://doi.org/10.1111/j.1432-1033.1988.tb13811.x
	NAD(P)H dehydrogenase, quinone 1	NQO1	CCTGCCATTCTGAAAGGCTGGT	GTGGTGATGGAAAGCACTGCCT	119	NM_000903.3	https://doi.org/10.1016/j.ecoenv.2023.115103
	Nuclear factor, erythroid 2-like 2 (Nrf2)	NFE2L2/NRF2	TGCTTTATAGCGTGCAAACCTCGC	AATCCAT GTCCCT TGACAGCACAGA	181	NM_001313904.1, NM_001145413.3, NM_001145412.3	10.1097/MD.0000000000035155
	Superoxide dismutase 1	SOD1	TGAAGGTGTGGGGAAGCATTA	TTACACCACAAGCCAAACGAC	360	NM_000454.5	https://doi.org/10.1002/ijc.10408
Inflammation	Homo sapiens C-X-C motif chemokine ligand 8 (CXCL8)	IL-8 (CXCL8)	CTTCCTGATTTCTGCAGCTCT	AACTTCTCCACAACCCTCTGC	240	NM_001354840.3, NM_000584.4	https://doi.org/10.1159/000027650
	Interleukin 6 (IL-6)	IL-6	ACTCACCTCTTCAGAACGAATTG	CCATCTTTGGAAGGTTCAGGTTG	149	NM_000600,	https://doi.org/10.1111/odi.14766
	Nuclear factor of kappa light polypeptide gene enhancer in B-cells 1	NF-κB1	CCTGGATGACTCTTGGGAAA	CTTCGGTGTAGCCCATTTGT	386	NM_003998, NM_001382627.1, NM_001382626.1	https://doi.org/10.1177/17534259124547761
	Tumor necrosis factor	TNF-α	CCTCTCTCTAATCAGCCCTCTG	GAGGACCTGGGAGTAGATGAG	220	NM_000594.4	https://doi.org/10.1111/odi.14766